REPORT DOCUMENTATION PAGE	Form Approved OMB No. 0704-0188

1. AGENCY USE ONLY *(Leave blank)*	2. REPORT DATE	3. REPORT TYPE AND DATES COVERED
	23.Sep.02	THESIS

4. TITLE AND SUBTITLE
RESIN COMPOSITE RESTORATIONS: EFFECT OF ENERGY DENSITY ON PROPERTIES AND MARGINAL INTEGRITY

5. FUNDING NUMBERS

6. AUTHOR(S)
COL VANDEWALLE KRAIG S

7. PERFORMING ORGANIZATION NAME(S) AND ADDRESS(ES)
OREGON HEALTH SCIENCES UNIVERSITY

8. PERFORMING ORGANIZATION REPORT NUMBER
CI02-647

9. SPONSORING/MONITORING AGENCY NAME(S) AND ADDRESS(ES)
THE DEPARTMENT OF THE AIR FORCE
AFIT/CIA, BLDG 125
2950 P STREET
WPAFB OH 45433

10. SPONSORING/MONITORING AGENCY REPORT NUMBER

11. SUPPLEMENTARY NOTES

12a. DISTRIBUTION AVAILABILITY STATEMENT
Unlimited distribution
In Accordance With AFI 35-205/AFIT Sup 1

12b. DISTRIBUTION CODE

13. ABSTRACT *(Maximum 200 words)*

DISTRIBUTION STATEMENT A
Approved for Public Release
Distribution Unlimited

20021017 100

14. SUBJECT TERMS	15. NUMBER OF PAGES
	221
	16. PRICE CODE

17. SECURITY CLASSIFICATION OF REPORT	18. SECURITY CLASSIFICATION OF THIS PAGE	19. SECURITY CLASSIFICATION OF ABSTRACT	20. LIMITATION OF ABSTRACT

ABSTRACT

Resin composite (Z250, 3M, St Paul, MN) was bonded in bulk with various degrees of cure into Class 2 preparations in extracted human molar teeth. Two control groups consisted of a highly-cured incrementally-placed group and a non-fatigued low-cure group. The restorations were subjected to 1000 thermal-cycles and 500,000 fatigue cycles from 18 to 85 Newtons using a stainless-steel sphere. Marginal integrity was evaluated using visual rating (ridit analysis) and microleakage. The degree of conversion had a significant effect on marginal defects but not on microleakage. Water had a significant dissolving effect on gingival margin integrity at very low degrees of conversion. Gingival marginal defects were maximized at 25% of maximum conversion and 3% of maximum hardness. There was no overall significant effect of thermal-mechanical stressing on marginal defects or microleakage. A recommended lower limit of gingival margin acceptability in a bulk-filled resin composite restoration was created by 80% of maximum conversion, 73% of maximum hardness and approximately 70% of maximum flexural strength and modulus in the gingival marginal area.

Resin Composite Restorations: Effect of Energy Density on Properties And Marginal Integrity

by

Kraig S. Vandewalle, DDS

A Thesis

Presented to the
Department of Biomaterials and Biomechanics
and the
Advanced Education Committee of the School of Dentistry
Oregon Health & Science University
in partial fulfillment of the requirements for the degree of
Masters of Science

30 May 2002

ACKNOWLEDEMENTS

I am extremely grateful to my supervisor and mentor, Dr. Jack Ferracane for his valuable advice, guidance and constant support. I am especially indebted to him for his inspiration, patience, and encouragement through the course of this project.

I would like to thank the other members of my thesis committee, Drs. Robert Erickson for his many hours in reviewing this project and Dr. Ron Sakaguchi for his assistance with strain measurements, FEA analysis and curing light radiometry.

I give my sincere gratitude to Dr. Tom Hilton for his help in developing the concept for the project and ongoing guidance.

I would also like to acknowledge, with many thanks, Jerry Adey for his Scanning Electron Microscopy support and John Condon for his technical guidance with the fatigue machine.

I appreciate the extra efforts of Drs. Lawrence Musanje and Jack Mitchem for their evaluation of specimens.

I am grateful to 3M ESPE Dental Products Division for funding this project and especially Rolf Halvorson for the constant supply of products.

I am thankful to the Dental Corp, United States Air Force for giving me the opportunity to take part in this fellowship and especially Col Kevin Gureckis for his support in gaining a second year and a mastership opportunity.

Finally, I would like to thank my family, [redacted]or being so understanding and supportive.

TABLE OF CONTENTS

	Page
LIST OF TABLES	vii
LIST OF FIGURES	viii
ABSTRACT	1
INTRODUCTION	2
REVIEW OF LITERATURE	4
OVERVIEW	28
PART ONE (Pilot Study)	
Methods and Materials	31
Results	35
Discussion	39
PART TWO	
Methods and Materials	47
Results / Discussion	52
PART THREE	
Methods and Materials	60
Results	63
OVERALL DISCUSSION	65
OVERALL CONCLUSIONS	80
BIBLIOGRAPHY	83
APPENDIX	95
[redacted] One	96
KHN and DC data (anatomic template)	97
KHN and DC data (flattened template)	101
KHN technique study	103
Statistics:	
2-way ANOVA Energy or Location on DC	106
2-way ANOVA Energy or Location on KHN	109
1-way ANOVAs Energy vs KHN or DC	112

Part Two
First Pilot 118
Photos, SEMs and gap width data 119
Second Pilot 128
Photos, SEMs and gap width data 129
Third Pilot 144
Photos, SEMs 145
Defect width data 159
Ridit data (n = 3) 167
Final Method 168
Ridit Scale 169
Ridit data (n = 8) 170
Microleakage raw scores 172
Microleakage photos 173
Statistics:
2-way ANOVA Energy or Stress on Ridit 180
2-way ANOVA Energy or Stress on Microleakage 185
1-way ANOVA Energy vs Pre or Post Stressing 189
Part Three 195
Flexure bar data
KHN 196
Flexural strength / Flexural modulus 197
Curing Light Transmission Study 198
Strain Gauge Study 201
Statistics:
1-way ANOVAs Time vs Flexural strength or modulus 203
1-way ANOVAs Time vs KHN surface or KHN center 207

Equipment: 211

Fourier Transform Infrared Spectroscopy 212

Knoop Hardness 215

Fatigue cycler 217

Scanning Electron Microscopy 219

LIST OF TABLES

		Pg.
1	Knoop Hardness (anatomic template)	35
2	Degree of Conversion (anatomic template)	36
3	Percentages of Maximum KHN and DC for Various Energy Densities	38
4	Knoop Hardness and Degree of Conversion (new groups)	40
5	Selected Groups	41
6	Degree of Conversion (flattened template)	43
7	Knoop Hardness (flattened template)	45
8	Defect Widths and Percent Defective (n=3)	54
9	Defect Widths and Ridit (n=3)	56
10	Ridit Analysis (n=8)	57
11	Microleakage Scores: Percent of Margin (n=8)	59
12	Mechanical Properties	63

LIST OF FIGURES

		Pg.
1	Re-usable template (anatomic)	31
2	Mounting Jig	31
3	Creation of Test Surface	32
4	Gridded Specimen	33
5	KHN vs DC (anatomic template): Gingival Increment	36
6	KHN or DC vs log Energy Density (anatomic temp): Gingival Increment	37
7	Flattened Template	42
8	Vertically Mounted Specimens for KHN Testing	44
9	KHN vs DC (flattened template): Gingival Increment	46
10	KHN or DC vs log Energy Density (flattened temp): Gingival Increment	46
11	Fatigue Cycler	48
12	Cross Section of Restoration after Silver Nitrate Stain	50
13	Width vs Ridit	56
14	Center KHN measurement	61
15	Surface KHN vs flexural modulus	63
16	Surface KHN vs flexural strength	64
17	KHN Indentation at 200x	66
18	Gingival Marginal Defect at 1000x	68
19	Dentinal Gingival Margin at 500x	71
20	5 mm Composite Restoration after 500,000 cycles	71
21	Microleakage Section (pre-op & 500,000 cycles)	72
22	Layering of Increments	75
23	KHN or DC vs Energy Density (no log) (flattened temp) Ging Increment	77
24	Strain gauge Measurements	78

ABSTRACT

Resin composite (Z250, 3M, St Paul, MN) was bonded in bulk with various degrees of cure into Class 2 preparations in extracted human molar teeth. Two control groups consisted of a highly-cured incrementally-placed group and a non-fatigued low-cure group. The restorations were subjected to 1000 thermal-cycles and 500,000 fatigue cycles from 18 to 85 Newtons using a stainless-steel sphere. Marginal integrity was evaluated using visual rating (ridit analysis) and microleakage. The degree of conversion had a significant effect on marginal defects but not on microleakage. Water had a significant dissolving effect on gingival margin integrity at very low degrees of conversion. Gingival marginal defects were maximized at 25% of maximum conversion and 3% of maximum hardness. There was no overall significant effect of thermal-mechanical stressing on marginal defects or microleakage. A recommended lower limit of gingival margin acceptability in a bulk-filled resin composite restoration was created by 80% of maximum conversion, 73% of maximum hardness and approximately 70% of maximum flexural strength and modulus in the gingival marginal area.

INTRODUCTION

New light activation protocols (PAC lights and lasers) and new composites (packables) claim the advantage of shorter exposure times and bulk curing.[1] The negative consequences of these approaches would be a composite with regions of lower properties at the base of the restoration. Laboratory research shows that many of the suggested new protocols do not produce composites with maximum depth of cure or uniform properties.[2] However, manufacturers and some clinicians claim clinical success. Current light-curing techniques may produce adequate marginal integrity though the properties of the base of these restorations are significantly less than the properties on the surface. The question is: "Are these lower properties clinically significant?" One danger is that repeated stressing of the interface between the base of the restoration and the tooth may deteriorate the marginal seal and integrity with time as a consequence of the "undercuring". In bonded restorations, would enough occlusal forces be transferred to the cavity walls allowing for an increase in marginal integrity that did not deteriorate under fatiguing?

Hypothesis.-- There is some minimal extent of cure required by the base of the resin composite restoration that allows it to support the rest of the filling and maintain its marginal seal under thermal and mechanical stress conditions.

Utilizing various photo-curing energy densities, a pilot study was used to determine the Knoop hardness and degree of conversion at incremental levels occlusal-gingivally throughout the depth of the resin composite in a 5 millimeter long sample created from an extracted tooth template.

Based on the pilot study, select energy densities were used to achieve variable degrees of gingival cure for resin composite restorations in prepared teeth. These restorations were subjected to thermal-mechanical stress to evaluate the effect on the gingival margins using scanning electron microscopy, stereomicroscopy and microleakage.

Additionally, bar-shaped specimens (2x2x25 mm) were tested in three-point bending to measure flexure strength and modulus. This data was correlated with the marginal breakdown data. The hypothesis tested was that marginal leakage and breakdown, as evaluated by silver nitrate and scanning electron microscopy and stereomicroscopy would increase for composites with low degree of conversion and low elastic modulus at the gingival margins.

REVIEW OF THE LITERATURE

Resin Composites.--

Introduction.-- The introduction of resin composites was one of the greatest milestones in esthetic restorative dentistry. Introduced in the early 1960's by R. L. Bowen with the development of the Bis-GMA molecule, it satisfied an initial need for an aesthetic anterior restorative material – eventually replacing silicate cement and acrylic resins.[3] Bowen began his experiments to reinforce epoxy resins with filler particles. However, epoxy resins were abandoned due to slow curing and discoloration. The monomer, Bis-GMA, prepared from bisphenol A and glycidyl methacrylate was bulky, but superior to the methyl methacrylate. It provided rapid hardening, less shrinkage and stronger and more rigid resins.[4]

With anterior resin composite restorations providing satisfactory performance, most research is now focused at developing a resin composite capable of replacing amalgam. Improvements in formulations, optimization of properties and the development of new placement techniques have made esthetic direct posterior restorations more commonplace and dependable. A concern with resin composite is polymerization shrinkage. A major step in solving this problem would be the development of a polymer that experiences only enough contraction on curing to offset any expansion from water absorption.

Composition.-- A composite is a material that consists of two or more components of metals, ceramics or polymers. Dental resin composites typically contain a mixture of a soft, organic resin matrix (polymer) and hard, inorganic filler particles

(ceramic). Other components are included to improve the efficacy of the combination and initiate polymerization. The resin matrix consists of monomers, an initiator system, stabilizers and pigments. The inorganic filler consists of particles such as glass, quartz and colloidal silica. The matrix and filler are bonded together with a coupling agent. The performance of resin composites is obviously dependent on these basic components.[4] The current improvement of these materials has primarily focused on filler technology, but the resin monomers have remained largely unmodified. The majority of resin composites are still based on variations of Bis-phenol A glycidyl methacrylate (Bis-GMA).[5]

The most common monomers used are Bis-GMA, urethane dimethacrylate (UEDMA), and triethylene glycol dimethacrylate (TEGDMA). Bis-GMA is extremely viscous at room temperature due to hydrogen bonding by hydroxyl groups (-OH). Lower viscosity is obtained by mixing Bis-GMA with dimethacrylate monomers (TEGDMA) of lower molecular weight to facilitate the addition of fillers. Addition of the diluents allows greater degree of conversion and more extensive cross-linking to occur between chains – providing a matrix that is more resistant to solvents.[4,6] However, this increased conversion and crosslinking increases the polymerization shrinkage.[7] Resin composites undergo volumetric shrinkage of 1.9 to 7.1 percent.[8,9] The shrinkage in the resin matrix results from the conversion of weak intermolecular attractions to primary covalent bonds.[10] Polymerization shrinkage and the resultant stress can contribute to gap formation at the margins of restorations. The current goal of resin composite restorative materials remains to be the improvement or elimination of contraction stress – possibly through low or non-shrinking monomers. Recent research has focused on ring opening

spiro-orthocarbonates, epoxy-based resin systems and a new class of difunctional monomers called oxybismethacrylates which exhibit cyclopolymerization.[5]

Polymerization shrinkage can also be reduced by increasing the concentration of filler particles because the overall shrinkage depends on the amount of polymer matrix present.[4] However, the modulus of elasticity of the resin composite is also increased at high filler levels contributing to higher polymerization stress.[11] Inclusion of filler particles into a resin matrix drastically improves the mechanical properties of the composite material. Improvement is seen in properties such as tensile and compressive strength, modulus of elasticity, abrasion resistance, radiopacity, esthetics and handling.[4] As a general rule, the higher the filler loading, the higher the physical properties of the resin composite. Most current resin composites have filler loaded between 50 and 86 percent by weight and 35 to 71 percent by volume.[12] Percentage filler is best expressed by volume instead of weight because the mechanical properties of composites are mainly dictated by their filler volume fraction.[13]

The type of filler directly influences radiopacity and is typically accomplished through the inclusion of elements of high atomic number. Barium and strontium are the most common elements used in filler particles to increase radiopacity.[14]

Various classification systems for resin composites have developed through the years based on particle size.[4] A very traditional system includes traditional, small particle, microfilled and hybrid filler particles.[15]

Originally, crystalline quartz was used as a filler for resin composites because of its availability, excellent optical properties, and chemical inertness.[4,16] However, it proved to be extremely hard, a challenge to grind and difficult to polish with the potential

to abrade opposing tooth structure.[4] The softer polymer would wear away easily, exposing the hard quartz particle, only to be plucked and perpetually roughen the surface.[16] These traditional quartz particles were produced by grinding or milling and typically were quite large – average 8 to 12 microns in size.[4]

Microfills were developed to provide better esthetics and polishability.[16] These tiny particles of silica are only 0.04 microns in diameter and are literally "born in fire" through a pyrolytic process.[4] The large surface area of these filler particles demands much more resin matrix to wet the surface. This creates extremely high viscosity that limits the percentage filler content possible. In order to maximize filler loading and minimize viscosity, prepolymerized resin and microfiller is used. The heavily filled polymerized resin is ground into 30-65 micron particles and mixed with more resin and microfiller to provide a composite that is filled 30 to 50% by volume. A smoother surface can be produced due to the smaller size of the silica particles.[4] However, mechanical properties such as strength and stiffness are generally inferior to larger quartz or glass filled composites because of the lower filler content.[16]

Small particle composites were developed to combine the esthetics of microfills with the mechanical properties of traditional composites. The average filler size ranged from 1 to 5 microns.[4]

The most common filler today is barium glass with average particle size of 0.6 to 1 micron.[4] A small amount of microfiller is added to improve handling and reduce stickiness.[16] To incorporate a maximum amount of filler into a resin matrix, a distribution of particle sizes is necessary. These so-called hybrids are potentially superior because increased filler loading improves the stress transfer between particles in the composite.[4]

The current trend is to maximize filler loading and minimize filler size.[16] The table below compares and contrasts various mechanical properties of these various resin composite types:[4]

Composite Resin Mechanical Properties

Property	Traditional	Microfilled	Small Particle	Hybrid
Compressive strength (MPa)	250-300	250-300	350-400	300-350
Tensile strength (MPa)	50-65	30-50	75-90	70-90
Elastic Modulus (GPa)	8-15	3-6	15-20	7-12
CTE	25-35	50-60	19-26	30-40
Knoop Hardness	55	5-30	50-60	50-60

Other classification systems have been developed over the years due to the difficulty in categorizing the newer complicated formulations of resin composites based on a wide range of filler sizes, loading and compositions. Willems proposed a system based on volume fraction in 1992.[17] More recently, a newer re-classification based on particle size was introduced. The various groups included megafill – 0.5 to 2 millimeters; macrofill – 10 to 100 microns; midifill – 1 to 10 microns; minifill – 0.1 to 1 microns; microfill – 0.01 to 0.1 microns and nanofill – 0.005 to 0.01 microns. Most new systems are minifill hybrids with a new trend toward nanofillers.[12]

It is important that the filler particle be bonded to the resin matrix via a coupling agent to improve mechanical and physical properties. The most commonly used coupling agent is an organosilane such as gamma-methacryloxypropyltrimethoxy silane. The silane reduces hydrolytic breakdown and allows stress transfer between the filler and the matrix. The silane agent is a bifunctional molecule with a methacrylate group on one end

and a silanol group on the other. The methacrylate end undergoes addition polymerization with the composite resin and the silanol end bonds to the hydroxyl groups on the filler particle via a condensation reaction.[4]

Resin composites undergo addition polymerization by chemical, heat or light energy activation. In chemical activation, a tertiary amine activator reacts with a benzoyl peroxide initiator supplied as two separate pastes to produce free radicals. The radicals attack the carbon double bonds of the polymer to propagate the reaction.[18] In heat activation, higher temperatures activate the initiator. The most popular method of curing resin composites is with light activation.[16] Originally, ultraviolet light was used to initiate free radicals. Today, visible light provides greater depth of cure and safety.[19,20]

Light activation is achieved with blue light that is absorbed by the photoinitiator, camphoroquinone in the 400 to 500 nanometer range. The excited initiator reacts with an amine activator to form free radicals and initiate the addition polymerization.[4] Compared to chemical curing of direct restorative resin composites, visible light activated systems provide longer working time, reduced porosity, greater color stability and reduced waste of material. A possible disadvantage with visible light materials is limited depth of penetration by the curing light.[18]

An inhibitor is added to resin systems to rapidly scavenge propagating radicals and prevent spontaneous polymer chain formation from heat or light. The inhibitor delays the start of the reaction, but once begun, the reaction proceeds at a normal rate. A typical inhibitor is butylated hydroxytoluene.[4]

Different metal oxides are added to resin composites in tiny amounts to provide shading and opacity to match natural tooth color.[18]

Polymerization Chemistry.-- Many types of dental resin composites utilize free radical polymerization with monomers containing double carbon bonds reacting to produce longer polymer chains of single carbon bonds. The reaction takes place in three stages: initiation, propagation and termination.

Initiation involves the production of highly reactive free radicals with either the use of heat, chemicals or light.

Heat activation is typically used in denture resins to initiate the heat sensitive benzoyl peroxide molecules. These benzoyl peroxide molecules split quite easily into two free radicals at temperatures between 50 and 100 degrees Centigrade, which initiate the polymerization of methyl methacrylate monomer.[4]

Chemical activation typically involves the mixing of two reactants that initiate the polymerization of self-cure dental resins. Benzoyl peroxide is again the usual initiator, but instead of heat energy, a tertiary amine activator catalyzes the split of the benzoyl peroxide molecule.[4]

Light activation is the most common method of initiating the polymerization process in resin composites for use in restorative dentistry. Initially, ultraviolet light activated resin composites were introduced as a welcomed replacement to the chemically cured resins. Utilizing a benzoin methyl ether photoinitiator, they offered command setting, no mixing and unlimited working time. The potential for retinal and skin damage ushered in the incorporation of visible light initiators by the early 1980s.[20]

In visible light activated polymerization, camphoroquinone is most commonly used to induce photoinitiation.[18] Camphoroquinone (CQ) requires a tertiary amine co-

initiator to photocure composite in a reasonable amount of time.[21] CQ absorbs energy in the visible region of 400 to 500 nanometers with a peak at 468 nanometers. Photons associated with this frequency range will be absorbed by camphoroquinone, raising it from the ground state to an excited, but short-lived, activated triplet state. However, if the energy is removed or diminished, the complex may de-energize and return to the ground state. If the excited triplet manages to bump into an amine co-initiator, an exciplex forms, with the subsequent transfer of an electron and then a proton to CQ to create an aminoalkyl free radical capable of initiating polymerization.[22,23]

Propagation is a chain reaction that results in the incorporation of hundreds of monomer units into the polymeric network. The rigidity of Bis-GMA molecules reduces its ability to rotate during polymerization and to participate efficiently in the polymerization process. The complete conversion of the methacrylate double bonds is eventually hindered by the reduction of diffusion rate of free radicals and unreacted methacrylate molecules as the polymer undergoes vitrification.[4] Therefore, only 50 to 75% of the methacrylate groups convert into polymer.[24] The process continues with considerable velocity until terminated either by direct coupling or by the exchange of a hydrogen atom from one growing chain to another.[4] The extent of the reaction is important in developing physical and mechanical properties of the composite.[16]

Light-Curing.--

Light generation.-- Light is a form of electromagnetic radiation. Other forms of electromagnetic radiation include radio waves, microwaves, infrared radiation, ultraviolet rays, X-rays, and gamma rays. All of these, known collectively as the electromagnetic

spectrum, are fundamentally similar in that they move at 186,000 miles per second - the speed of light. The only difference between them is their wavelength, which is directly related to the amount of energy the waves carry. Shorter wavelengths have higher energy. The rainbow of colors that we see in visible light represents only a very small portion of the electromagnetic spectrum. On one end of the spectrum are radio waves with wavelengths billions of times longer than those of visible light. On the other end of the spectrum are gamma rays. These have wavelengths millions of times smaller than those of visible light. Visible light is the portion of the electromagnetic spectrum with wavelengths between 400 to 700 nanometers.[25]

Quartz-tungsten-halogen lamps are integrated into most dental curing lights in use today. The principle output from these lamps is infrared energy with the generation of high heat. An infrared filter is used to reduce the heat energy to the oral structures.[26] Next, a band-pass filter provides further restriction of visible light to the narrower spectrum of the photoinitiator. Finally, the dichroic filter, a silver coated surface passes infrared energy out the back and reflects and focuses the light forward to provide a focal area of energy at defined distance. Ultimately, 99.5% of the original radiation is eliminated.[25] Due to the high operating temperatures, the halogen bulbs have a limited efficient lifetime.[26] The reflector, bulb and filters can break down over time, reducing the curing effectiveness.[25]

Less noticeable on the surface to the operator, a decreased light intensity could dramatically affect the cure in deeper areas of the restoration. Therefore, curing lights should be periodically tested with a dental radiometer.[27] However, recent research suggests that the accuracy of the commercial radiometers vary widely depending on the

diameter of the curing tip. Commercial radiometers have fixed apertures, while an industrial radiometer measures all light intensity from the curing tip, regardless of the diameter.[28] A study in dental offices revealed that 46% of the halogen lights provided inadequate intensity to sufficiently cure resin composites.[29]

Increased levels of light can be developed within the composite depths if the intensity of the curing source is increased. With curing procedures considered highly time consuming, the demand for expensive high energy plasma-arc and laser light sources has increased.[30] However, polymerization stress and contraction gaps increase as the mechanical properties are maximized and perhaps, as the rate of polymerization is increased.[31]

Plasma-arc (PAC) lights generate a high voltage pulse that creates hot plasma between two electrodes in a Xenon filled bulb.[32] The irradiance of up to 2400 mW/cm^2 is much higher than typical halogen bulbs, but the PAC light generates very high heat with an inefficient emission spectrum similar to halogen bulbs.[25]

Light emitted from an argon laser is very different from that emitted from the halogen or PAC lights. The photons produced are coherent and do not diverge, therefore they concentrate more photons of specific frequency into a tiny area. The laser has a power of only 250 mW, but the energy is restricted to only a few wavelengths. With very little infrared output, unwanted heat is minimized. If the 250 mW is transmitted through a 50 micron fiber it results in an irradiance of more than 12 million mW/cm^2 However, the tiny spot size of only 50 micrometers makes clinical application more tedious. Some systems utilize diffusers that increase the spot size, however, the irradiance will be

reduced. Other clinicians will use the tiny fiber itself, placing it directly on the tooth until it actually appears to glow.[25]

Light emitting diodes (LED) use special semiconductors for the electroluminescence of light rather than a hot filament found in halogen lights providing a longer life span, consistent output and lower power consumption.[33] No significant ultraviolet or infrared light is emitted thereby reducing heat and minimizing the need for a noisy fan. Since the energy is clearly defined by the semiconductor, most of the light emitted is concentrated in a narrow band around 470 nanometers which is ideally suited for composite resins that use the photoinitiator camphoroquinone.[34] Initial claims of greater efficiency in curing resin composites have yet to be unequivocally established in vitro.[33-35] More laboratory and clinical data is needed to establish the significance of any increased efficiency and determine the overall efficacy of this potentially promising technique in light curing.[36]

Light-Restorative Interaction.—

Light transmission.-- Light is reflected, scattered and absorbed as it passes into the polymerizing resin composite.[37] There are many factors that may alter the transmission of light, such as filler type and size, composite shade, and refractive index.

Light scattering may be related to filler particle size in resin composite. Kawaguchi et.al. showed that microfilled composites had a lower transmission coefficient and depth of cure than hybrid and small particle composites.[38] One theory suggests that light scattering is maximized when the filler particle size is one-half the wavelength of the activation light.[39] One-half of the peak wavelength of the 450 to 500 nanometers

typically emitted from halogen curing lights would be 250 nanometers or 0.250 microns. However, microfill composites are, on average, only 0.04 microns in diameter. But at least one study found that microfills tend to clump in sizes that may closely approximate these critical sizes and increase light scattering and reduce depth of cure relative to hybrid composites.[40] Another study found resin composites with larger filler particles were capable of showing good transmission coefficient and cure depth.[41]

The content of pigment, or shade, appears to influence light scattering in resin composites. McCabe et. al. showed a strong correlation between depth of cure and light attenuation for various shades of microfilled composite.[40] However, Ferracane et. al. suggested that the depth of cure may be less dependent upon shade than upon other factors, such as translucency.[42]

Transmission of light is facilitated through composite when the refractive index is closely matched between the filler particles and the resin matrix. Refractive index is the ratio of the velocity of propagation of an electromagnetic wave (light) in vacuum to its velocity in the medium (composite). However, this coordination produces a translucent composite. Therefore, a compromise is needed to provide some obvious esthetic qualities. Some mismatch in refractive index between the filler particle and the resin matrix is needed to provide some opacity. [43]

Light absorption.-- There are many factors that may be altered with light absorption, such as depth of cure, degree of conversion, and biocompatibility.

Numerous studies have suggested that depth of cure is affected by light intensity, spectral distribution and exposure time.[43,44] The more intense the light intensity, the

more photons available. With more photons, more camphoroquinone molecules are raised to the excited state, react with the amine and form free radicals. At the top surface, polymerization proceeds quickly and more completely. However, deeper in the composite, attenuation of light leads to a potential gradation of cure within the depths of the material and is responsible for what has become known as "depth of cure".[45] To compensate for this decreased potential, the duration of exposure can be increased, providing enhanced opportunity for the creation of a free radical. A study by Rueggeberg and others found that at depths greater than 2 millimeters, poorer cure may result and polymerization is very susceptible to changes in light intensity and exposure duration. Routine exposure times of 60 seconds are recommended using light-source intensities of at least 400 mW/cm^2.[46]

The maximum degree of conversion of monomer into polymer of resin composites is between 50 and 80%.[47] However, only a small amount of unreacted monomer actually remains. Most of the remaining unreacted double carbon bonds are bonded to the polymer chain. Therefore, less than 10% of the available methacrylate is extractable, thereby significantly reducing biological effects.[48] Most of the unreacted monomers are believed to be TEGDMA molecules.[49] However, with decreased degree of conversion, there is greater residual monomer available to be leached.[48,50] And as the percentage of monomer conversion decreases, the potential for cellular toxicity increases.[51] Several *in vivo* studies have shown that complete or incompletely polymerized resin composites cause little pulpal irritation if the restorations are sealed.[52,53]

In addition to biocompatibility issues, less degree of conversion may reduce the mechanical properties of resin composites. There appears to be a good correlation between increasing degree of conversion and increasing hardness,[54] fracture toughness [55] and abrasive wear resistance.[56]

Restorative Response.-- The prognosis of the restoration may depend on how the resin composite is placed and how it is light activated.

One disadvantage of resin composite is the polymerization shrinkage that arises during curing and the potential for subsequent marginal gap formation.[57,58] Marginal gap formation may facilitate secondary caries[59-61] and post-operative sensitivity[62] - especially in posterior resin composite restorations with greater technique sensitivity.[63]

Various studies have advocated incremental instead of bulk placement and curing for resin composite to decrease the effects of polymerization shrinkage and to provide complete polymerization in deeper cavities.[2,58,64-65] Incremental placement may also reduce the configuration factor – the ratio of bonded to unbonded surfaces – and reduce the stress by making more resin available for flow.[66] The superiority of the incremental technique has not been totally proven. Tjan and others found that when resin composite was cured in bulk from the occlusal, there was no difference in marginal gap formation at the dentin margin compared to incremental placement.[67] Another study found no significant difference between bulk and incremental cure and its effect on fluid permeability in dentin under class 1 resin composite restorations.[68]

Another approach to stress reduction is the application of various liners. Glass ionomer liners may provide some advantages when used with resin composite

restorations. The setting reaction is much slower and less polymerization stress may result.[69] Less bulk of resin composite is necessary to fill the lined restoration, thereby reducing the amount available for shrinkage. Resin-modified glass-ionomer restorative materials have been placed in areas of the preparation with dentinal margins in an "open-sandwich" technique to reduce marginal leakage.[70] However, the use of glass ionomer liners has decreased with the improvement in efficacy and ease of use of resin adhesive bonding agents.[63]

The use of a relatively thick layer of resin adhesive to serve as a flexible intermediary between the stiff dentinal cavity wall and the shrinking restorative resin composite has been proposed. This "elastic bonding theory" proposes that the stretching of a 100 micron thick layer may provide enough elasticity to reduce the polymerization contraction stresses of the restorative resin composite to below dentin bond strengths.[11,63,71-72]

Soft-start polymerization is a method recently advocated to reduce polymerization stresses. During early polymerization, the composite cross-linking network is relatively weak - allowing flow fairly easily to accommodate stresses and prevent damage to adhesive bonds. With further polymerization, contraction and flow decrease, while stiffness and stress increase. This can cause adhesive failure. The bond strength must exceed the contraction stress to provide a stable marginal adaptation. The resin-enamel bond interface may survive the shrinkage, but the weaker resin-dentin interface may not.[73] Soft-start polymerization proposes that a slower rate of conversion will allow better flow of resin with a decrease in contraction stress. However, the final mechanical properties must be obtained in a reasonable amount of chair time. Three different types

of techniques are currently advocated. "Stepped" uses a short, low-level initial burst followed by full intensity. "Ramped" uses a gradual increase from an initial low level. And "pulsed" uses a short low level burst, a delay for polishing followed by full intensity. Although the majority of studies suggest that soft-start polymerization may be statistically beneficial *in vitro,*[74-81] further research is necessary to see if any clinically significant differences can be found.

Assessment of Polymerization.-- The assessment of the effectiveness of polymerization may be done directly or indirectly. Indirect methods include surface hardness,[82] optical,[83] and scraping.[84] Direct methods include laser Raman spectroscopy[85] and infrared spectroscopy.[86] DeWald and Ferracane compared four modes of evaluating depth of cure of light-activated composites and found that the optical and scraping methods correlated well, but both over-estimated depth of cure when compared to hardness and degree of conversion values. Degree of conversion was the most sensitive testing mode for evaluating depth of cure.[87] A good correlation can be found between hardness and relative degree of conversion for a specific composite at different time periods or under variable conditions.[82] Hardness testing appears to be a popular method of assessing effectiveness of polymerization because of its simplicity and reasonable correlation with other methods. [87]

Johnston et. al. suggested that the depth of cure may be defined as the level at which the hardness value is equivalent to at least 90% of the hardness at the top of the composite.[88] Others have suggested that this top-to-bottom gradient should not exceed 20% [89] and should be considered a realistic measure of depth of cure.[90] Research is

needed to determine the minimal extent of cure required by the base of the resin composite restoration that allows it to support the rest of the filling and maintain its marginal seal under thermal and mechanical stress conditions. The marginal integrity of resin composites has been routinely examined *in vitro* with marginal gap and microleakage evaluations.

Assessment of Marginal Integrity.-- Ideally, evaluation of restorative margins should be repeatable, sensitive enough to discriminate between variables, recognize marginal discrepancies easily, and require little evaluator training. One of the first measures for quality assessment of restorations was the Ryge criteria.[91] Popular as a clinical assessment, the procedure cannot detect small differences between various materials or variables.[92] Scanning electron microscopy (SEM) provides a high magnification inspection of the marginal integrity of the restoration.[93] Disadvantages include its potential of distortion through desiccation, lack of penetration, the destructive nature of the process and difficulty in quantifying the results.[94] However, epoxy replicas may be used to avoid artifacts and provide observations over time.[95] Researchers have used the SEM to measure marginal gap formation.[96,97] Common *in vitro* methods to characterize marginal quality include gap or defect size, ridit analysis, ranking and microleakage.

Interfacial gaps may provide a route for bacteria to the pulp, whereas discrepancies such as marginal ditching or material defects create a site for plaque accumulation and potential secondary caries.[92] Determining gap size involves measurement of the largest gap,[98] average gap,[99] or percent gapped.[100] Using the

measuring capabilities of the SEM, Roulet assigned the largest gap measurement to one of five classes on the basis of gap size: 0; 0<30 microns; >30<50 microns; >50<100 microns and >100 microns<150 microns.[98] Lutz and Krejci determined the percentage of continuous margins by digitizing the restorations using a three dimensional scanner and superimposing before and after images using a custom-made software program.[100]

The ridit analysis[101] in marginal restoration evaluation uses a numbered scale of restoration images that exhibit progressively increasing degrees of marginal defects. The procedure involves assigning to the restoration being evaluated, the number of the scale image to which it is most similar with respect to the extent of marginal defect. A ranking system described by Osborne and others consists of assigning the entire margin of each restoration in a rank of descending order from the one showing the best margin to the one showing the worst.[102]

Images may be created by enlargement of scanned computer images,[100] photographic film,[103] or SEM photographs of the entire margin.[104] Using enlarged images or photographs may be labor intensive, time consuming and produce pictures of inconsistent quality.[92] Although useful for gross marginal defects,[103] it may not be possible, in some cases, to see or estimate the width of micron-sized marginal gaps to any degree of accuracy.[92]

Microleakage is defined as the clinically undetectable passage of fluids, bacteria, molecules or ions between the walls of the preparation and the restorative material.[95] Microleakage is detected indirectly with the use of dyes, chemical tracers, radioactive isotopes, air pressure, bacteria, and artificial caries.[95]

One of the most common methods of detecting leakage is the use of organic dyes or chemical tracers. There has been a wide variation in the choice, size, concentration and duration of dyes or chemical tracers.[95] A chemical tracer, silver nitrate, is considered a severe test because of the very tiny size of the silver ion – much smaller than common bacteria. The sample is typically immersed in a fifty percent solution of silver nitrate and later developed with a photographic solution.[105]

Another technique for evaluating microleakage is the use of radioisotopes. The most popular method is immersion in Ca^{45}. The sample is rinsed, sectioned and applied to photographic film.[106]

The use of bacteria to study microleakage may be the most clinically relevant. However, the relatively larger size of bacteria, 0.5 –1 micrometers, may not account for other detrimental products such as toxins. A somewhat qualitative test exists where the sectioned or shaved samples are cultured in broth to note the presence or absence of bacteria.[95]

A more quantifiable method for leakage is the use of air pressure. The release of air bubbles is examined from a submerged sample, which does not need to be sectioned or destroyed. This gives an added advantage of leakage evaluation over time.[107]

Bacterial cultures or an acidified-gel are used to produce artificial carious lesions. The acidified-gel technique has the advantage of expediency over bacterial induced lesions. Lesions produced are examined with polarized light and an outer and cavity wall lesion is described.[108]

Many of these techniques - dyes, bacteria, chemical and radioactive tracers - necessitate the destruction of the sample, making it difficult to study the margins over

time.[109] Most studies section the tooth and restoration with a single cut through the center, allowing visualization of interfaces and dentinal tubules. Three dimensional techniques are more representative of penetration, but are tedious and extremely time consuming. The use of multiple sections is perhaps more practical.[110]

Most researchers use a subjective ordinal ranking system to score the leakage. The ordinal scale has the advantage of relating relevant landmarks such as dentin-enamel junction and axial walls. However, non-parametric statistics must be used.[111,112] Others have recently tried more objective techniques by measuring the microleakage directly[113]or expressing the amount of leakage as a percentage of the total cavity-restoration interface length[114] and through the use of imaging software.[115,116] Although more time consuming, continuous measurements allow greater precision and the use of more robust parametric statistics.

Many studies examining marginal integrity include thermocycling and load cycling in the design of the experiment.[117-119] Thermocycling is simply a way of applying stress to the restorative interface at the limits of temperature found intra-orally.[120] One researcher found a direct correlation between the degree of mismatch in the coefficient of thermal expansion between various restorative materials and tooth structure and the extent of microleakage.[121] Thermal-cycling was found to be detrimental to bond strengths of two older generation dentin adhesive agents[122-123] and the microleakage of bonded amalgam restorations.[124] However, several studies suggest that thermocycling resin composite restorations may not significantly affect microleakage.[124,125] Although resin composites have high coefficients of thermal expansion relative to tooth structure, they are relatively good insulators. Harper and others theorized with their clinical

measurement of thermal diffusion through restorations of various materials that the relatively low rate of thermal change beneath resin composite restorations might reduce the significant effect of thermal expansion.[126] The significance of thermocycling resin composite restorations remains questionable and perhaps the procedure is unnecessary.

There appears to be little consensus on temperatures, dwell time and number of cycles among research studies involving microleakage. Investigators have used temperature ranges from 15 to 45°C, 4 to 60°C and 5 to 55°C. Dwell times have varied from 10, 15, 30, 60 and 120 seconds.[95] Shorter dwell times are more clinically relevant, however, longer dwell times may stress the interface greater and accelerate the evaluation process. One study concluded that the depth of microleakage was correlated with the thermal conductivity of the restorative material.[124] Composite restorations, with low thermal conductivity compared to amalgam appeared to be unaffected by differences in dwell time.[124] Also, microleakage tests on composite restorations should be delayed 24 hours to permit the potential for water absorption.[117] The number of thermocycles recommended has ranged from 1 to 2500.[95] However, the stresses from thermocycling may act quickly to produce microleakage thereby reducing the need for extended cycles.[127]

Water is absorbed as resin composite restorations are placed intraorally and may lead to hydrolytic breakdown of the silane coupling and filler particles, reducing the strength of the material.[128] Water decreases the elastic modulus, fracture strength, and flexure fatigue limits.[129] Water has a plasticizing effect on the matrix. Debonded fillers may act as stress concentrators, significantly increasing the number of potential crack growth sites.[130] The breakdown can contribute to lower wear and abrasion resistance.

However, the expansion of resin composite associated with the water uptake could counteract some setting contraction. Studies show that microfilled composites absorb more water than hybrid composites. [131] Most resin composites require 4 days to show the majority of expansion and 7 days to reach equilibrium.[18]

Researchers have proposed that mechanical loading of teeth may temporarily or permanently cause gap formation in restorations[119] and the combination of thermal and mechanical loading may simulate intra-oral conditions more accurately.[132] However, studies have shown conflicting results on load cycling, reinforcing the need for careful evaluation and interpretation due to differences in experimental designs.[100,116,133-142] Several researchers found no effect on microleakage from load cycling of resin composite restorations.[125,133-138] However, a few authors did find an effect from load cycling[116,134,140] and a couple of investigators found an effect from a simultaneous combination of thermocycling and loading.[100,139] The type of restoration, either Class 2 or Class 5, did not appear to have any effect on the conclusions reached in these studies.[100,116,133-142] Many studies used a combination of cyclic loading while the tooth soaked in dye solution to potentially help detect transient gaps formed during the loading.[116,133,139-141] Again, this combination did not appear to have any effect with some studies showing increased microleakage[116,140]and some no increase.[133,136]

Different materials, bonding systems and types and location of load were used. Most studies used axial compressive loading to stress the restorations by using a stainless steel ball or rod that rests on the buccal and lingual inclines of the occlusal surface.[116,133,136,137] Very few studies stress the actual restorative material itself.[125,142] Two studies used oblique forces.[134,135] Jang and others loaded the buccal aspect of the

buccal cusp on teeth with class 5 restorations and found an effect of load cycling.[134] While Hakimeh and others alternated the loading of the buccal and lingual inclines of the occlusal surface and found no effect on class 5 compomer restorations.[135]

All studies used varying load levels and various cycles and cycling rates.[100,116,133-142] Some investigators oscillated cycles between a low of just a few Newtons to a maximum of 170 Newtons.[100,116,133-135,137,140] Others reported just a maximum load.[136-139] Number of cycles varied widely from a low of 1000 cycles[133] to a high of 1.2 million.[100] Cycling rate varied from a low of 1 Hertz[116,134,140] to a high of 5 Hertz.[137]

Admittedly, however, there appears to be a wide variance in the literature as to the magnitude of actual clinical masticatory forces with an estimated range of 9 to 180 Newtons.[143,144] The duration of the occlusal forces is estimated to be from 0.25 to 0.33 seconds or 3 to 4 Hertz.[145] Dietschi et al, loaded his inlay samples with a stainless steel cusp at 80 Newtons and 1.5 Hertz for 250,000 cycles and related this to approximately one year of clinical use.[146-148]

Behavior of resin composites *in vivo* is complex and is not clearly defined and is often described in terms of wear, marginal breakdown or fatigue. Fatigue is a major factor affecting the life expectancy of resin composite restorations.[149] and is due to progressive fracture under repeated loading.[18] Several mechanisms may participate in fatigue-induced damage of composite materials including matrix cracking, multidirectional cracking, and filler debonding.[150] Fatigue in resin composites largely depends on the materials properties, especially filler loading.

Higher filled hybrid resin composites deform little under function. Filler particles act to arrest or retard crack propagation through the matrix resulting in more localized

destruction. Under function, however, cracks can propagate, weaken the matrix and favor further crack growth resulting in a worn surface at the occlusal contact area.[149]

Microfilled composites with a relatively lower filler content, lower modulus of elasticity and a weaker interface between resin matrix and prepolymerized filler particles have greater fatigue sensitivity and are more prone to mechanical deformation. Initially, while under function, cracks propagate in the subsurface area. Over the first two years, while under continued stress, the matrix is weakened as the cracks begin to connect. Eventually, after four or five years, the subsurface cracks interconnect and the restoration fails catastrophically and often, surprisingly.[149]

There appears to be a need for more standardized testing procedures of fatigue to gain insight into the complex behavior of resin composite restorations.[149] Currently, specimens may be cyclically tested in tension-tension, flexure, torsion, shear, or compression.[150] Contact fatigue is used to study the wear process by cyclic loading of an indenter into the surface of the material. A study by Htang[151] and others found the existence of an optimal or critical filler level in resin composites in fatigue endurance. Resin composites with low (<60% wgt) or high filler content (>80% wgt) were significantly lower in fatigue resistance. A higher susceptibility to crack development in very highly filled composites under impact stresses is probably due to the brittle nature of filler particles with fractures occurring through the filler particles as well as the matrix.[151] The dynamic fatigue test is useful for determining crack velocity parameters.[150] Finally, with a stair-case technique, the material is cycled at a preset stress level and cycles. If the specimen fails, a lower stress is chosen, if the specimen survives, a higher stress level is used on the next specimen.[152]

OVERVIEW

The following is an overview of this project. The study is presented in three separate parts – effects of energy density on hardness and degree of conversion, effects of degree of conversion on marginal integrity and effects of degree of conversion on flexural strength and modulus.

The first part details the materials and methods, results and discussion of an initial pilot study to determine the Knoop hardness and degree of conversion at incremental levels occlusal-gingivally throughout the depth of the resin composite in a 5 millimeter long sample created from an extracted tooth template. As can be seen in the discussion of this pilot study, there were many changes in the methods that spanned the whole project. But, the final procedure that was utilized provided the necessary information to select the various energy densities needed to achieve variable degrees of gingival cure for Z250 resin composite restorations in prepared teeth for the final method in part two of the study.

The second part details the materials and methods, results and discussion of the primary objective – to determine the minimal extent of cure required by the base of the resin composite restoration that allows it to support the rest of the filling and maintain its marginal seal under thermal and mechanical stress conditions. This section was broken up into three pilots and a final method. Again, various techniques were modified before a final version was agreed upon. Please note that the energy density groups selected changed with knowledge gained concurrently in part one of the study.

The third part details the materials and methods, results and discussion of a supplementary goal of determining mechanical properties of the composite at the marginal area at various degrees of conversion. See overview chart on next page.

Overview

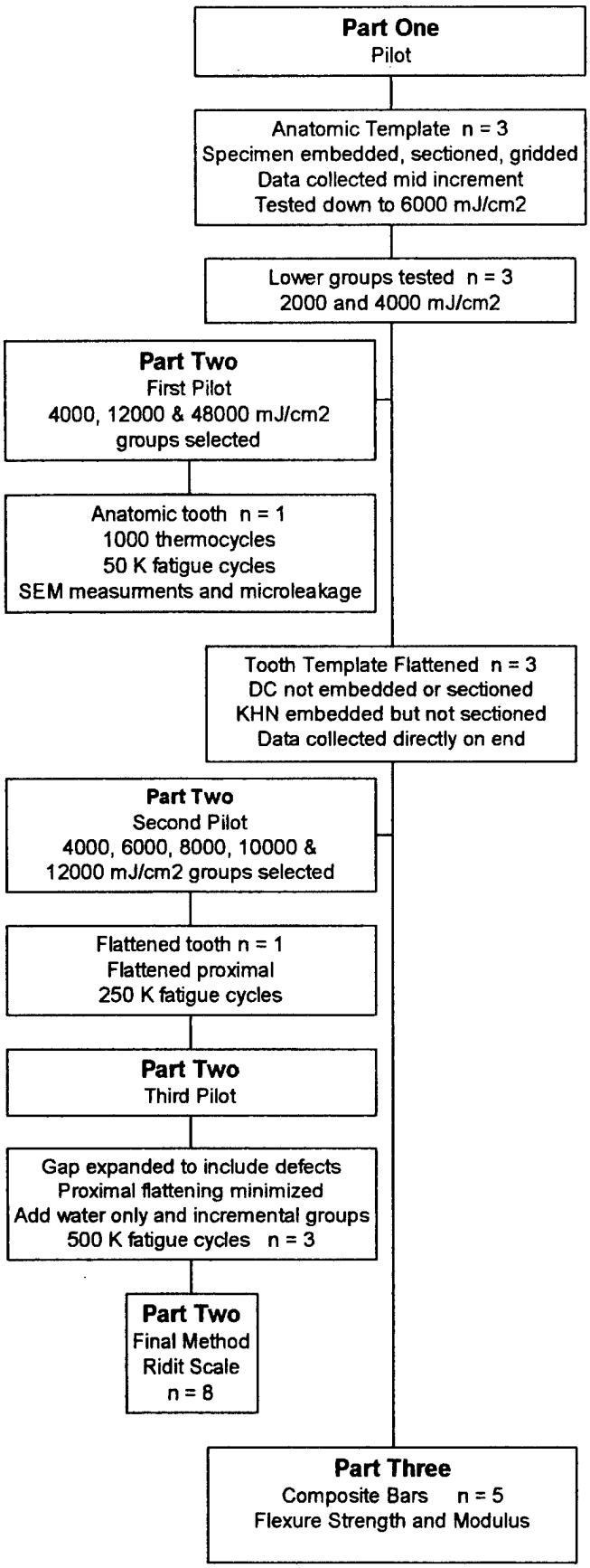
Part One
Pilot
Anatomic Template n = 3
Specimen embedded, sectioned, gridded
Data collected mid increment
Tested down to 6000 mJ/cm2
Lower groups tested n = 3
2000 and 4000 mJ/cm2
Part Two
First Pilot
4000, 12000 & 48000 mJ/cm2
groups selected
Anatomic tooth n = 1
1000 thermocycles
50 K fatigue cycles
SEM measurments and microleakage
Tooth Template Flattened n = 3
DC not embedded or sectioned
KHN embedded but not sectioned
Data collected directly on end
Part Two
Second Pilot
4000, 6000, 8000, 10000 &
12000 mJ/cm2 groups selected
Flattened tooth n = 1
Flattened proximal
250 K fatigue cycles
Part Two
Third Pilot
Gap expanded to include defects
Proximal flattening minimized
Add water only and incremental groups
500 K fatigue cycles n = 3
Part Two
Final Method
Ridit Scale
n = 8
Part Three
Composite Bars n = 5
Flexure Strength and Modulus

PART ONE

PILOT STUDY

MATERIALS AND METHODS

Effects of Energy Density on Hardness and Degree of Conversion.-- The first objective was to determine which energy densities would produce sequentially decreasing degrees of gingival cure and hardness in a 5 millimeter long resin composite restoration. One extracted human molar, stored in 0.525% NaOCl served as a reusable template. A tapered Class II slot cavity preparation (Figure 1) was created with a #57 carbide bur and high-speed handpiece with water coolant with the following dimensions: buccolingual (occlusal) – 4.5 mm; buccolingual (gingival) – 4.0 mm; mesiodistal (gingival) 1.5 mm; occlusalgingival height of 5 mm. Composite specimens were created as outlined below. The tooth was stored in 37 degree Centigrade tap water while not in use.

Figure 1: Re-usable template (anatomic)

A thin layer of Bis-GMA and TEGDMA (50% each by weight) containing no polymerization promoters was placed in the cavity preparation to act as a lubricant and to simulate the layer of dentin bonding. A metal matrix band was placed on the tooth and held in place with a hemostat. A minifill resin composite was placed in bulk (Z250, Shade A-2, 3M, St. Paul, MN) using a resin composite syringe system (CR

Figure 2: Mounting jig

Figure 3: Creation of test surface

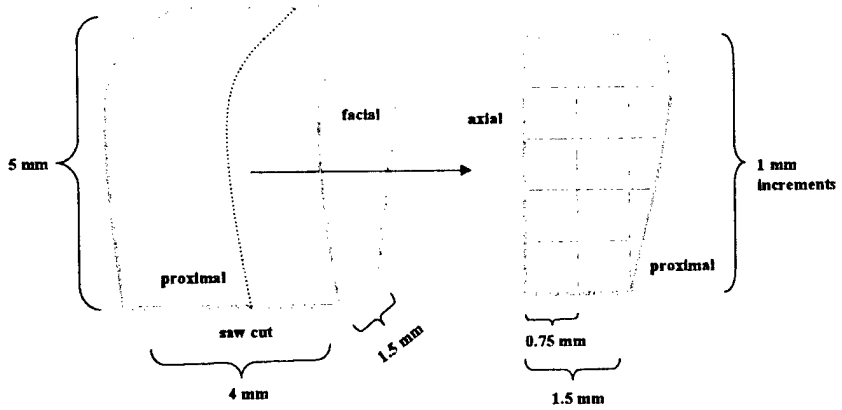

tubes, Centrix, Inc, Shelton, CT) until the preparation was full. Large condensers were used to smooth the occlusal portion. The composite was cured from the occlusal with a curing light (VIP, Bisco, Schaumburg, IL) after utilizing its internal calibration feature. The light output of the curing light was confirmed using a power meter (Power Max 5200, Molectron, Portland, OR). A 10.25 millimeter curing tip was utilized and held in place with a mounting jig (Figure 2). The light tip rested on the occlusal cusp tips and a blue ink line on the occlusal surface helped to reduce variation in angulations and position. The distance between the light guide and the composite surface was approximately 0.75 millimeters. The approximate center of the light guide was over the center of the occlusal composite surface. The power density of the curing light was 600 mW/cm^2 and the time was varied between 10 and 100 seconds (10, 20, 40, 60, 80 and 100 seconds) to produce the various levels of cure at the gingival margin. Three specimens were made per energy density. The specimens were removed from the tooth template and stored dry throughout the entire testing process in a black film canister when not handled. The same day, the specimens were suspended in acrylic rings using a wax sprue and embedded in epoxy resin (Buehler, Lake Bluff, IL) and allowed to cure overnight in a dark box container to eliminate light exposure. The next day, the specimens were sectioned using a 0.3 millimeter thick diamond saw (Isomet, Buehler, Lake Bluff, IL) under a water coolant. The lights were dimmed in the room to reduce exposure. One

saw cut was made through the specimen in the approximate center from the buccal and lingual surfaces respectfully. The test surface became the cut inner surface of the section (Figure 3) and was polished using 5 micron aluminum oxide powder (Buehler, Lake Bluff, IL) and de-ionized water on a 8 inch nylon polishing cloth (Buehler, Lake Bluff, IL) for 30 seconds.

A grid area was inscribed on the surface with a pencil to facilitate testing (Figure 4). Measurements were taken within the center of each increment at 24 hours for Knoop hardness and between 3 and 7 days for degree of conversion. The gridded specimen was tested at 2 points in the mesiodistal direction in 0.75 millimeter increments and 1 millimeter in the occlusalgingival direction for the entire length of the specimen for Knoop hardness (KHN) (Kentron Microhardness, Torsion Balance Co., Clifton, NJ) Due to the heavy time expenditure, only the occlusal and gingival increments were tested for degree of conversion (DC) using Fourier Transform Infrared Spectroscopy (FTIR) (DS20, Analect Instruments, Irvine, CA). Tiny chips of composite - 10 to 30 microns in thickness - to be placed in the FTIR were removed from the center of each increment using the tip of a razor blade after completing the Knoop hardness test. Knoop hardness values were determined using the following formula: $KHN = L / l^2 \times Cp$ where L is the load in kilograms and l is the length of the indentation in millimeters and Cp is the constant 0.007028. A 200 gram load was used with a dwell time of 10 seconds.

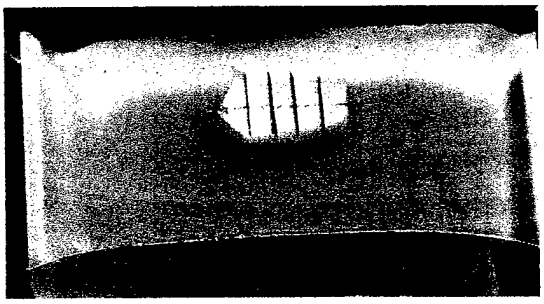

Figure 4: Gridded specimen

The degree of conversion of the Z250 resin composite was determined using FTIR analysis. The intensities of the carbon double bond (C=C) absorbance peak at 1637.3 cm^{-1} and the aromatic (C...C) reference peak at 1608.3 cm^{-1} were measured with 30 scans at a resolution of 4.0 in transmission mode. The C...C peak originates from the aromatic rings in the Bis-GMA molecule and remains unchanged during the polymerization reaction. The ratio of the absorbance intensities of C=C/C...C were compared before and after polymerization using the following equation to determine the percent of reacted carbon double bonds or degree of conversion:

1 – [Abs (C=C) / Abs (C...C)] cured resin / [Abs (C=C) / Abs (C...C)] uncured resin X 100

See Appendix under Equipment for more details on FTIR and Knoop Hardness testing.

Data Analysis. Three specimens were created for each energy density level. Three hardness and two degree of conversion values were determined per axial and proximal increment examined per specimen and a mean calculated. The percentage of maximum KHN and DC was determined for the gingival regions. A two-way analysis of variance (ANOVA) was used to test the effect of energy density or location (axial vs proximal) on Knoop hardness in the 5 millimeter increment. The same tests were done for degree of conversion. Tukey's post-hoc tests were utilized to perform *a posteriori* pair-wise comparisons to determine which groups showed a significant difference (α=0.05). SPSS software (SPSS Inc, Chicago, IL) was used and the printout is provided in the Appendix under Part One. Also, paired student t-tests were used to compare axial with proximal increments for both Knoop hardness and degree of conversion. See tables in Appendix under Part 1.

RESULTS

Effects of Energy Density on Hardness and Degree of Conversion.-- The mean of three hardness values per increment per specimen (Appendix Part 1) and the mean of two degree of conversion values per occlusal and gingival increment per specimen (Appendix Part 1) was determined and a percentage of maximum KHN and DC determined for the gingival regions. The highest value for KHN and DC was found to be 98.7 kg/mm^2 and 60.6% respectively and was therefore designated as the maximum KHN and DC. Paired t-tests revealed no significant difference between axial wall and proximal surface increments for all but a few of the paired increments found typically in the lower energy levels (Appendix, Part 1). Pooled versions of the tables combining axial with proximal values are shown below (Tables 1 and 2).

A linear regression analysis (R^2=0.95) was performed using SPSS software relating Knoop hardness with degree of conversion at the gingival increment using pooled axial and proximal average values (Figure 5). Also, Knoop hardness (R^2=0.96) or degree of conversion (R^2=0.94) was plotted versus the log of energy density (Figure 6).

Table 1: Knoop Hardness in kg/mm^2 (anatomic template) n=6 max KHN =98.7

6000 mJ/cm^2	mean	st dev
1 mm	89.4	4.8
2	86.1	5.3
3	78.5	5.7
4	70.3	4.4
5 mm	45.8	4.2
% of max	46.4	4.3

12000 mJ/cm^2	mean	st dev
1 mm	89.3	5.2
2	89.6	3.6
3	84.8	2.7
4	79.3	6.5
5 mm	64.6	9.2
% of max	65.3	9.4

24000 mJ/cm^2	mean	st dev
1 mm	90.2	5.0
2	87.6	5.5
3	85.8	6.1
4	79.2	8.3
5 mm	70.6	11.3
% of max	71.5	11.6

36000 mJ/cm^2	mean	st dev
1 mm	90.2	4.6
2	89.9	3.8
3	90.8	4.7
4	85.7	4.2
5 mm	76.4	12.0
% of max	77.3	12.1

48000 mJ/cm^2	mean	st dev
1 mm	91.6	2.4
2	91.7	3.1
3	90.3	4.2
4	83.9	5.3
5 mm	80.0	6.0
% of max	80.9	6.1

60000 mJ/cm^2	mean	st dev
1 mm	90.8	2.3
2	90.7	4.5
3	92.5	5.4
4	92.5	6.2
5 mm	88.7	2.3
% of max	89.8	2.3

Table 2: Degree of conversion in % (anatomic template) n=6 max DC = 60.6

6000 mJ/cm²	mean	st dev
1 mm	53.7	2.7
2		
3		
4		
5 mm	40.0	2.2
% of max	66.0	3.6

12000 mJ/cm²	mean	st dev
1 mm	56.1	2.4
2		
3		
4		
5 mm	47.2	3.0
% of max	77.9	4.9

24000 mJ/cm²	mean	st dev
1 mm	57.3	2.2
2		
3		
4		
5 mm	49.2	3.3
% of max	81.2	5.5

36000 mJ/cm²	mean	st dev
1 mm	57.5	2.5
2		
3		
4		
5 mm	50.0	4.6
% of max	82.6	7.6

48000 mJ/cm²	mean	st dev
1 mm	58.0	2.4
2		
3		
4		
5 mm	54.6	1.5
% of max	90.2	2.5

60000 mJ/cm²	mean	st dev
1 mm	58.9	1.9
2		
3		
4		
5 mm	54.7	1.1
% of max	90.3	1.9

Figure 5: Knoop Hardness vs degree of conversion at the gingival increment

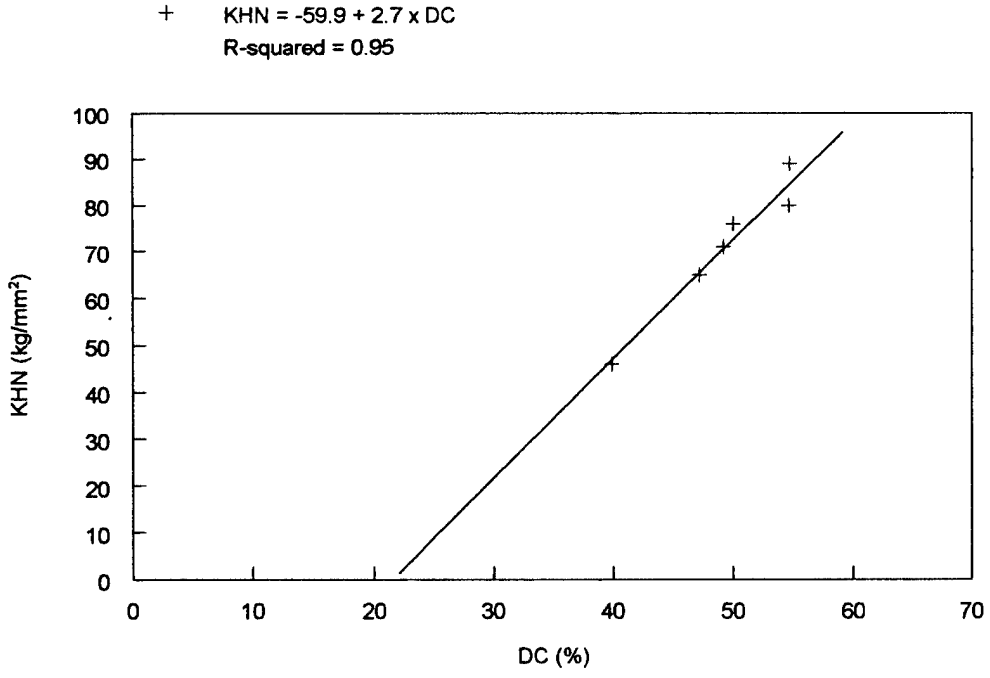

Figure 6: Knoop Hardness or degree of conversion vs log energy density at the gingival increment

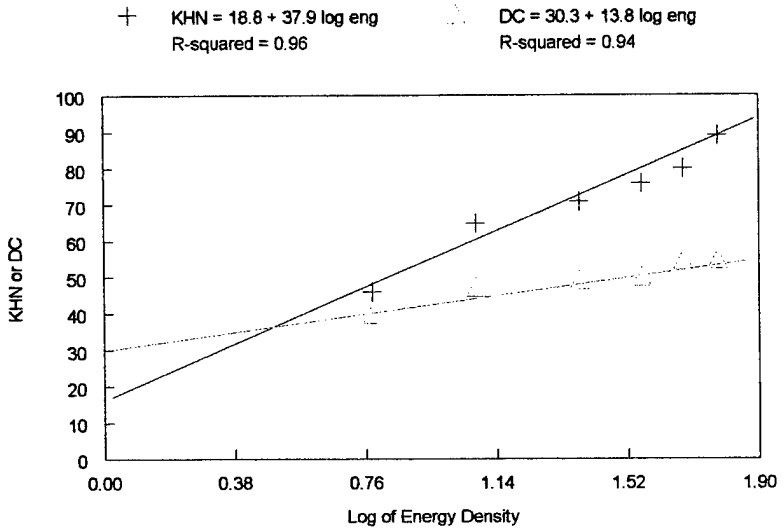

A percentage of maximum Knoop hardness and degree of conversion were determined for the gingival increments. A two-way analysis of variance (ANOVA) was completed (Appendix, Part 1) using non-pooled axial and proximal average values (n=6) to test the effect of energy density or location (axial vs proximal) on Knoop hardness in the 5 millimeter increment. The same tests were done for degree of conversion. Significant differences in Knoop hardness and degree of conversion were found based on energy levels using a two-way ANOVA and Tukey's post hoc tests. (α=0.05). The percentages of maximum Knoop hardness and degree of conversion of the pooled gingival increment is shown below in Table 3. Letters (a-d) denote significant differences across rows. At least 36000 mJ/cm^2 was necessary to produce maximum gingival degree of conversion and Knoop hardness in a 5 millimeter deep restoration of Z250 resin composite.

Table 3: Percentages of maximum KHN and DC at the gingival increment for various energy densities n=6/group

a - d denotes significant differences across rows

	6000 mJ/cm^2	12000 mJ/cm^2	24000 mJ/cm^2	36000 mJ/cm^2	48000 mJ/cm^2	60000 mJ/cm^2
KHN	46.4 % a	65.3 % b	71.5 % b,c	77.3 % b,c,d	81.0 % c,d	89.8 % d
DC	66.0 % a	77.9 % b	81.2 % b	82.7 % b,c	90.2 % c	90.3 % c

DISCUSSION

Effects of Energy Density on Hardness and Degree of Conversion.-- Although the two-way ANOVA showed no significant difference overall between axial wall and proximal surface increments at the 5 millimeter level, the individual paired T-tests did show a few differences at lower energy levels (Tables in Appendix under Part One). This variation could be due to the orientation of the light guide and the effect of tooth or band shadowing.

Regression analysis (Figure 5) revealed a significant correlation when relating Knoop hardness and degree of conversion ($R^2 = 0.95$). This agrees with Ferracane who found a similar relationship during the setting reaction of three unfilled dental resins.[54] However, the attainment of hardness relative to maximum hardness fell behind the degree of conversion of the carbon double bonds (Tables 1 and 2). This is possibly due to the late formation of networking links in the polymer chains. A greater increase in hardness relative to maximum hardness occurred with higher energy levels and subsequent increases in crosslinking.[54] Lag of hardness behind degree of conversion could also be due to the overestimation of percent cure at lower energy levels. The "overestimation" may be due to the sectioning and polishing that might cause a loss of free monomer.

Knoop hardness ($R^2= 0.96$) or degree of conversion ($R^2 = 0.94$) at the gingival increment had a strong linear relationship to the log of the energy density. However, the KHN and DC values fell dramatically at the gingival increment below a threshold level of approximately 12000 mJ/cm^2.

The first objective was to determine which energy densities would produce sequentially decreasing degrees of gingival cure and hardness. However, having

examined the results of this first objective, it became obvious that the minimum energy density in the gingival increment had not been determined. Two new energy density groups were created lower than the 6000 mJ/cm^2. A 2000 mJ/cm^2 group (200mW/cm^2 x 10 secs) and a 4000 mJ/cm^2 (400mW/cm^2 x 10 secs) group were tested for hardness and degree of conversion. Three specimens were created for each energy density level. Three hardness and two degree of conversion values were determined per axial and proximal increment examined per specimen and a mean calculated (Tables in Appendix, Part 1). The percentage of maximum KHN and DC was determined for the gingival regions. A summarized version of each table is shown below in Table 4.

Table 4: Knoop Hardness and degree of conversion (new groups)
n=6 max KHN = 98.7 max DC = 60.6

KHN (kg/mm^2)

2000 mJ/cm^2	mean	st dev
1 mm	78.2	10.3
2	83.0	8.8
3	71.1	10.4
4	47.3	8.3
5 mm	16.7	3.8
% of max	17.0	3.8

4000 mJ/cm^2	mean	st dev
1 mm	86.4	5.2
2	79.7	3.6
3	72.0	2.7
4	65.2	6.5
5 mm	43.5	9.2
% of max	44.0	7.9

DC (%)

2000 mJ/cm^2	mean	st dev
1 mm	52.7	4.6
2		
3		
4		
5 mm	27.9	12.0
% of max	46.0	8.5

4000 mJ/cm^2	mean	st dev
1 mm	54.0	2.4
2		
3		
4		
5 mm	36.1	6.0
% of max	59.1	6.0

Table 5: Selected groups for Part 2, 1st Pilot, based on max KHN or DC of gingival increment

% Gingival KHN/DC of max	Energy density (mJ/cm^2)	Power x time (mW/cm^2 x secs)
45/60	4000	400 x 10
65/80	12000	600 x 20
80/90	48000	600 x 80

The Knoop hardness of the gingival increment of the 2000 mJ/cm^2 group was undeterminable and soft to touch in one specimen and near the limits of the filar scale in the other two. Therefore, 4000 mJ/cm^2 was chosen as the lowest energy density. Table 5 shows the selected groups to be used in the first pilot of the second part of the study (Part 2) based on percent of maximum Knoop hardness or degree of conversion of the gingival increment.

Inspection of the initial data (Tables in Appendix under Part 1) raised certain questions concerning the possible inflation of the Knoop hardness and degree of conversion numbers. Various efforts were undertaken to review existing data and to implement improvements before further testing.

First, it became apparent that the variability in length and occlusal shape created from preparing an anatomic tooth could result in extreme inconsistency in degree of conversion in the gingival areas of the restoration, especially at the lower energy densities. A solution was to flatten the occlusal table to provide a uniform 5 millimeter depth and shape to the preparations of the teeth. Also, as noted earlier, variation between individual values in the axial/proximal regions, particularly for low energy conditions, suggested that the curing conditions were variable – possibly due to angulations of the

light guide or differences in surface reflectance. Flattening the tooth surface was expected to reduce the potential for light guide angulations.

Second, since the data collected per increment was only representative of the middle third of the increment, it did not represent the true values at the apical portions of that increment. At lower energy densities it became apparent that the Knoop hardness and degree of conversion values could decrease dramatically in the apical half millimeter in the gingival increment. Knowing the true conversion value of the absolute gingival marginal level would become critical in Part 2 of this study.

Third, concerns were raised over the possibility of heat generation causing an increase in conversion from embedding the specimens in epoxy prior to FTIR evaluation and possible leaching of monomer from sectioning and polishing. Therefore, a new set of removable specimens was evaluated based on a flattened tooth template (Figure 7). A total of three specimens were created per group. These 5 millimeter long specimens were not sectioned, polished or embedded in epoxy, but were evaluated directly on the gingival and occlusal edges after lightly sanding away 0.1 millimeters to remove any unfilled resin and air inhibited layer. Testing was conducted 24 hours after dry storage at room temperature in a black film canister. Tiny chips of composite to be placed in the FTIR were removed from the occlusal or gingival area of the specimen in a darkened room. The average of three degree of conversion (DC) values per specimen was determined. Table 6 lists the occlusal and gingival degrees of conversion for the various energy densities. The percentage of maximum DC was

Figure 7: Flattened template

determined at 5 millimeters. A analysis of variance (ANOVA) was used to test the effect of energy density on DC at the gingival margin. SPSS software was used and the results are shown in the table and the printout is provided in the Appendix under Part 1.

Table 6: Occlusal and gingival degrees of conversion with percentage of maximum DC (58.2) of gingival increment using flattened template. (a – e denotes significant differences) n = 3

mJ/cm^2	occ DC	st dev	ging DC	st dev	% max
4000	54.1	1.0	14.3	5.1	24.5 a
6000	53.4	1.9	26.2	4.4	44.9 b
8000	55	1.2	33.4	0.2	57.3 b,c
12000	55.2	1.9	39.4	2.3	67.6 c,d
24000	56.2	1.9	46.5	0.9	80 d
Control 72000	57.4	0.7	56.4	1.6	97 e

It became apparent that a significant descending gradient of degree of conversion values was seen below the 12000 mJ/cm^2 level at the gingival margin providing greater opportunity to evaluate even more levels of conversion, especially in the critical lower levels. Therefore recommended groups for the second part of the study would eventually expand to include 4000, 6000, 8000, 10000, 12000 and 72000 (control) mJ/cm^2.

Finally, the Knoop hardness indenter utilized in this study displayed variability between operators and possibly overestimated actual Knoop hardness when evaluating resin composites. The poor contrast between the indentation and surrounding resin matrix may have provided a hindrance to reproducing filar length determinations. To reduce the potential for altering the hardness values in the poorly converted portions of

the specimens, a high level of polish was not attempted. A simple study found that Knoop hardness values varied a plus or minus 10 – 20 % between operators reading the same indentation. See Appendix under Part 1 for details. Care should be taken to use the same operator throughout the testing process to preserve the relative significance of the numbers between groups. The same study found a potential overestimation of Knoop hardness values by an average of 14. The ability to read the indentation may be enhanced by covering the composite test surface with graphite prior to testing to greatly increase contrast. Overall, the use of graphite appeared to increase the ability to read the actual lengths of the indentations and reduce the variability between operators and even within the same operator.

A new set of removable specimens was evaluated for Knoop hardness based on the same flattened tooth template (Figure 8). A total of three specimens were created per group. These 5 millimeter long specimens were mounted vertically in a square acrylic tube with epoxy resin with the occlusal and gingival portions exposed. These specimens were not sectioned, but evaluated directly on the gingival and occlusal edges after gently sanding away 0.1 millimeters to remove any unfilled resin and the air inhibited layer with 600 grit sand paper and polishing with 5 micron aluminum oxide paste for 30 seconds on a 8 inch nylon wheel. Testing was conducted 24 hours after dry storage at room temperature in a black film canister. Graphite from a mechanical pencil was rubbed on the lightly polished surface of the composite specimens before indentation. The average of three

Figure 8: Vertically mounted specimens for KHN testing

Knoop hardness values per occlusal or gingival surface was determined. The following table lists the occlusal and gingival Knoop hardness values for selected 5 millimeter specimens. The percentage of maximum KHN was determined at 5 millimeters. A one-way analysis of variance (ANOVA) was used to test the effect of energy density on KHN at the gingival margin. SPSS software was used and the results are shown in Table 7 and the printout is provided in the Appendix (Part 1).

Table 7: Occlusal and gingival Knoop Hardness with percentage of maximum KHN (72.7 kg/mm^2) of gingival increment using flattened template
(a – f denotes significant differences) n = 3

mJ/cm^2	occ KHN	st dev	ging KHN	st dev	% of max
4000	69.3	2.3	2.1	3.6	2.8 a
6000	69.9	2.3	16.4	0.8	22.6 b
8000	69.1	3.1	28.5	4.5	39.2 c
12000	68	2.1	39.3	0.3	54.1 d
24000	68.8	1.7	52.9	0.3	72.8 e
Control 72000	71.7	1.1	70.2	1.2	96.5 f

A linear regression analysis (R^2 = 0.99) was performed using SPSS software relating Knoop hardness with degree of conversion at 5 millimeters (Figure 9 (l)). The lowest data point, representing 4000 mJ/cm^2 had a high standard deviation and was dropped from the analysis to obtain a better fit (R^2 = 1.0; Figure 9 (r)).

Also, Knoop hardness (R^2 = 0.96) or degree of conversion (R^2 = 0.93) was plotted versus the log of energy density (Figure 10). A more linear fit was seen in the lower energy densities. If the curve was extended to include higher energy densities, the curve would plateau and an exponential equation would be more appropriate.

Figure 9: Knoop Hardness vs degree of conversion (flattened template) at the gingival increment [(l) all data points; (r) dropped data point]

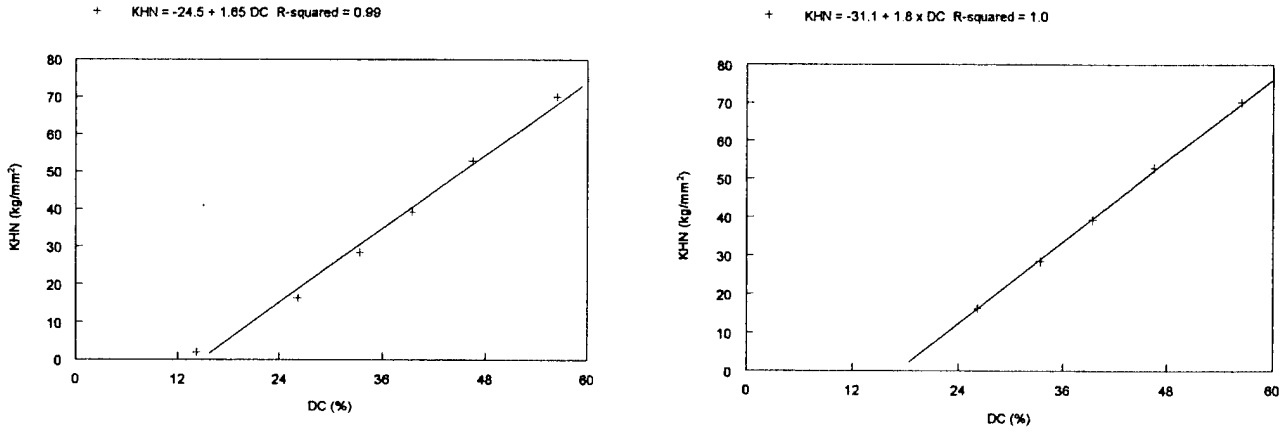

Figure 10: Knoop Hardness or degree of conversion vs log energy density (flattened template) at the gingival increment

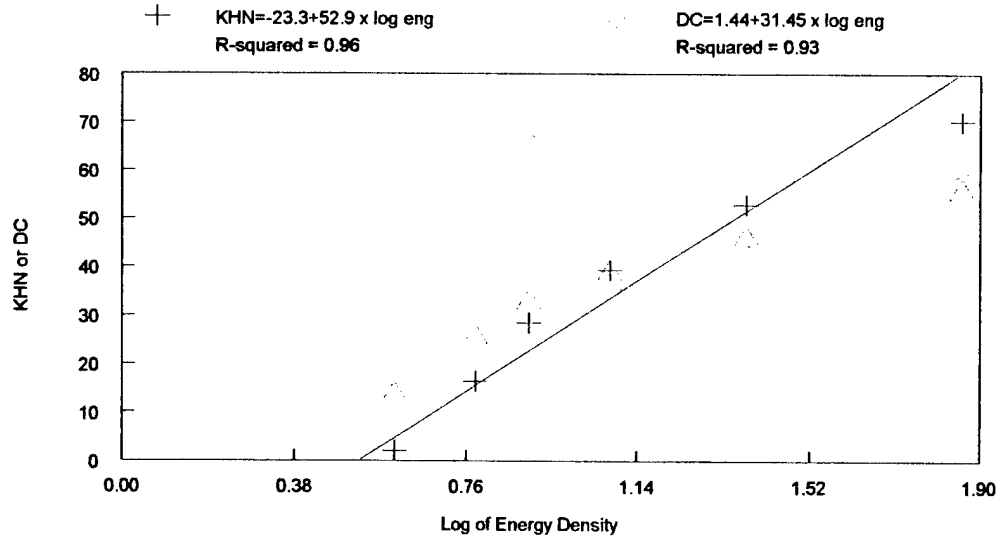

PART TWO

MATERIALS AND METHODS

Effects of Degree of Conversion on Marginal Integrity.-- First Pilot

The first objective was to determine which energy densities would produce sequentially decreasing degrees of gingival cure and hardness. Next, selected energy densities from this data were used to bond resin composite specimens in prepared teeth to find the minimal extent of cure required by the base of the resin composite restoration that allowed it to support the rest of the filling and maintain its marginal seal under thermal and mechanical stress conditions.

Extracted human molars originally stored in 0.525% NaOCl were mounted in acrylic rings (14 mm x 22 mm) with epoxy resin (Buehler, Lake Bluff, IL). A Class II slot cavity preparation was created with a #57 carbide bur and high-speed handpiece with water coolant with the following dimensions: buccolingual (occlusal) – 4.5 mm; buccolingual (gingival) – 4.0 mm; mesiodistal (gingival) 1.5 mm; the gingival margin placed 0.5 mm into dentin. A 0.5 millimeter bevel was placed on the buccal and lingual margins. The teeth were stored in 37 degree C tap water while not in use.

A metal matrix band was placed on the tooth and held in place with a hemostat. The preparation was acid-etched for 15 seconds with 35% phosphoric acid, gently rinsed for 15 seconds with water from a three-way syringe, and lightly dried leaving the dentin moist. Two consecutive thin layers of Single Bond bonding agent (3M, St. Paul, MN) was placed in the cavity, gently thinned for 5 seconds and light cured for 10 seconds at 600 mW/cm^2 after internally calibrating as before (VIP, Bisco, Schaumburg, IL). A minifill composite resin was placed in bulk (Z250, Shade A-2, 3M, St. Paul, MN) using a

composite resin syringe system (CR tubes, Centrix, Inc, Shelton, CT) until the preparation was full. Large condensers were used to smooth the occlusal portion. The composite was cured from the occlusal with a VIP curing light. The light output of the curing light was assessed using a power meter (Power Max 5200, Molectron, Portland, OR). A 10.25 mm curing tip was utilized and held in place with a mounting jig. The cusp tips were flattened very slightly using a belt sander (Surfmet I, Buehler, Lake Bluff, IL) to provide a uniform distance of 0.75 millimeters from the light tip to the occlusal surface of the resin composite restoration. Various energy densities were selected based on the results of the first part of study detailed earlier for profiling the degree of conversion and Knoop hardness at the 5mm gingival levels. See Table 5.

Completed specimens were finished immediately with polishing discs (Soflex, 3M, St. Paul, MN), photographed with 2x magnification (Elite Chrome, Kodak, Rochester, NY), impressed with polyvinylsiloxane impression material (Express, 3M, St. Paul, MN), and then stored in 37 degree Centigrade water for 24 hours. The specimens received 1000 thermocycles with a 30 second dwell time at 5 to 55 degrees Centigrade in a custom-made thermocycler. After thermocycling, the specimens were photographed and impressed.

Next, the specimens were stressed in a custom-made OHSU mechanical fatigue-cycling machine. See Appendix under Equipment for more details. A 2 millimeter stainless steel ball was cemented onto the occlusal surface of the restoration with a chemically-curing resin cement. (C&B Cement, Bisco, Schaumburg, IL). The specimens (Figure 11)

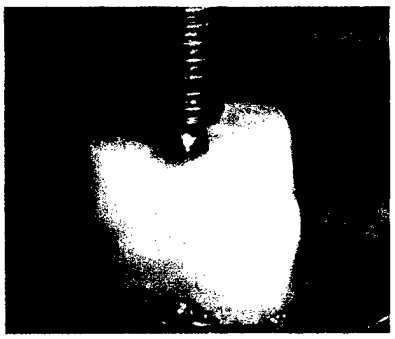

Figure 11: Fatigue cycler

were then placed in the fatigue-cycler and stressed with a stainless steel bolt contacting the ball for 50,000 cycles under a cyclic load of 18 to 85 Newtons at 1.25 Hertz and verified using a Material Testing System machine (MTS Systems Corp, Eden Prairie, MN) by placing the load cell in the fatigue-cycler and loading with the stainless steel bolt. The specimens were constantly bathed in re-circulated 37 degree Centigrade water. After 50,000 cycles the specimens were removed from the fatigue machine and photographed and impressed as before. The estimated range of actual clinical masticatory forces range from 9 to 180 Newtons at 3 to 4 Hertz.[143-145] Two hundred fifty thousand cycles has been related to approximately one year of clinical use.[146-148]

Replicas of the specimens were created using epoxy resin (Buehler, Lake Bluff, IL). The replicas were mounted on aluminum stubs, sputter-coated with 50 nanometers of gold-palladium (Hummer VII, Anatech Ltd, Alexandria, VA) and the gingival margin was examined and quantified by Scanning Electron Microscopy (SEM) (JXA-6000, JEOL, Tokyo, Japan). Examination of the marginal breakdown took place for each specimen at the pre-operative, post-thermal, and 50,000 cycle steps. Quantitation consisted of 25 equally-spaced measurements of the width of the gingival defect along the entire length of the four millimeter gingival margin. A percentage of the margin deemed defective was determined by dividing the number of the 25 locations with defects by 25 and expressed as percentage. Polaroid (T-52, Cambridge, MA) photographs at 14x magnification were taken of restorations and representative photographs were taken at 1000x magnification of select marginal defect areas. See Appendix under Equipment for more SEM details.

Marginal leakage of each specimen was determined with silver nitrate dye penetration (J.T. Baker, Palmyra, N.J) after completion of the fatigue cycling. New preparations and composite restorations were created with identical energy densities as the fatigue specimens. They were polished, left in 37 degree Centigrade water as before, but served only as pre-operative, non-fatigue specimens for marginal leakage examination.

The staining technique was the same as that used in previous studies.[10] All tooth surfaces were covered with two coats of fingernail polish to within 1.0 mm of the tooth-restoration margin. The occlusal surface of resin composite restoration was also covered with nail polish because of the concern for enhanced microleakage from the occlusal margins due to the reduction of the occlusal surface pre-operatively and the subsequent reduction in circumscribing enamel. The specimens were immersed in 3 moles per liter silver nitrate for 24 hours in a dark drawer. They were then removed, rinsed with de-ionized water, and placed in film developer (Eastman Kodak, Rochester, NY) under fluorescent lights for 24 hours. On removal from the developer, the teeth were rinsed in de-ionized water, embedded in epoxy resin (Buehler, Lake Bluff, IL) and allowed to set overnight. Three mesiodistal sections were made through the restorations using a 0.3 millimeter thick diamond saw (Isomet, Buehler, Lake Bluff, IL) in order to assess marginal leakage along the entire length of the preparation interface.

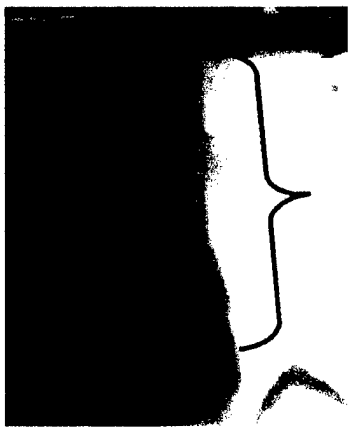

Length of Stain/
Length of preparation x 100%

Figure 12: Cross-section of restoration after silver nitrate stain

Leakage scores were assessed on the six resultant surfaces using IP Lab software (Scanalytics, Fairfax, VA) and the extent of the dye penetration was expressed as a percentage of the entire cross-sectional length of the preparation interface. See Figure 12. The most severe dye penetration of the six surfaces was used as the score representing that specimen.

RESULTS / DISCUSSION

Effects of Degree of Conversion on Marginal Integrity.-- First Pilot

The first pilot study used the results of the initial data evaluating the effects of energy density on hardness and degree of conversion as seen in Table 1 and 2. The initial groups selected were summarized in Table 5 earlier. Only one sample from each group was created for an "n" of 1. Photos of the restorations, SEMs and gap width data per energy group can be seen in Appendix under Part 2, First Pilot. Several problems were encountered and identified during this initial pilot study.

First, as stated earlier, the variability in length and occlusal shape created from preparing an anatomic tooth could result in extreme inconsistency in gap formation in the gingival margin of the restoration, especially at the lower energy densities. Therefore, the occlusal table was flattened to provide a uniform 5 millimeter depth and shape to the preparations of the teeth. A folded piece of electrical tape 0.75 mm in thickness, placed on the occlusal surface opposite the preparation, would serve as a spacer to provide consistent light curing distance.

Second, it was noted that the gingival margin was difficult to polish to the exact margin without leaving slight overhangs of resin, especially at higher energy densities. Therefore, the proximal area was flattened slightly to provide better access to polishing.

Third, it was obvious that the 4000 mJ/cm^2 group had significant degradation in the gingival marginal area. However, as stated earlier, the original hardness and degree of conversion testing only evaluated the middle third of each increment. Therefore, a new set of removable specimens was created from a flattened tooth template to determine the degree of conversion directly from the apical portion of the specimen. It then became

apparent that a significant descending gradient of degree of conversion values was seen at the gingival margin below the 12000 mJ/cm^2 level, providing an opportunity to evaluate even more levels of conversion (Table 6).

Fourth, a higher number of cycles on the mechanical fatigue cycling machine was used to see if greater differences could be discerned in the gingival margin, especially at higher energy densities. Mechanical cycling was increased to 250,000 from 50,000 cycles.

Second Pilot.-- Photos of the restorations, SEMs and gap width data per energy group can be seen in the Appendix under Part 2, Second Pilot. Only one sample from each group was produced for an "n" of 1. Several problems were encountered and identified during this second pilot study.

First, the definition of "gap width" needed to be expanded to include defective marginal areas instead of areas that had a true space or gap. This allowed a better assessment of all marginal areas, especially in the 4000 mJ/cm^2 group, which had an obvious loss of resin composite but still maintained relatively small "gaps".

Second, it was felt that the amount of proximal flattening to facilitate polishing was too severe. This could compromise the effect of enamel bonding, especially as the gingival margin was approached. Future groups would include subtle flattening only in the immediate gingival margin area.

Third, it was recommended to include two control groups. One group would be at 4000 mJ/cm^2 without any thermal or mechanical cycling to see the effects of water storage only on the marginal defects. The second control group would be more

traditional with 2 millimeter incremental placement of the resin composite and 40 seconds at 600 mW/cm^2 irradiance per increment. The first increment would only be 1 millimeter in thickness.

Fourth, a higher number of cycles on the mechanical fatigue cycling machine was attempted to see if greater differences could be discerned in the gingival margin, especially at higher energy densities. Maximum mechanical cycling was increased to 500,000, with specimens also evaluated after 100,000. In addition, specimens were created after 300,000 cycles, to be evaluated if necessary.

Third Pilot.— Representative photos of the restorations, SEMs and all of the defect width and percent defective data can be seen in the Appendix under Part 2, Third Pilot. Three specimens from each group were produced for an "n" of 3. A summarized version of the data can be seen in Table 8.

Table 8: Defect widths & percent defective margin n = 3 (width in microns)

	Pre-op			Post-Thermal			100K			500K		
	width	st dev	% def	width	st dev	% def	width	st dev	% def	width	st dev	% def
4000-W mJ/cm2	230.7	345.5	58.5	229.2	342.3	60.3	228.5	342.9	58.3	229.5	343.1	59.0
4000 mJ/cm2	466.1	247.5	100.0	474.0	246.3	100.0	479.5	248.6	100.0	488.4	245.9	100.0
6000 mJ/cm2	5.9	5.9	15.7	11.0	1.5	71.0	11.6	3.3	70.7	13.2	7.0	74.0
8000 mJ/cm2	11.8	5.0	36.7	25.1	8.6	97.0	22.2	14.0	61.0	25.2	7.6	82.3
10000 mJ/cm2	20.6	16.7	40.0	26.5	12.8	93.7	27.6	10.7	94.3	27.3	10.1	83.3
12000 mJ/cm2	26.9	3.0	88.7	30.5	4.0	100.0	26.0	5.0	98.3	24.0	12.3	84.7
24000 mJ/cm2	13.8	5.1	63.7	20.3	3.7	80.7	18.5	1.7	77.0	17.1	1.6	78.7
Control	3.4	5.3	7.8	8.0	9.1	81.3	6.3	7.0	57.3	5.5	6.0	60.3

4000-W mJ/cm^2 specimens placed in water only for equivalent time of stressed groups

A couple of problems were encountered and identified during this third pilot study. It became apparent after analyzing the data that the defect widths did not fully represent the true nature of the defects, especially in the 4000 mJ/cm^2 groups. The current technique of measuring defect width using the SEM could not account for the increase in depth of the defect. This became more significant as greater amounts of cycling or time occurred. Therefore, it was determined that the gingival margins be assessed by visual rating of the sputter-coated epoxy replicas by three examiners at 50X magnification (SMX-10, Nikon, Oak Ridge, TN). A ridit scale from 1 to 11 was created using techniques modeled after Mahler, et.al.[153] See scale in Appendix under Part 2, Final Method. This scale uses a numbered scale of restoration images that exhibit progressively increasing degrees of marginal defects. The procedure involves assigning to the restoration being evaluated, the number of the scale image to which it is most similar with respect to the extent of marginal defect. The data may be analyzed using parametric or non-parametric statistical methods. The defect and ridit data is provided in Table 9.

The tooth specimens outlining the ridit scale were available in the form of sputter-coated epoxy replicas to view at 50X magnification. The evaluators were calibrated with several practice specimens and were encouraged to rate a specimen overall with a score that may reflect a mental averaging of a combination of scores within the same specimen. For example, one half of the gingival margin could rate a "2" on the scale and the other half could rate a "6" to give a final score of "4" for that specimen. The specimens were rated blindly and randomly, with the examiners unaware of the specimen type. Any scoring discrepancy of greater than "2" between the evaluators was reassessed and the

evaluators were allowed to change their score, if desired.

Table 9: Defect widths and ridit scores n = 3 (width in microns)

	DC at 5mm	Pre-op				Post-Thermal				100K				500K			
Energy Density	% of max	width	st dev	ridit	st dev	width	st dev	ridit	st dev	width	st dev	ridit	st dev	width	st dev	ridit	st dev
4000-W mJ/cm2	20	340.7	345.5	4.8	2.3	329.2	342.3	5.3	2.6	328.9	342.9	5.9	3.1	329.5	343.1	6.4	3.3
4000 mJ/cm2	20	466.1	247.5	7.4	0.8	474.0	246.3	8.1	0.2	479.5	248.6	9.1	0.5	488.4	245.9	10.3	1.2
6000 mJ/cm2	45	5.9	5.9	2.2	1.3	11.0	1.5	2.7	1.6	11.6	3.3	2.1	1.0	13.2	7.0	2.6	1.1
8000 mJ/cm2	58	11.8	5.0	2.2	0.6	25.1	8.6	3.8	1.6	22.2	14.0	3.3	3.3	25.2	7.6	3.7	1.7
10000 mJ/cm2	68	20.6	16.7	3.7	2.3	26.5	12.8	4.1	1.8	27.6	10.7	4.2	1.5	27.3	10.1	4.1	1.8
12000 mJ/cm2	71	26.9	3.0	3.7	0.8	30.5	4.0	4.3	1.2	26.0	5.0	4.0	1.4	24.0	12.3	3.6	1.3
24000 mJ/cm2	84	13.8	5.1	2.9	0.2	20.3	3.7	3.0	0.7	18.5	1.7	3.2	0.2	17.1	1.6	3.4	1.0
Control (24000x3)	98	3.4	5.3	2.2	1.8	8.0	9.1	2.3	1.8	6.3	7.0	2.3	1.7	5.5	6.0	2.3	1.8

4000-W mJ/cm^2 specimens placed in water only for equivalent time of stressed groups

Figure 13: Width vs ridit

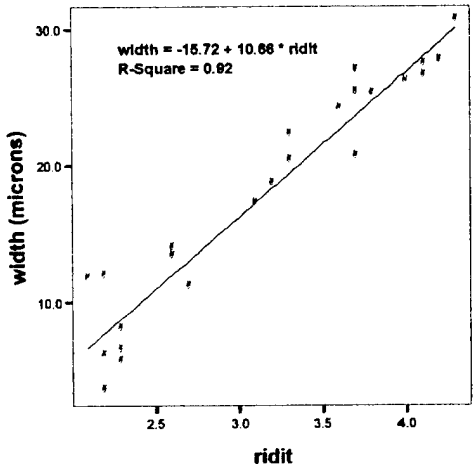

A linear regression analysis was performed using SPSS software relating defect width with ridit scores. When the 4000 mJ/cm^2 groups were left out because of the obvious lack of relationship between width and ridit scores, the correlation has an R^2 of 0.92. See figure 13. Including the 4000 mJ/cm^2 groups gives a correlation with an R^2 of 0.89 (not shown).

Final Method.-- As expected, there is a high standard deviation in many of the groups and especially the 4000 mJ/cm^2 groups (both water only and fatigued) in both the defect analysis and microleakage study. Therefore, the number of specimens was increased to 8 per group and a ridit analysis only was conducted with 3 evaluators. The results are summarized in table 10. The raw data of the 3 evaluators is provided in the Appendix under Part 2, Final Method.

A paired t-test was completed comparing the pre-operative margins with the margins cycled 500,000 times. A significant degradation was found only in the 4000 mJ/cm^2 groups ($p < 0.05$). However, since the degradation was seen both in the water-

Table 10: Ridit analysis n=8 3 evaluators

	KHN at 5mm		DC at 5mm		Pre op		Post thrmal		100K		500K		t-test	
Energy Density	% max	st dv	% max	st dv	ridit	st dv	ridit	st dv	ridit	st dv	ridit	st dv	pre-500K	
4000-W mJ/cm^2	[illegible]	3.6	[illegible]	5.1	4.0	1.9	4.5	2.0	5.6	2.0	6.3	2.4	0.002	c
4000 mJ/cm^2	2.8 a	3.6	24.5 a	5.1	4.7	2.7	4.8	3.0	5.4	3.2	6.0	3.8	0.035	c
6000 mJ/cm^2	22.6 b	0.8	45 b	4.4	2.5	1.2	2.9	1.2	2.7	1.0	2.8	1.3	0.402	a
8000 mJ/cm^2	39.2 c	4.5	57.3 b,c	0.2	3.3	1.4	4.3	0.8	4.2	1.1	4.2	1.0	0.113	b,c
12000 mJ/cm^2	54.1 d	0.3	67.6 c,d	2.3	3.9	0.9	4.1	1.4	4.0	0.9	4.1	0.8	0.407	b,c
24000 mJ/cm^2	72.8 e	0.3	80 d	0.9	3.0	0.6	3.3	0.6	3.3	0.5	3.2	0.6	0.516	a,b
Control (24000x3)	96.5 f	1.2	97 e	1.6	2.4	1.2	2.2	0.8	2.3	0.9	2.3	0.8	0.487	a

a – f denotes significant differences in columns

4000-W mJ/cm^2 specimens placed in water only for equivalent time of stressed groups

only and the stressed groups, it can be concluded that the water was primarily responsible for the degradation and not the thermal-mechanical stressing.

A two-way analysis of variance (ANOVA) was completed with SPSS software to test the effect of energy density or thermal-mechanical stressing on gingival marginal defects (ridit scores). See printout in Appendix under Part 2, Final Method. Significant

differences in the ridit scores were found based on energy levels. Tukey's post hoc test was used to determine differences between individual groups ($\alpha = 0.05$; Table 10). No overall significant difference was seen based on stressing ($p = 0.167$). Differences were seen based on energy density ($p = 0.0001$). There were no significant differences between the incrementally-filled control group, and the bulk-filled 24000 and 6000 mJ/cm^2 groups.

The results of the microleakage study are summarized in Table 11. The raw data and photos of all of the sectioned specimens used for scoring are shown in the Appendix under Part 2, Final Method. An unpaired t-test was completed comparing microleakage of pre-operative with post-operative margins (1000 thermal-cycles and 500,000 fatigue-cycles). No significant difference was seen between these two comparisons at any energy density. The microleakage scores of the groups had an overall normal distribution ($p > 0.05$). See SPSS printouts in Appendix under Part 2, Final Method. A two-way analysis of variance (ANOVA) was completed to test the effect of energy density or thermal-mechanical stressing on microleakage. No overall significant difference was seen based on stressing or energy level ($p = 0.167$ & 0.212). A one-way analysis of variance (ANOVA) was used to test the effect of energy density on microleakage pre-operatively and also post-operatively. No significant differences were found. SPSS software was used and the results are shown in Table 11. See printouts in Appendix under Part 2, Final Method.

Table 11: Microleakage scores: percent of cross-sectional length of preparation interface n = 8

Energy Density	Avg Pre	st dv	Avg Post	st dv	Unpaired t-test	Two way anova
4000-W mJ/cm^2	53 a	31	52 a	21	0.96	a
4000 mJ/cm^2	53 a	31	56 a	27	0.86	a
6000 mJ/cm^2	58 a	28	55 a	30	0.85	a
8000 mJ/cm^2	57 a	25	47 a	24	0.44	a
12000 mJ/cm^2	59 a	18	56 a	31	0.84	a
24000 mJ/cm^2	38 a	14	30 a	5	0.15	a
Control (24000x3)	68 a	25	41 a	32	0.11	a

All "a" denotes no significant differences between groups in columns
4000-W mJ/cm2 specimens placed in water only for equivalent time of stressed groups

PART THREE

MATERIALS AND METHODS

Effects of Degree of Conversion on Flexural Strength and Modulus.--

Resin composite bars were produced having the same approximate degree of conversion as the gingival margins created by various energy densities in Part 1 and 2. These bars were tested to determine their flexural strength and flexural modulus. Knoop hardness testing was used to approximate the degree of conversion because it was quicker and easier and because it correlated so well with degree of conversion in previous testing ($R^2 = 0.99$; Figure 9).

Specimens were made in square glass rods with dimensions of 2 millimeters by 2 millimeters by 25 millimeters. The Z250 resin composite shade A-2 was light-cured in a Triad II (Dentsply, York, PA) laboratory curing unit for various time intervals to produce surface Knoop hardness levels corresponding to the marginal Knoop hardness levels found in the previous procedures. This approach was taken because it was difficult to measure the power output from the three bulbs in the Triad II unit. In addition, the light in the Triad II unit was unfiltered, and could not be directly compared to the VIP light in terms of curing efficacy or total energy density. The specimens were cured in a vertical position in the center of a rotating platform in the center of the Triad oven to produce the most uniform degree of conversion possible. The specimens were stored dry in a light-proof film canister for 48 hours, polished on each side for 10 seconds with 5 micron aluminum oxide paste on an 8 inch nylon polishing cloth, and then tested in 3-point bending (20 mm span) on a universal testing machine (Instron, Instron Engineering Corp., Canton, MA) at a crosshead speed of 0.254 mm/min. The flexure strengths were

determined from the maximum load using the equation: Flexural strength = $3Fl/2bh^2$ where "F" is the resultant force in pounds, "l" is the length of the specimen over the support beams (20mm) and "b" and "h" are the base and height width of the bar (2mm). The flexural modulus was determined from the initial slope of the force-deflection curve using the following equation: $E = L^3/4bh^3 \times F/Y$ with "F" (force in pounds) determined on a straight portion of the curve and Y as the crosshead speed per minute (0.01 inches / minute) divided by the chart speed (1 inch/min) with "L, b and h" as before. Five specimens of each group were tested. Specimens from the flexure strength tests were evaluated for Knoop hardness in the Kentron hardness tester as before. The specimens were polished on each side for 10 seconds with 5 micron aluminum oxide paste on an 8 inch nylon polishing cloth (Buehler, Lake Bluff, IL). Graphite from a mechanical pencil was rubbed on the lightly polished surface of the composite specimens before indentation. A load of 200 grams was applied through a diamond pyramid indenter with a dwell time of 10 seconds. The length of the indention was measured and a hardness number calculated. Three measurements were made on two opposing sides of each bar and averaged. The average from three bars was calculated (n = 3). These averages were then expressed as a percentage of maximum hardness (71.8 kg/mm^2) from this test and compared with the previous data of Knoop hardness values produced in the gingival margin of the 5 millimeter specimens under various energy densities. In addition to the surface hardness, the center hardness of each bar was tested by embedding the previously fractured bars

Figure 14: Center KHN measurement

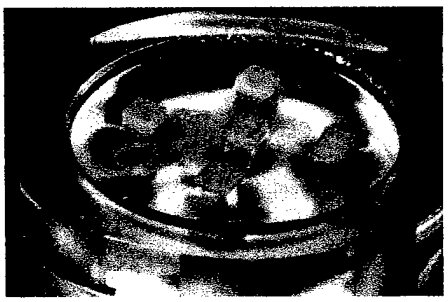

vertically in epoxy resin (Buehler, Lake Bluff, IL) in an acrylic ring and allowing them to cure overnight in a light proof container (Figure 14). The specimens were polished and rubbed with graphite before indentation. One hardness value was taken at the center of both ends of a bar and an average taken. The average of three bars was expressed as a percentage of maximum hardness (n = 3). A one-way analysis of variance (ANOVA) was used to test the effect of curing time on Knoop hardness (surface or center), elastic modulus and flexure strength. SPSS software was used and the results are shown in Table 12. See printouts in Appendix under Part 3. Detailed data can be seen in Appendix under Part 3.

RESULTS

Effects of Degree of Conversion on Flexural Strength and Modulus.--

Table 12 below shows the various hardness ratios and mechanical properties obtained at various Triad II curing times and compares them to similar hardness ratios found at the gingival margin at various energy densities with Part 1 and 2.

Table 12: Mechanical properties compared to KHN in Part 1 and 2

Part 1 n = 3 n = 3 n = 5 n = 5

	KHN at 5mm	
Energy Density	% max	st dv
4000 mJ/cm^2	2.8 a	3.6
6000 mJ/cm^2	22.6 b	0.8
8000 mJ/cm^2	39.2 c	4.5
12000 mJ/cm^2	54.1 d	0.3
24000 mJ/cm^2	72.8 e	0.3
Control (24000x3)	96.5 f	1.2

Time	KHN surf		KHN center		Flexural Mod			Flexure Strength		
secs	% max	st dv	% max	st dv	GPa	st dv	% max	MPa	st dv	% max
4	31.4 a	3.9	22 a	0.9	2.5 a	0.5	20.0	35.2 a	5.5	26.1
8	50 b	2.7	50.7 b	3.1	6 b	0.6	47.5	71.4 b	5.8	52.8
16	70.1 c	1.3	69.1 c	2.1	9.1 c	1.2	72.5	90.2 c	12.4	66.7
80	91.1 d	0.9	91.2 d	5.5	12.3 d	0.3	97.4	125.2 d	7.4	92.6

a – f denotes significant differences within columns

A correlation was performed using SPSS software relating the surface Knoop hardness of the flexure bars with flexural modulus (Figure 15) $R^2 = 0.100$ or flexural strength (Figure 16) $R^2 = 0.98$.

Figure 15: Surface KHN of flexural bars vs. flexural modulus

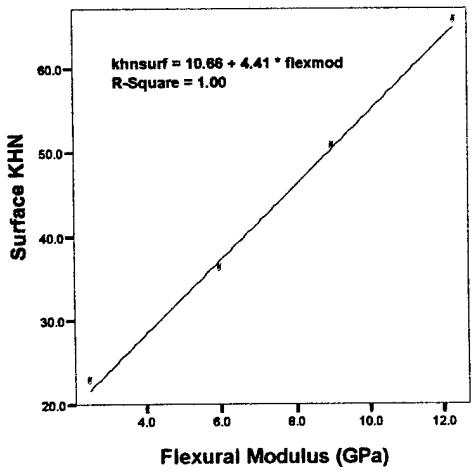

Figure 16: Surface KHN of flexural bars vs. flexural strength

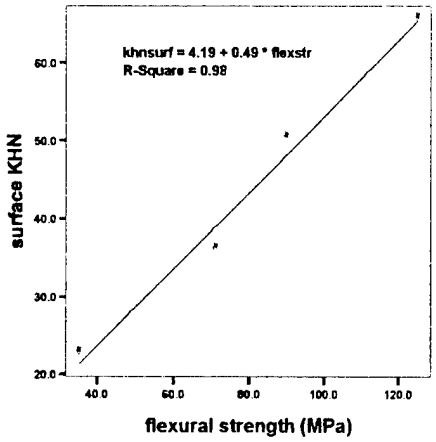

It may be possible to extrapolate from these excellent correlations a good relationship between the mechanical properties of the flexural bars produced with various energy densities and the mechanical properties found at the gingival margin at various energy densities seen in Part 1 or 2 (Table 12).

OVERALL DISCUSSION

Many of the problems with the initial pilot study investigating the effect of energy density on degree of conversion and hardness in the gingival portion of the restoration were resolved with modifications in technique. These modifications consisted of standardizing the length and shape of the specimen by flattening the occlusal of the template and testing the specimens directly on the occlusal and gingival surfaces. The flattened occlusal surface reduced the potential variation in data, especially in the gingival margin area, that could occur from inconsistent lengths in specimens produced from an anatomic occlusal. It allowed greater standardization of the position and angulation of the light guide and permitted the testing of the most apical portion corresponding to the gingival margin. At lower energy densities it became apparent that the Knoop hardness and degree of conversion values decreased markedly in the apical half millimeter of the gingival increment. However, the new technique did not allow data determination within the body of the specimen.

There was a strong correlation when relating Knoop hardness and degree of conversion ($R^2 = 0.99$) with the direct technique. Once again, the attainment of hardness fell behind the degree of conversion of the carbon double bonds (Table 10) and this could be due to the late formation of networking links in the polymer chains.[54] A greater increase in hardness relative to maximum hardness occurred with higher energy levels and subsequent increases in crosslinking.[54] The theory reported earlier that the lag of hardness behind degree of conversion resulting from an overestimation of percent cure at lower energy levels from sectioning and polishing is unlikely with the new technique.

Another significant modification in technique consisted of improving the visualization of the Knoop hardness indentations with the use of graphite. It was noticed in the course of working with the hardness tester that a potentially significant variation existed between operators or even within the same operator when reading or re-reading the same indentation. Poor contrast between the indentation and the surrounding resin may have contributed to this variation and potential underestimation of the length. A high level of polish may have improved the contrast, but was not attempted in order to reduce the potential of altering the properties of the lower cured areas. Graphite from a lead pencil placed on the specimen before indentation provided dramatically improved visualization and substantially reduced the standard deviation. See figure 17. A concern was expressed over the possibility of the graphite altering the test or test surface. Therefore, graphite was also placed on the nearby epoxy mounting resin, on which the indentations were readily observed without the graphite. No differences were seen in hardness measurements with or without graphite. See data in Appendix under Part One.

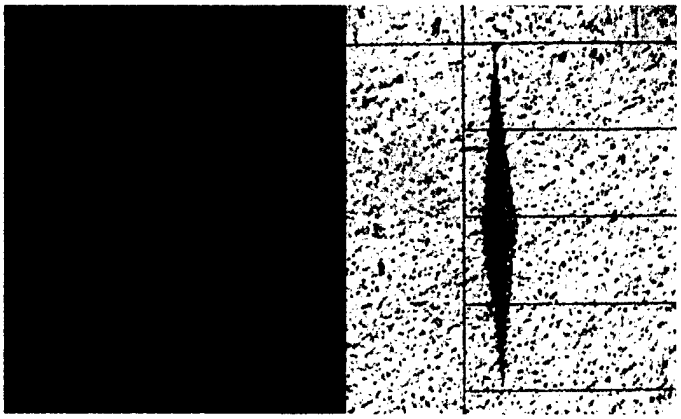

Figure 17: Knoop hardness indentation at 200x
(l) Non-graphite enhanced; (r) graphite enhanced

It is common in hardness testing to express the hardness values as a percentage of the top or upper surface of the composite with 80 percent typically chosen to be the critical level for adequate depth of cure. That was modified slightly in this study to

reduce the potential error in comparing groups with softer top surfaces. The values were standardized by expressing the hardness and the degree of conversion numbers as a percentage of maximum. The maximum Knoop hardness value found for Z250 was originally 98.7 but changed to 72.7 after using the graphite technique that provided easier visualization of the indentation. The original data served primarily as a pilot to provide initial guidance to energy density estimation. The study was essentially repeated using modified techniques.

Many of the problems with the next part of the study investigating the effect of degree of conversion on marginal integrity in the gingival portion of a restoration were resolved with multiple modifications in technique.

The flattening of the occlusal surface became even more critical in this next phase of the project due to the variability in anatomic form of the multiple teeth used. A uniform 5 millimeter depth and shape to the preparations was produced.

In the higher energy density groups, especially the control group, it was difficult to finish and polish the gingival margins to the exact margins without leaving a slight overhang of resin composite. This became especially difficult in teeth with any sort of furcal concavities or deep contours. Many of these overhangs did not become obvious until observed under 50X magnification. Flattening the gingival marginal area with a disc just before preparation helped to create a more manageable surface. A recent study found that 51.3% of bonded Class 2 resin composite restorations had significant flash at the interproximal margins in teeth restored in a phantom head after a typical finishing and polishing procedure.[154]

It was difficult when using scanning electron microscopy to consistently identify the true width or length of gaps or defects. A gap could be defined as a space or lack of restorative material whereas a defect may be defined as a loss of material or both.

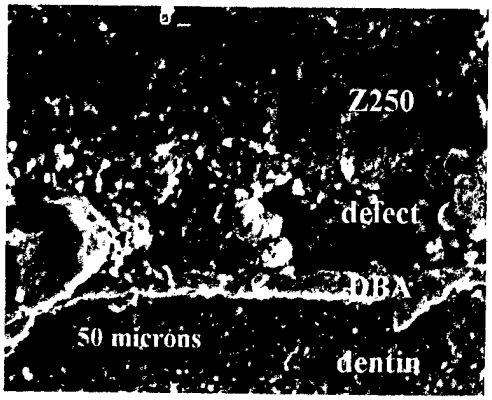

Figure 18: Gingival marginal defect at 1000 X

It was often difficult to differentiate between the two. Some areas were occupied with a thicker layer of bonding agent, but it was problematic to determine if it was intact or fractured or simply filling a void (Figure 18). Variation in the angulation of the interface could produce variable results when attempting to measure gap width. Also, analysis at various magnifications seemed to produce variable interpretations by itself. The procedure was technically complex, expensive and very time consuming – taking up to one hour to examine and quantify a single specimen. Finally, the technique was abandoned when it was realized that the SEM could not adequately measure the depth of defects. This became significant in the gingival marginal areas of the lowest energy density groups.

It was determined that the gingival margins would best be assessed by a visual rating or ridit analysis that used a numbered scale of restoration images that exhibited progressively increasing degrees of marginal defects. This technique has been used successfully in the past by Mahler et. al. to evaluate amalgam margins.[153] However, instead of enlarged photographic images, the sputter-coated replicas were examined using 50X stereomicroscopy by three examiners. Stereomicroscopy allowed the necessary assessment of the depth of the defects in addition to width and length. The interval nature of the ridit scale also lends itself to the use of the more powerful parametric

statistics.[153] A good correlation was found between defect widths as measured by SEM and ridit scores ($R^2 = 0.92$).

It was interesting to see no significant effect of thermal-mechanical stressing on microleakage or marginal defects. Several studies suggest that thermocycling resin composite restorations may not significantly affect microleakage in Class 2 resin composite restorations.[124,125,155] In a recent study, Wibowo used Z100 and Single Bond in Class 2 restorations with gingival margins in dentin. He found no significant difference between the thermal-cycled and non thermal-cycled groups using a computer imaging technique of the gingival floor after breaking away the entire resin restoration.[155] The effects of thermal-cycling resin composite restorations on microleakage remains questionable and perhaps the procedure is unnecessary.

Studies have shown conflicting results of load cycling, reinforcing the need for careful evaluation and interpretation due to differences in experimental designs.[100,116,133-142] Several researchers found no effect on microleakage from load cycling of resin composite restorations.[125,133-138] However, a few authors did find an effect from load cycling.[116,134,140] A couple of investigators found an effect from a simultaneous combination of thermal-cycling and loading,[100,139,156] while another had mixed results.[157] Virtually all of the studies evaluate only microleakage with thermal-mechanical loading. However, a couple of recent studies have found conflicting results when evaluating marginal gap formation and a combination of thermal-mechanical loading. Friedl and others,[158] using testing conditions fairly similar to this study (5000 thermal cycles and 500,000 load cycles at 1.7 Hz and 72.5 N in Class 2 restorations), found no significant increase in marginal gaps using ProBond and Prisma TPH, but found a significant

increase using Scotchbond MP and Z100. Interestingly, these investigators using a measurement technique similar to this study, found an actual decrease in microleakage at the dentinal gingival margin in both groups after thermal-mechanical loading.[158] They theorized that the decrease could have been due to hygroscopic expansion. However, a recent study by Lutz and Krejci utilized a three dimensional scanner and found an increase in the percentage of marginal gap formation in MOD resin composite restorations after a combination of simultaneous thermal and load cycling (3000 thermal cycles and 1,200,000 load cycles at 1.7 Hz and 49 N).[100]

Several studies have found no correlation between gap formation and microleakage.[157,159-161] Similar results were found in this investigation. A linear regression analysis was performed using SPSS software relating the ridit scores and the microleakage values and found a poor correlation with an R^2 of 0.24. Any significant increase in marginal gap or defect would probably not contribute to an increase in microleakage, once the threshold width for dye penetration is met.

The preparation and placement of the resin composite in this study was based on techniques supported in the literature. One study found a significant reduction in microleakage by placement of a conservative bevel along the facial and lingual enamel margins.[110] Also, the use of the syringe tip for resin composite placement has been shown to decrease the viscosity of the material and decrease voids along the preparation walls.[162,163]

Various techniques have been utilized to assess dye penetration in microleakage studies. Many utilize a single section through the center of the restoration.[134-137,140,164,165] However, a three dimensional technique whereby the entire restoration is removed has

been shown to reveal more extensive dye penetration,[166-169] but it is more time consuming and does not allow good visualization of dentin tubule leakage.[169] Using multiple sections, as used in this study, seems to be a practical compromise.[124,133,139,141,169] It was not surprising to see extensive leakage between resin composite and the dentinal gingival margin. This agrees with many studies utilizing dentin bonding agents.[116,124,133,136,138,169] A recent study by Hagge and others found extensive microleakage under composite using a 5th generation bonding agent with and without flowable liners. The only group not to suffer heavy leakage utilized a resin-modified glass ionomer in an open sandwich technique.[164] The enhanced performance of resin-modified glass ionomer liners on dentinal gingival margins has been substantiated in several laboratory and clinical studies.[158,165,170]

It was interesting to find, however, no significant increase in microleakage in the groups with very low levels of gingival marginal cure. Microleakage testing using silver nitrate dyes is a very stringent test that perhaps overestimates the amount of leakage that will occur clinically.[157] The dye is of considerably smaller size and molecular weight than bacteria, or endotoxins.[171] Gap formation found at the dentinal gingival margin found in this study and other studies was much larger than the silver nitrate dye.[100,158]

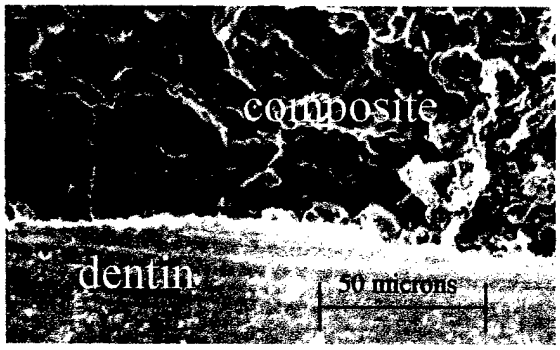

Figure 19: 500X
Dentinal gingival margin
4000 mJ/cm^2 500K cycles

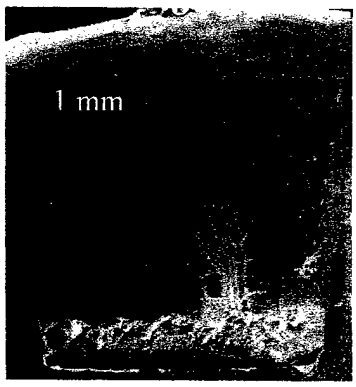

Figure 20: 14X
5 mm composite restoration
4000 mJ/cm^2 500K cycles

Perhaps any significant increase in marginal gap or defect would not contribute to an increase in microleakage, once the threshold width for dye penetration is met. Even the poorest cured group (4000 mJ/cm^2) that sustained significant marginal degradation or defects over time was found in pilot studies to have relatively small marginal "gaps" at the depths of these defects (Figures 19,20). Therefore, except for the obvious loss of superficial marginal resin composite material, these lower cured groups would possibly not leak any more or less than the higher cured groups (Figure 21).

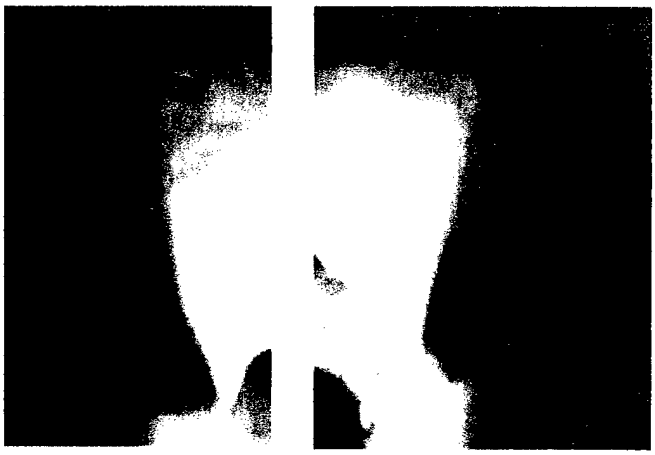

Figure 21:
Microleakage: (l) pre-op; (r) 500K cycles
4000 mJ/cm^2

There was a significant loss in marginal integrity in the gingival margins with the lowest degrees of conversion after thermal-mechanical stressing. However an identical group stored only in water suffered similar degradation. This suggests that water, not the thermal-mechanical stressing contributed to the increase in marginal defects in these susceptible groups. The lesser the extent of the polymerization reaction, the more residual monomers are available to be leached.[48] This inverse relationship ($R^2 = 0.95$) between degree of cure and percent elution was confirmed in a study by Rueggeberg and Craig. [50] In that study, resin composite was cured through various thicknesses of cured

resin composite in order to reduce the irradiance and degree of conversion. After storing the variably cured resin composite in water for four weeks, the elution of residual monomers was determined gravimetrically.[50]

There was no significant difference in marginal defects between the incrementally-filled control group and the bulk-filled 24000 and 6000 mJ/cm^2 groups. Although the 6000 mJ/cm^2 group was statistically similar to the control and 24000 mJ/cm^2 groups, it was on the edge of significant marginal deterioration as seen by the 4000 mJ/cm^2 groups and could not be recommended clinically. Any slight variation in light guide angulation or loss in power density could result in severe undercuring and marginal degradation. Also, these lower energy groups could be susceptible to solvents and enzymes not tested in this study. The lack of marginal degradation in the 6000 mJ/cm^2 group may have been a combination of reduced shrinkage stress and just enough degree of conversion to prevent degradation primarily from water. Therefore, a recommended lower limit of gingival margin acceptability in a bulk-filled resin composite restoration was created by 80% of maximum conversion, 73% of maximum hardness and approximately 70% of maximum flexural strength and modulus in the gingival marginal area as seen in the 24000 mJ/cm^2 group.

Caution should be exercised when attempting to extrapolate the results of this study to resin composites other than minifilled hybrid Z250. Direct comparisons of the sufficiency of irradiation using absolute surface hardness are not generally appropriate because the hardness is influenced by both the nature of the resin matrix and of the inorganic filler.[88] Johnston and others used a mathematical model to suggest that the depth of cure may be defined as the level at which the hardness value is equivalent to at

least 90% of the hardness at the top of the composite.[88] Others have suggested that this top-to-bottom gradient should not exceed 20% [89] and should be considered a realistic measure of depth of cure.[90]

Various studies have advocated incremental instead of bulk placement and curing for resin composite to decrease the effects of polymerization shrinkage and to provide complete polymerization in deeper cavities. [2,58,64-65] Incremental placement may also reduce the configuration factor – the ratio of bonded to unbonded surfaces – and reduce the stress by making more surface resin available for flow.[66] However, other studies found no difference between bulk and incremental placement on marginal gap formation[67] or fluid permeability.[68] A finite element study by Versluis and others showed that incremental filling yields higher polymerization shrinkage stresses.[172] Polymerization contraction of each individual filling increment causes some deformation of the cavity, forcing the walls to bend and decreasing cavity volume. Less composite placed for the next filling increment results in a cavity that is volumetrically filled with less composite material than the original volume of the cavity and that results in a higher stress state.[172] Using photo-elastic material, Jedrychowski and others found that bulk resin composite placement generated the lowest shrinkage stresses compared with various other incremental techniques.[173]

This study found no significant difference in gingival marginal defects between incremental cure and bulk curing at an energy density of 24000 mJ/cm^2. The reasons for these findings despite the great disparity in energy density between the groups may be due to a complex interaction of multiple factors. With incremental curing, the mechanical properties of the resin composite adjacent to the gingival margin and the

bond between resin composite and adhesive are maximized. These factors favoring improved gingival margin performance are balanced with the increased polymerization shrinkage that occurs with the high energy density. With bulk cure, polymerization shrinkage is lessened due to a decrease in applied energy density. Counteracting this is a decrease in the mechanical properties of the resin composite adjacent to the gingival margin. However, with the higher energy density group (24000 mJ/cm^2) adequate mechanical properties at the gingival margin may result since functional forces through the restoration are likely dissipated to the tooth via adhesion. Another factor opposing gingival margin integrity in the bulk cure group may be a decreased adhesion of resin composite at the gingival margin as a result of the reduced energy density.

The incremental placement of resin composite utilized in this study was difficult to accurately place and reproduce, requiring magnification to insure uniformity among specimens. Unlike bulk placement, an obvious demarcation could be seen on occasion between sequential layers of the incremental technique. Separate silver nitrate staining along the internal restoration interface could be seen on occasion corresponding to the demarcation areas[164]. See Figure 22.

Figure 22: Layering of increments

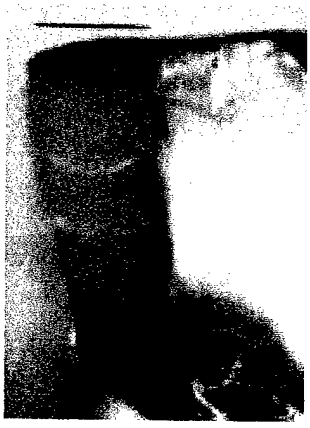

The 5 millimeter long posterior resin composite restorations were created with various energy densities, but these energy densities were determined based on the power density recorded at the end of the light guide. It became of interest to know just how much power density was actually transmitted through the resin composite to the gingival surfaces. Therefore, a simple study was conducted to determine what percentage of the

power density delivered to the occlusal surface actually reached the gingival margin. See details and data in Appendix under Part 3.

The 1.6 percent value of this study agrees with a recent study by Price and others that found an average of only 1.1 percent of initial light energy transmitted through 5 millimeters of various resin composites (1.6 for Z250).[174]

It was difficult to consistently record the lower levels of power found at the gingival surface of the specimens. The Power Max reads heat energy and the ambient level of heat in the room of 1 mW tended to complicate testing at these very low levels. Also, the measurements reported with the Power Max tended to float slightly. Although not a problem at the higher levels recorded at the end of the light guide, greater variation and less reproducibility of the data was evident at these lower levels of recorded power.

Knoop hardness (R^2= 0.96) or degree of conversion (R^2 = 0.93) at the gingival increment had a strong linear relationship to the log of the energy density (Figure 10). This agrees with Nomoto and others who reported a linear relationship between the depth of cure and the logarithm of total amount of exposure.[175] Cook described the intensity of light transmitted by the cured resin composite by the equation:[176]

$$I = I_o \times 10^{-eL}$$

where I_o is the intensity of the light at the surface of the resin composite; L is the depth of cure and e is the attenuation coefficient due to the heterogeneity in resin composites altering the optical properties. Light is absorbed and scattered by matrix and fillers. When the specimen is irradiated for time t, the amount of light transmitted is defined by:

$$E = I \times t = I_o \times t \times 10^{-cL}$$

where E is defined as the minimum total amount of exposure required to activate polymerization. This equation can be expressed:

$$L = \{\log (I_o \times t) - \log E\}/e$$

which indicates that a linear relationship exists between the depth of cure (L) and logarithm of total amount of exposure as was found in this study. [175,176]

Figure 23 shows the correlation between Knoop hardness or degree of conversion and energy density without the logarithmic conversion. Notice the sudden drop in KHN or DC at lower energy densities consistent with the dramatic attenuation of energy exposure.

Figure 23: Knoop Hardness or degree of conversion vs energy density (flattened template) at the gingival increment

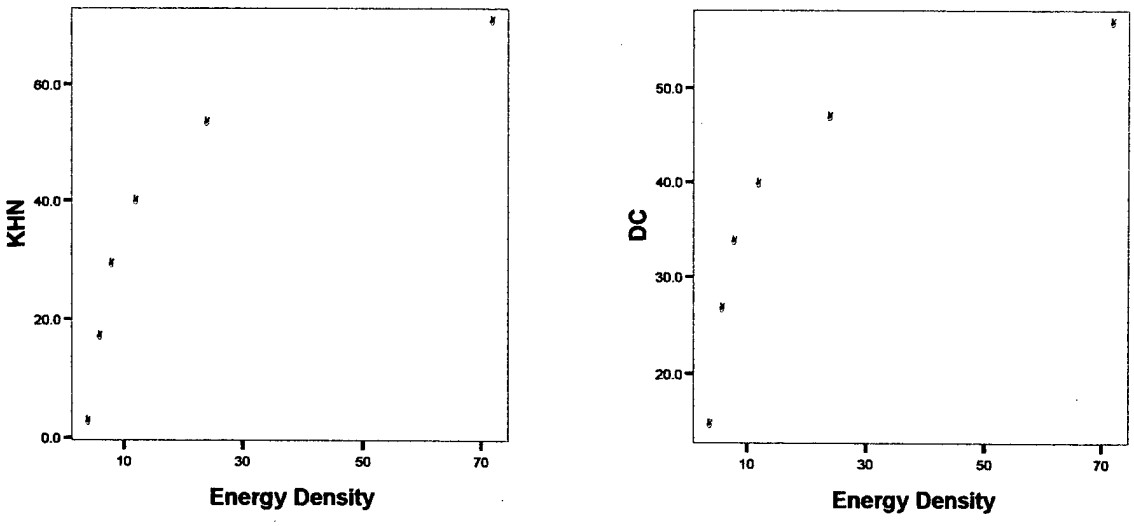

The maximum load of 85 Newtons used in this study could have been increased in an attempt to produce gingival marginal degradation or until the restoration failed catastrophically. However, the clinical significance of such high forces and the likelihood of producing localized changes in the gingival area would be questionable. A simple study was conducted to determine the stress developed at the occlusal and gingival marginal area of the restoration. Three single strain gauges (CEA-06-032UW-120, Measurements Group, Raleigh, NC) were bonded on the resin composite (Control Group) near the occlusal, at the gingival margin, and on dentin near the gingival margin using cyanoacrylate and the tooth was subjected to the same cyclic forces as before (Figure 24). The generated strain was conditioned by a strain gauge conditioner (2100 System, Measurements Group, Raleigh, NC). Data indicates that the maximum amount of stress transmitted to the gingival marginal resin composite area is less than 12.4 Megapascals (MPa). The maximum stress near the occlusal marginal ridge was 15.5 MPa and near the gingival marginal dentin was 11.5 MPa. The bonded resin composite restoration appears to absorb most of the available stress, transferring the energy through the resin composite, the bonding agent and the supporting

Figure 24: 3 Strain gauges at the occlusal, gingival and dentinal margins

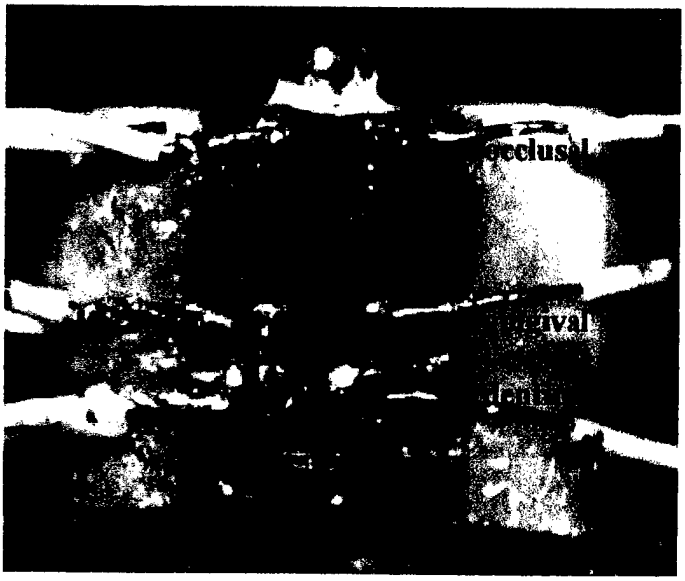

walls of the restoration without affecting marginal integrity. See details and data in the Appendix under Part 3.

Future studies are needed to determine the effect of energy density on caries resistance, interproximal wear resistance and post-operative sensitivity. Also, a less photosensitive material such as a microfill composite should be evaluated under similar conditions of this study to evaluate the opposite end of the spectrum of available restorative resin composites. This additional information may provide a more general description of the minimum hardness ratio necessary at the base of a resin composite restoration to maintain marginal integrity. Also, a yellowish discoloration was seen in the gingival areas of the poorly cured groups (4000 and 6000 mJ/cm^2) after thermal-mechanical stressing. See the photos of the restorations in the Appendix under Part Two, 1^{st}, 2^{nd} and 3^{rd} Pilot. A future study could examine the effect of water immersion on composite discoloration over time in resin composites with variable degrees of conversion using a colorimeter.

OVERALL CONCLUSIONS

Based on the limitations of this study, the following conclusions can be made concerning Z250 shade A-2 resin composite by 3M ESPE in class 2 slot preparations with gingival margins in dentin with various degrees of conversion. (see summary sheet following conclusions):

1) There was a strong correlation between degree of conversion and Knoop hardness at the gingival margins. ($R^2 = 0.99$)

2) There was a good correlation between degree of conversion or Knoop hardness and the log of energy density at the gingival margin. ($R^2 = 0.96$ & 0.93)

3) There was a good correlation between average defect widths and visual rating (ridit scores). ($R^2 = 0.92$)

4) Energy density had a significant effect on gingival marginal defects and no significant effect on microleakage.

5) Water had a significant dissolving effect on the resin composite with very low degrees of conversion at the gingival margin producing defects.

6) The maximum defect formed at the gingival margin with a Knoop hardness of 2.1 or 2.8% of maximum and a degree of conversion of 14.3 or 24.5% of maximum.

7) There was no significant difference in gingival marginal defects between the incrementally-filled control group and the bulk-filled 24000 and 6000 mJ/cm^2 groups.

8) A recommended lower limit of gingival margin acceptability in a bulk-filled Z250 resin composite restoration was created by 80% of maximum conversion or 73% of maximum hardness as seen in the 24000 mJ/cm^2 group (600 mW/cm^2 for 40 seconds). There was no significant difference between bulk curing and incremental filling resin composite within these limits.

9) There was no overall significant effect of thermal-mechanical stressing on gingival marginal defects or microleakage in class 2 resin composite restorations with gingival margins in dentin.

Summary Sheet

Ridit Analysis 3 evaluators n = 8

	KHN at 5mm		DC at 5mm		Pre op		Post thrmal		100K		500K		t-test	
Energy Density	% max	st dv	% max	st dv	ridit	st dv	ridit	st dv	ridit	st dv	ridit	st dv	pre-500	ANOVA
4000-W mJ/cm^2	2.8 a	3.6	24.5 a	5.1	4.0	1.9	4.5	2.0	5.6	2	6.3	2.4	0.002	c
4000 mJ/cm^2	2.8 a	3.6	24.5 a	5.1	4.7	2.7	4.8	3.0	5.4	3.2	6.0	3.8	0.035	c
6000 mJ/cm^2	22.6 b	0.8	45 b	4.4	2.5	1.2	2.9	1.2	2.7	1.0	2.8	1.3	0.402	a
8000 mJ/cm^2	39.2 c	4.5	57.3 b,c	0.2	3.3	1.4	4.3	0.8	4.2	1.1	4.2	1.0	0.113	b,c
12000 mJ/cm^2	54.1 d	0.3	67.6 c,d	2.3	3.9	0.9	4.1	1.4	4.0	0.9	4.1	0.8	0.407	b,c
24000 mJ/cm^2	72.8 e	0.3	80 d	0.9	3.0	0.6	3.3	0.6	3.5	0.3	3.2	0.6	0.516	a,b
Control (24000x3)	96.5 f	1.2	97 e	1.6	2.4	1.2	2.2	0.8	2.3	0.9	2.3	0.8	0.487	a

Microleakage % of margin n = 8

Energy Density	Avg Pre	st dv	Avg Post	st dv	t-test	
4000-W mJ/cm^2	53 a	31	52 a	21	0.96	a
4000 mJ/cm^2	53 a	31	56 a	27	0.86	a
6000 mJ/cm^2	58 a	28	55 a	30	0.85	a
8000 mJ/cm^2	57 a	25	47 a	24	0.44	a
12000 mJ/cm^2	59 a	18	56 a	31	0.84	a
24000 mJ/cm^2	38 a	6	30 a	5	0.15	a
Control (24000x3)	68 a	25	41 a	32	0.11	a

Mechanical Properties

Part 1 n = 3

	KHN at 5mm	
Energy Density	% max	st dv
4000 mJ/cm^2	2.8 a	3.6
6000 mJ/cm^2	22.6 b	0.8
8000 mJ/cm^2	39.2 c	4.5
12000 mJ/cm^2	54.1 d	0.3
24000 mJ/cm^2	72.8 e	0.3
Control (24000x3)	96.5 f	1.2

n = 3 n = 5 n = 5

Time	KHN surf		KHN center		Elastic Mod			Flexure Strength		
secs	% max	st dv	% max	st dv	GPa	st dv	% max	MPa	st dv	% max
4	31.4 a	3.9	22 a	0.9	2.5 a	0.5	20.0	35.2 a	5.5	26.1
8	50 b	2.7	50.7 b	3.1	6 b	0.6	47.5	71.4 b	5.8	52.8
16	70.1 c	1.3	69.1 c	2.1	9.1 c	1.2	72.5	90.2 c	12.4	66.7
80	91.1 d	0.9	91.2 d	5.5	12.3 d	0.3	97.4	125.2 d	7.4	92.6

a-f denote significant differences in columns

BIBLIOGRAPHY

1. Dentsply. Surefil High Density Posterior Restorative: Technical Manual. 1998; Milford, DE: Dentsply-Caulk International pp. 9-11.

2. Yap AUJ. Effectiveness of polymerization in composite restoratives claiming bulk placement: impact of cavity depth and exposure time. Oper Dent 2000;25:113-120.

3. Bowen RL. Dental filling material comprising vinyl-silane treated silica and a binder consisting of the reaction product of bisphenol and glycidyl methacrylate. US Patent 1962;3,066, 112.

4. Phillips RW, Phillip's Science of Dental Materials, 10th edition, Philadelphia, PA: W.B Saunders Co., 1996. p274.

5. Peutzfeldt A. Resin composites in dentistry: the monomer systems. Eur J Oral Sci 1997;105:97-116.

6. Ferracane JL, Greener EH. The effect of resin formulation on the degree of conversion and mechanical properties of dental restorative resins. J Biomed Mater Res 1986;20:121-131.

7. Asmussen E. Composite restorative resins. Composition versus wall-to-wall polymerization contraction. Acta Odontol Scand 1975:33:337-344.

8. De Gee AJ, Feilzer AJ, Davidson CL. True linear polymerization shrinkage of unfilled resins and composites determined with a linometer. Dent Mater 1993;9:11-14.

9. Labella R, Lambrechts P, Van Meerbeek B, Vanherle G. Polymerization shrinkage and elasticity of flowable composites and filled adhesives. Dent Mater 1999;15(2):128-137.

10. McMurray J. Fundamentals of Organic Chemistry. Monterey CA: Brooks Pub. Co., 1986.

11. Choi KK, Condon JR, Ferracane JL. The effects of adhesive thickness on polymerization contraction stress of composite. J Dent Res 2000;79(3):812-817.

12. Bayne SC, Heymann HO, Swift EJ. Update on dental composite restorations. J Am Dent Assoc 1994;125:687-701.

13. Ferracane JL. *In vitro* evaluation of composite resins. Structure-property relationships, development of assessment criteria. Trans Acad Dent Mater 1989;2:6-35.

14. Bouschlicher MR, Cobb DS, Boyer DB. Radiopacity of compomers, flowable and conventional resin composites for posterior restorations. Oper Dent 1999;24(1):20-25.

15. Lutz F, Phillips RW. A classification and evaluation of composite resin systems. J Prosthet Dent 1983;50:480-488.

16. Ferracane JL. Current trends in dental composites. Crit Rev Oral Biol Med. 1995;6(4):302-318.

17. Willems G, Lambrechts P, Braem M, Celis JP, Vanherle G. A classification of dental composites according to their morphological and mechanical characteristics. Dent Mater 1992;8:310-319.

18. Craig RG. Restorative Dental Materials. 10th edition, St. Louis, MO: Mosby Pub Co., 1997. p245.

19. Cook WD. Factors affecting the depth of cure of UV-polyermized composites. J Dent Res 1980;59:800-808.

20. Burdsell DC, Bannon PJ, Webb PB. Harmful effects of near ultraviolet radiation used for polymerization of sealant and composite resin. J Amer Dent Assoc. 1976;92(4):775-776.

21. Rueggeberg FA, Ergle JW, Lockwood PE. Effect of photoinitiator level on properties of a light-cured and post-cure heated model system. Dent Mater 1997;12:360-364.

22. Cook WD. Photopolymerization kinetics of dimethacrylates using camphoroquinone amine initiator system. Polymer 1992;33:600-609.

23. Stansbury JW. Curing dental resins and composites by photopolymerization. J Esthet Dent 2000;12:300-308.

24. Asmussen E. Factors affecting the quantity of remaining double bonds in restorative resin polymers. Scand J Dent Res 1982;90:490-496.

25. Rueggeberg FA. Contemporary issues in photocuring. Compend 1999;20:S4-15.

26. Nagel R. Operation and diagnostic features of the VIP light. Compend 1999;20:S55-59.

27. Ruggeberg FA. Precision of hand-held dental radiometers. Quintessence Int 1993;391-6.

28. Leonard DL, Charlton DG, Hilton TJ. Effect of curing-tip diameter on the accuracy of dental radiometers. Oper Dent 1999;24:31-37.

29. Pilo R, Oelgiesser D, Cardash HS. A survey of output intensity and potential for depth of cure among light-curing units in clinical use. J Dent 1999;27:235-241.

30. Davidson CL, de Gee AJ. Light-curing units, polymerization, and clinical implications. J Adhesive Dent 2000;2:167-173.

31. Unterbrink GL, Muessner R. Influence of light intensity on two restorative systems. J Dent 1995;23:183-189.

32. Althoff O, Hartung M. Advances in light curing. Am J Dent 2000;13:77D-81D.

33. Jandt KD, Mills RW, Blackwell GB, Ashworth SH. Dept of cure and compressive strength of dental composites cured with blue light emitting diodes (LEDs). Dent Mater 2000;16:41-47.

34. Kurachi C, Tuboy AM, Magalhaes DV, Bagnato VS. Hardness evaluation of a dental composite polymerized with experimental LED-based devices. Dent Mater 2000;17:309-315.

35. Mills RW, Jandt KD, Ashworth SH. Dental composite depth of cure with halogen and blue light emitting diode technology. Br Dent J 1999;186(6)388-391.

36. Duke ES. Light-emitting diodes in composite resin photopolymerization. Compendium 2001;22(9);722-725.

37. Balland D, Guillard R, Andre JC. Experimental studies and modeling of light distribution in photopolymerizable composite materials. Dent Mater 1984;3:93-98.

38. Kawaguchi M, Fukushima T, Miyazaki K. The relationship between cure depth and transmission coefficient of visible-light-activated resin composites. J Dent Res 1994;73(2):516-521.

39. Ruyter IE, Oysaed. Conversion in different depths of ultraviolet and visible light activated composite materials. Acta Odontol Scand 1982;40:179-192.

40. McCabe JF, Carrick TE. Output from visible-light activation units and depth of cure of light-activated composites. J Dent Res 1989;68:1534-1539.

41. Campbell PM, Johnston WM, O'Brien WJ. Light scattering and gloss of an experimental quartz-filled composite. J Dent Res 1986;65:892-894.

42. Ferracane JL, Aday J, Matsumoto H, Marker VA. Relationship between shade and depth of cure for light-activated dental resin composites. Dent Mater 1986;2:80-84.

43. Yearn JA. Factors affecting cure of visible light activated composites. Int Dent J 1985;35:218-225.

44. Swartz ML, Phillips RW, Rhodes B. Visible light-activated resins – depth of cure. J Amer Dent Assoc 1983;106:634-637.

45. Ruyter IE, Conversion in different depths of ultraviolet and visible light activated composite materials. Acta Odontol Scand 1982;40:179-192.

46. Rueggeberg FA, Caughman WF, Curtis JW. Effect of light intensity and exposure duration on cure of resin composite. Oper Dent 1994;19:26-32.

47. Ruyter IE. Svendsen SA. Remaining methacrylate groups in composite restorative materials. Acta Odontol Scand 1978;36:75-82.

48. Ferracane JL. Elution of leachable components from composites. J Oral Rehabil 1994;21:441-452.

49. Tanaka K, Taira M, Shintani H, Wakasa K, Yamaki M. Residual monomers of a set visible-light-cured dental composite resin when immersed in water. J Oral Rehabil 1991;18:353.

50. Rueggeberg FA, Craig RG. Correlation of parameters used to estimate monomer conversion in a light-cured composite. J Dent Res 1989;67:932.

51. Caughman WF, Caughman GB, Shiflett RA, Rueggeberg F, Schuster GS. Correlation of cytotoxicity, filler loading and curing time of dental composites. Biomaterials 1991;12(8):737-740.

52. Cox CF, Keall CL, Keall HJ. Biocompatibility of surface-sealed dental materials against exposed pulp. J Prosthet Dent 1987;57:1.

53. Stanley HR, Bowen RL, Folio J. Compatibility of various materials with oral tissues. II. Pulp responses to composite ingredients. J Dent Res 1979;58:1507.

54. Ferracane JL. Correlation between hardness and degree of conversion during the setting reaction of unfilled dental restorative resins. Dent Mater 1985;1:11-14.

55. Ferracane JL, Berge HX. Fracture toughness of experimental dental composites aged in ethanol. J Dent Res 1995;74:1418-1423.

56. Ferracane JL, Mitchem JC, Condon JR, Todd R. Wear and marginal breakdown of composites with various degrees of cure. J Dent Res 1997;76(8):1508-1516.

57. Lutz F, Krejci I, Barbakow F. Quality and durability of marginal adaptation in bonded composite restorations. Dent Mat 1991;7:107-113.

58. Lambrechts P, Braem M, Vanherle G. Evaluation of clinical performance for posterior composite resins and dentin adhesives. Oper Dent 1987;12:53-87.

59. Collins CJ, Bryant RW, Hodge KV. A clinical evaluation of posterior composite resin restorations: 8-year findings. J Dent 1998;26:311-317.

60. Letzel H. Survival rates and reasons for failure of posterior composite restorations in multicentre clinical trial. J Dent 1989;17:S10-S17.

61. Qvist V, Qvist J, Mjor IA. Placement and longevity of tooth-colored restorations in Denmark. Acta Odontol Scand 1990;48:305-311.

62. Stangel I, Barolet RY. Clinical evaluation of two posterior composite resins; two-year results. J Oral Rehabil 1990;17:257-268.

63. Summitt JB, Robbins JW, Schwartz RS. Fundamentals of Operative Dentistry,. 2nd edition, Chicago, IL: Quintessence Publishing Co., 2001. p265-271.

64. Crim GA. Microleakage of three resin placement techniques. Am J Dent 1991;4:69-72.

65. Opdam NJ, Feilzer AJ, Roeters JJ, Smale I. Class I occlusal composite resin restorations: in vivo post-operative sensitivity, wall adaptation, and microleakage. Am J Dent 1998;11:229-234.

66. Feilzer AJ, de Gee AJ, Davidson CL. Setting stress in composite resin in relation to configuration of the restoration. J Dent Res 1987;66:1636-1639.

67. Tjan AHL, Bergh BH, Lidner C. Effect of various incremental techniques on the marginal adaptation of class 2 composite resin restorations. J Prosthet Dent 1992;67:62-66.

68. Ciucchi B, Bouillaguet S, Delaloye M, Holz J. Volume of the internal gap formed under composite restorations in vitro. J Dent 1997;25:305-312.

69. Feilzer AJ, de Gee AJ, Davidson CL. Curing contraction of composites and glass ionomer cements. J Prosthet Dent 1988;59:297.

70. Feilzer AJ, de Gee AJ, Davidson CL. Curing contraction of composites and glass ionomer cements. J Prosthet Dent 1988;59:297.

71. Kemp-Scholte CM, Davidson CL. Complete marginal seal of Class V resin composite restorations effected by increased flexibility. J Dent Res 1990;69:12401243.

72. Van Meerbeek B, Willems G, Celis JP, Roos JR, Braem M, Lamberts P. Assessment by nano-indentation of the hardness and elasticity of the resin-dentin bonding area. J Dent Res 1993;72:1434-1442.

73. Davidson CL, de Gee AJ. Relaxation of polymerization contraction stress by flow in dental composites. J Dent Res 1984;63:146.

74. Silikas N, Eliades G, Watts DC. Light intensity effects on resin-composite degree of conversion and shrinkage strain. Dent Mat 2000;16:292-296.

75. Bouschlicher MR, Rueggeberg FA. Effect of ramped light intensity on polymerization force and conversion in a photoactivated composite. J Esthet Dent 2000;12:328-339.

76. Koran P, Kurschner R. Effect of sequential versus continuous irradiation of a light-cured resin composite on shrinkage, viscosity, adhesion, and degree of polymerization. Am J Dent 1998;10:17-22.

77. Goracci G, Mori G, Casa de'Martinis L. Curing light intensity and marginal leakage of resin composite restorations. Quint Int 1996;27:355-362.

78. Uno S, Asmussen E. Marginal adaptation of a restorative resin polymerized at reduced rate. Scand J Dent Res 1991;99:440-444.

79. Sakaguchi RL, Berge HX. Reduced light energy density decreases post-gel contraction while maintaining degree of conversion in composites. J Dent 1998;26:695-700.

80. Feilzer AJ, Dooren LH, de Gee AJ, Davidson CL. Influence of light intensity on polymerization shrinkage and integrity of restoration-cavity interface. Eur j Oral Sci 1995;103:322-326.

81. Kanca J, Suh BI. Pulse activation: reducing resin-based composite contraction stresses at the enamel cavosurface margins. Am J Dent 1999;12:107-112.

82. Ferracane JL. Correlation between hardness and degree of conversion during setting reaction of unfilled dental restorative resins. Dent Mat 1985;1:11-14.

83. Murray GA, Yates JL, Newman SM. Ultraviolet light and ultraviolet light-activated composite resins. J Prosthet Dent 1981;46:167-170.

84. Cook W. Factors affecting the depth of cure of ultraviolet-polymerized composites. J Dent Res 1980;59:800-808.

85. Shin WS, Li XF, Schwartz B, Wunder SL, Baran GR. Determination of the degree of cure of dental resins using Raman and FT-Raman spectroscopy. Dent Mater. 1993 Sep;9(5):317-24.

86. Ferracane JL, Greener EH. Fourier Transform Infrared Analysis of Degree of Polymerization in Unfilled Resins – Methods of Comparison. J Dent Res 1984;63(8):1093-1095.

87. DeWald JP, Ferracane JL. A comparison of four modes of evaluating depth of cure of light-activated composites. J Dent Res 1987;66(3):727-730.

88. Johnston WM, Leung RL. Fan PL. A mathematical model for post-irradiation hardening of photoactivated composite resins. Dent Mat 1985;1;191-194.

89. Pilo R, Cardash HS. Post-irradiation polymerization of different anterior and posterior visible-light activated resin composites. Dent Mat 1992;8:299-304.

90. Skeeters TM, Timmons JG, Mitchell RJ. Curing depth of visible light cured resin. J Dent Res 1983;62:219, abstr. # 448.

91. Ryge G. Clinical criteria. Inter Dent J 1980;30:347.

92. Grossman ES, Matejka JM. Amalgam marginal quality assessment: a comparison of seven methods. J Oral Rehab 1997;24:496-505.

93. Boyde A, Knight PJ. The use of scanning electron microscopy in clinical dental research. Br Dent J 1969;127:313-322.

94. Kidd EAM. Microleakage: a review. J Dent 1976;4:199-206.

95. Alani AH, Toh CG. Detection of microleakage around dental restorations: a Review. Oper Dent 1997;22:173-185.

96. Davila JM, Gwinnett AJ, Robles JC. Marginal adaptation of composite resins and dental bonding agents. J Dent Child 1988;55:25-28.

97. Van Dijken JWV, Horsted BP. The effects of Gluma and Gluma/Scotchbond on in vivo marginal adaptation of a composite resin to dentin. Dent Mater 1989;5:165-167.

98. Roulet JF. Quality Evaluation of Dental Resorations. Chicago, IL: Quintessence Publishing Co., 1989. pp.223-242.

99. Andrews P, Davis RD, Overton JD, Vandewalle KS. Effect of base thickness on cervical gaps in sandwich restorations. J Dent Res 2000;79:abstr #3632.

100. Lutz F, Krejci I. Amalgam substitutes: a critical analysis. J Esthet Dent 2000;12:146-159.

101. Bross IDJ. How to use ridit analysis. Biometrics 1958;3:18.

102. Osborne JW, Phillips RW, Gale EN, Binon PP. Three-year clinical comparison of three amalgam alloy types emphasizing an appraisal of the evaluation methods used. J Amer Dent Assoc 1976;93:784.

103. Mahler DB, Marantz RI. The effect of time on the marginal fracture behaviour of amalgam restorations. J Oral Rehab 1979;6:391.

104. Mjor IA, Espevik S. Assessment of variables in clinical studies of amalgam restorations. J Dent Res 1980;59:1511.

105. Hammesfahr PD, Huang CT, Shaffer SE. Microleakage and bond strength of resin restorations with various bonding agents. Dent Mater 1987;3:194-199.

106. Going RE. Microleakage around dental restorations: a summarizing review. J Amer Dent Assoc 1972;84:1349-1357.

107. Granath LE, Svensson A. Studies of microleakage with restorative materials. A new air pressure method. Scand J Dent Res 1970;78:353-366.

108. Kidd EAM. Microleakage in relation to amalgam and composite restoration. A laboratory study. Br Dent J 1976;141:305-310.

109. Crisp S, Wilson AD. Radioactive tracer technique for monitoring of microleakage: an interim report. J Biomed Mat Res 1980;14:373-382.

110. Hilton, TJ, Schwartz RS, Ferracane JL. Microleakage of four class II resin composite insertion techniques at intraoral temperature. Quintessence Int 1997;28:135-144.

111. Swift EJ, Triolo PT, Barkmeier WW, Bird JL, Bounds SJ. Effect of low viscosity resins on the performance of dental adhesives. Am J Dent 1996;9:100-104.

112. Vargas MA, Swift EJ. Microleakage of resin composites with wet versus dry bonding. Am J Dent 1994;7:187-189.

113. Fortin D, Swift EJ, Denehy GE, Reinhardt JW. Bond strength and microleakage of current dentin adhesives. Dent Mater 1994;10:253-258.

114. Sano H, Takatsu T, Ciucchi B, Horner JA, Mathews WG, Pashley DH. Nanoleakage: leakage within the hybrid layer. Oper Dent 1995;20:18-25.

115. Fayyad MA, Shortall AC. Microleakage of dentine-bonded posterior composite restorations. J Dent 1987;15:67-72.

116. Ausiello P, Davidson CL, Cascone P, de Gee AJ, Rengo S. Debonding of adhesively restored deep class 2 MOD restorations after functional loading. Am J Dent 1999;12:84-88.

117. Rossomando KJ, Wendt SL. Thermocycling and dwell times in microleakage evaluation for bonded restorations. Dent Mater 1995;11:47-51.

118. Grieve AR, Saunders WP, Alani AH. The effects of dentine bonding agents on marginal leakage of composite restorations – long term studies. J Oral Rehab 1993;20:11-18.

119. Jorgensen KD, Matono R, Shimokobe H. Deformation of cavities and resin fillings in loaded teeth. Scand J Dent Res 1976;84:46-50.

120. Peterson EA, Phillips RW, Swartz ML. A comparison of the physical properties of four restorative resins. J Am Dent Assoc 1966;73:1324-1336.

121. Bullard RH, Leinfelder KF, Russell CM. Effect of coefficient of thermal expansion on microleakage. J Am Dent Assoc 1988;116:871-874.

122. Wakabayashi Y, Kondou Y, Suzuki K, Yatani H, Yamashita A. Effect of dissolution of collagen on adhesion to dentin. Int J Prosthodont 7:302-306.

123. Eliades GC, Caputo AA, Vougiouklakis GJ. Composition, wetting properties and bond strength with dentin of 6 new dentin adhesives. Dent Mater 1985;1:170-176.

124. Wendt SL, McInnes PM, Dickinson GL. The effect of thermocycling in microleakage analysis. Dent Mater 1992;8:181-184.

125. Prati C, Tao L, Simpson M, Pashley DH. Permeability and microleakage of Class 2 resin composite restorations. J Dent 1994;22:49-56.

126. Harper RH, Schnell RJ, Swartz ML, Phillips RW. In vivo measurements of thermal diffusion through restorations of various materials. J Prosthet Dent 1980;43(2)180-185.

127. Crim GA, Garcia-Godoy F. Microleakage: the effect of storage and cycling duration. J Prosthet Dent 1987;57:574-576.

128. Soderholm KJ. Degradation of glass filler in experimental composites. J Dent Res 1981. 60;1867-1875.

129. Braem MJA, Davidson CL, Lambrechts P, Vanherle G. In vitro flexural fatigue limits of dental composites. J Biomed Mater Res 1994;28:1397-1402.

130. Sakaguchi RL, Cross M, Douglas WH. A simple model of crack propagation in dental restorations. Dent Mater 1992;8:131-136.

131. Momoi Y, McCabe JF. Hygroscopic expansion of resin based composites during 6 months of water storage. Br Dent J 1994;176:91-96.

132. Mandras RS, Retief DH, Russell CM. The effects of thermal and occlusal stresses on the microleakage of the Scotchbond 2 dentinal bonding system. Dent Mater 1991;7:63-67.

133. Yap A, Stokes AN, Pearson GJ. An in vitro microleakage study of a new multi-purpose dental adhesive system. J Oral Rehab 1996;23:302-308.

134. Jang KT, Chung DH, Shin D, Garcia-Godoy F. Effect of eccentric load cycling on microleakage of class 5 flowable and packable composite resin restorations. Oper Dent 2001;26:603-608.

135. Hakimeh S, Vaidyanathan J, Houpt ML, Vaidyanathan TK, Von Hagen S. Microleakage of compomer class 5 restorations: effect of load cycling, thermal cycling, and cavity shape differences. J Prosthet Dent 2000;83:194-203.

136. Davidson CL, Abdalla AI. Effect of thermal and mechanical load cycling on the marginal integrity of class 2 resin composite restorations. Am J Dent 1993;6:39-42.

137. Darbyshire PA, Messer LB, Douglas WH. Microleakage in class 2 composite restorations bonded to dentin using thermal and load cycling. J Dent Res 1988;67(3):585-587.

138. Munksgaard EC, Itoh K, Jorgensen KD. Dentin-polymer bond in resin fillings tested in vitro by thermo and load cycling. J Dent Res 1985;64(2):144-146.

139. Rigsby DF, Retief DH, Bidez MW, Russell CM. Effect of axial load and temperature cycling on microleakage of resin restorations. Am J Dent 1992;5:155-159.

140. Sanders-Tavares da Cunha Mello F, Feilzer AJ, de Gee AJ, Davidson CL. Sealing ability of eight resin bonding systems in a class 2 restoration after mechanical fatiguing. Dent Mater 1977;13:372-376.

141. Abdalla AI, Davidson CL. Effect of mechanical load cycling on the marginal integrity of adhesive class 2 resin composite restorations. J Dent 1996;24:87-90.

142. Lundin SA, Noren JG. Marginal leakage in occlusally loaded, etched, class 2 composite resin restorations. Acta Odontol Scand 1991;49:247-254.

143. Anderson DJ. Measurement of stress in mastication. J Dent Res 1956;35:671.

144. Gibbs CH. Occlusal forces during chewing and swallowing as measured by sound transmission. J Prosthet Dent 1981;46(4):443.

145. Jent T, Karlsson S, Hedegard B. Mandibular movements of young adults recorded by intraorally placed light-emitting diodes. J Prosthet Dent 1979;42(6):669.

146. Dietschi D, Moor L. Evaluation of the marginal and internal adaptation of different ceramic and composite inlay systems after an in vitro fatigue test. J Adhesive Dent 1999;1:41-56.

147. Krejci, Heinzmann JL, Lutz F. Amalgam und ihrer schmelz-antagonism im computer gesteuerten kausimulator. Schweiz Monatsschr Zahnmed 1990;100:1285-1291.

148. Sakaguchi RL, Douglas WH, DeLong R, Pinatado MR. The wear of a posterior composite in an artificial mouth: a clinical correlation. Dent Mater 1986;2:235-240.

149. Braem M, Lambrechts P, Vanherle G. Clinical relevance of laboratory fatigue studies. J Dent 1994;22:97-102.

150. Baran G, Boberick K, McCool J. Failure of restorative materials. Crit Rev Oral Biol Med 2001;12(4):350-360.

151. Htang A, Ohsawa M, Matsumoto H. Fatigue resistance of composite restorations: effect of filler content. Dent Mater 1995;11:7-13.

152. Braim M, Lambrechts P, Gladys S, Vanherle G. In vitro fatigue behavior of restorative composites and glass ionomomers. Dent Mater 1995;11:137-141.

153. Mahler DB, Engle JH, Phillips DS. The interval nature of an ordinal scale for measuring the marginal fracture of amalgam. Dent Mater 1993;9:162-166.

154. Frankenberger R, Kramer N, Pelka M, Petschelt A. Internal adaptation and overhang formation of direct class 2 resin composite restorations. Clin Oral Invest 1999;3:208-215.

155. Wibowo G, Stockton L. Microleakage of class2 composite restorations. Am J Dent 2001;14:177-185.

156. Yap Auj, Mok BYY, Pearson G. An in vitro microleakage study of the bonded-base restorative technique. J Oral Rehab;24:230-236.

157. Pahsley DH, Livingston MJ. Effect of molecular size on permeability coefficients in human dentine. Archs Oral Biol 1978;23:391-395.

158. Friedl KH, Schmalz G, Hiller KA, Mortazavi F. Marginal adaptation of composite restorations versus hybrid ionomer/composite sandwich restorations. Oper Dent 1997;22;21-29.

159. Sano H, Shono T, Takatsu T, Hosoda H. Microporous dentin zone beneath resin-impregnated layer. Oper Dent 1994;19:59-64.

160. Sano H, Takatsu T, Ciucchi B, Horner JA, Mathews WG, Pashley DH. Nanoleakage: Leakage within the hybrid layer. Oper Dent 1995;20:18-25

161. Tay FR, Gwinnett AJ, Pang KM, Wei SHY. Variability in microleakage observed in a total-etch wet-bonding technique under different handling conditions. J Dent Res 1995;74(5):1168-1178.

162. Opdam NJM, Roeters JJ, Peters TCRB. Consistency of resin composites for posterior use. Dent Mater 1996;12:350-354.

163. Opdam NJ, Roeters JJ, Peters TCRB. Cavity wall adaptation and voids in adhesive Class I resin composite restorations. Dent Mater 1996;12:230-235.

164. Hagge MS, Lindemuth JS, Mason JF, Simon JF. Effect of four treatment layer treatments on microleakage of Class 2 composite restorations. Gen Dent 2001;49(5):489-495.

165. Aboushala A, Kugel G, Hurley E. Class 2 composite resin restorations using glass-ionomer liners: Microleakage studies. J Clin Pediatr Dent 1996;21:67-70.

166. Gwinnett JA, Tay FR, Pang KM, Wei SHY. Comparison of three methods of critical evaluation of microleakage along restorative interfaces. J Prosthet Dent 1995;74:575-585

167. Gale MS, Darvell BW, Cheung GSP. Three-dimensional reconstruction of microleakage pattern using a sequential grinding technique. J Dent 1994;22:370-375.

APPENDIX

PART ONE PILOT

Knoop Hardness

2000 mJ/cm²

	Axial			Occlusal Avg.	stdev	avg	stdev	Avg	Proximal			t-test
1	77.1	71.6	92.3	80	10.7	78	9.95	76	74.8	66.7	86.5	0.05
2	71.6	83.2	95.4	83	11.9	83	5.73	82.5	83.2	76.5	87.9	0.9
3	70	68.6	81.3	73	6.96	71	13.9	68.9	57.9	64.4	84.5	0.43
4	41.9	41.9	59.8	48	10.3	47	6.28	46.6	49.8	39.4	50.7	0.83
5	mush	15.2	19.1	17	2.76	17	4.74	16.3	mush	12.9	19.6	0.64
				Gingival								
5/max	mush	15.4	19.4	17	2.83	17	4.81	16.5	mush	13.1	19.9	

4000 mJ/cm²

	Axial			Occlusal Avg.	stdev	avg	stdev	Avg	Proximal			t-test
1	89.4	83.8	83.8	86	3.2	86	2.2	87	86.5	85.2	89.4	0.63
2	83.8	77.6	83.2	82	3.4	80	4.8	78	75.9	74.2	83.2	0.24
3	56.4	71.6	80.7	70	12	72	3.2	74	75.9	70.6	76.5	0.59
4	62.2	58.2	75.4	65	9	65	0.9	65	64.8	66.2	64.4	0.98
5	38.6	50.4	52.9	47	7.6	44	8.1	40	31.5	39.9	47.7	0.04
				Gingival								
5/max	39.1	51	53.5	48	7.7	44	8.2	40	31.9	40.4	48.3	

6000 mJ/cm²

	Axial			Occlusal Avg.	stdev	avg	stdev	Avg	Proximal			t-test
1	93.9	88.5	91.1	91	2.7	89	6.9	87.6	95.4	85.1	82.3	0.35
2	92.3	90.6	88	90	2.17	86	8.44	81.9	88.6	84.6	72.4	0.15
3	80.7	75.9	88	82	6.09	79	5.36	75.5	69.6	76.7	80.1	0.23
4	72.1	69.9	78	73	4.19	70	4.62	67.2	63.5	65.8	72.4	0.04
5	48.6	50.2	55.3	51	3.5	46	4.85	40.2	45	40.4	35.3	0.15
				Gingival								
5/max	49.2	50.8	56	52	3.56	46	4.95	40.7	45.6	40.9	35.7	

12000 mJ/cm²

	Axial			Occlusal Avg.	stdev	avg	stdev	Avg	Proximal			t-test
1	87.2	86.5	94.9	90	4.7	89	5.7	89	94.6	89.5	83.2	0.95
2	85.2	86	93.8	88	4.8	90	2.5	91	91.6	88	92.7	0.38
3	85.9	81.8	87.5	85	2.9	85	2.4	85	81.9	85.1	86.5	0.81
4	72.6	82.3	87.5	81	7.6	79	5.5	78	74.8	84.1	74.3	0.61
5	60.9	72.4	71.3	68	6.3	65	12	61	47.2	69.1	66.5	0.15
				Gingival								
5/max	61.3	73.3	72.1	69	6.6	65	12	62	47.8	70	67.3	

Knoop Hardness

24000 mJ/cm²

Occlusal

	Axial			Avg.	stdev	avg	stdev	Avg	Proximal			t-test
1	91.6	85.1	96.6	91	5.77	90	4.31	89.3	85.2	89	93.8	0.62
2	87.2	85.1	93.2	89	4.2	88	6.73	86.7	84.5	81.4	94.3	0.35
3	85.9	89.5	92.7	89	3.4	86	8.84	82.2	72.1	86	88.5	0.16
4	74.8	82.3	85.6	81	5.53	79	11.2	77.4	64.8	81.4	86	0.4
5	60.6	69.2	82.8	71	11.2	71	11.6	70.4	64.4	63	83.7	0.88

Gingival

5/max	61.3	70	83.9	72	11.4	71	11.7	71.2	65.2	63.8	84.7

36000 mJ/cm²

Occlusal

	Axial			Avg.	stdev	avg	stdev	Avg	Proximal			t-test
1	90.8	86.5	93.2	90	3.4	90	5.8	90	85.2	89	96.6	0.98
2	85.9	89	91.1	89	2.6	90	4.9	91	87.2	96.6	89.5	0.46
3	87.2	92.7	96	92	4.4	91	4.9	90	84.5	90	94.3	0.02
4	80.7	91.6	88.5	87	5.6	86	2.7	85	83.8	87.5	82.3	0.48
5	64.8	81	85.1	77	11	76	13	76	60.6	82.8	84.1	0.58

Gingival

5/max	65.6	82	86.1	78	11	77	13	77	61.3	83.8	85.1

48000 mJ/cm²

Occlusal

	Axial			Avg.	stdev	avg	stdev	Avg	Proximal			t-test
1	96.2	93.8	91.1	94	2.55	92	2.21	89.6	88.6	88	92.1	0.26
2	88.6	92.1	94.9	92	3.16	92	3.02	91.6	90.8	89	94.9	0.86
3	85.2	91.6	86	88	3.49	90	4.81	93	96.2	95.4	87.5	0.2
4	74.8	88	86.5	83	7.23	84	3.38	84.6	82.5	88.5	82.8	0.7
5	71.1	81.8	87.5	80	8.33	80	3.72	79.9	77.1	78.4	84.1	0.94

Gingival

5/max	71.9	82.8	88.5	81	8.43	81	3.78	80.8	78	79.3	85.1

60000 mJ/cm²

Occlusal

	Axial			Avg.	stdev	avg	stdev	Avg	Proximal			t-test
1	92.3	96.6	96	95	2.3	91	2.3	87	84.5	86.5	89	0.01
2	93.1	94.9	90	93	2.5	91	6.4	89	94.6	89.5	81.8	0.3
3	90.8	98.7	90.6	93	4.6	93	6.1	92	91.6	97.7	85.6	0.42
4	98.7	93.8	88	94	5.4	92	5.3	90	89.4	96	85.6	0.44
5	93.9	88	85.6	89	4.3	89	0.3	88	87.9	88.5	88.5	0.78

Gingival

5/max	95	89	86.6	90	4.3	90	0.3	89	88.9	89.5	89.5

FTIR Actual and Interpolated

interpolated

2000 mJ/cm²

Occlusal

	Axial			Avg.	stdev	avg	stdev	Avg	Proximal			t-test
1	54.1	52	55.4	54	1.72	52.7	1.2	51	52.6	51.6	50.2	0.24
2	49.2	54.1	59.3	54	5.04	54	2.4	54	54.1	51.3	56.1	0.9
3	48.5	47.9	53.3	50	2.95	49	5.9	48	43.4	46.1	54.7	0.43
4	43.9	41.7	41.1	42	1.47	40.1	6.2	38	43.6	39.2	31.3	0.28
5	29.5	36.1	26.3	31	5	27.9	5.3	25	31.1	21.4	22.7	0.37

Gingival

5/max	48.7	59.6	43.4	51	8.26	46	8.7	41	51.4	35.4	37.5

4000 mJ/cm²

Occlusal

	Axial			Avg.	stdev	avg	stdev	Avg	Proximal			t-test
1	53.7	55.4	53.3	54	1.1	54	2.3	54	52.1	53.2	56.5	0.92
2	54.4	51.7	54.1	53	1.4	52.6	2	52	51	50.3	54.1	0.24
3	42.8	49.2	53.1	48	5.2	49.3	1.4	50	51	48.8	51.3	0.59
4	49.5	45.3	47.8	48	2.1	47.2	1.7	47	48.4	46.9	45	0.61
5	33.4	32.2.	41.7	38	5.9	36.1	1.9	35	35.4	36.2	32.5	0.64

Gingival

5/max	57.6	53.2	68.9	60	8.1	59.1	4	58	61.1	59.8	53.7

6000 mJ/cm²

Occlusal

	Axial			Avg.	stdev	avg	stdev	Avg	Proximal			t-test
1	52	53.5	57.8	54	3.01	53.7	2.3	53	52.5	51	55.5	0.28
2	58	57.2	56.1	57	0.92	55.3	3.6	54	56.4	54.7	49.5	0.15
3	53.1	51	56.1	53	2.58	52.1	2.3	51	48.3	51.4	52.8	0.23
4	49.4	48.5	51.9	50	1.77	48.6	2	47	45.8	46.7	49.5	0.04
5	39	42.6	41.6	41	1.86	40	2.6	39	41	36	39.5	0.46

Gingival

5/max	64.4	70.3	68.7	68	3.05	66	4.2	64	67.7	59.5	65.2

12000 mJ/cm²

Occlusal

	Axial			Avg.	stdev	avg	stdev	Avg	Proximal			t-test
1	54	58.4	52	55	3.3	56.1	1.6	57	56.5	59.1	56.3	0.14
2	55	55.3	58.6	56	2	56.8	1	57	57.7	56.1	58.1	0.38
3	55.3	53.5	55.9	55	1.2	54.8	1	55	53.6	54.9	55.5	0.81
4	44.8	51.6	55	50	5.2	50	4.3	49	43.9	51.7	51	0.32
5	44	47.5	47.4	46	2	47.2	4	48	44	52	48	0.35

Gingival

5/max	72.7	78.4	78.3	76	3.3	77.9	6.6	79	72.7	85.9	79.3

FTIR Actual and Interpolated

24000 mJ/cm²

	Occlusal											
	Axial			Avg.	stdev	avg	stdev	Avg	Proximal			t-test
1	56	58.3	57.4	57	1.16	57.3	3.3	57	54	57.2	60.6	0.99
2	55.8	54.9	58.3	56	1.78	56	2.9	56	54.7	53.3	58.8	0.35
3	55.3	56.8	58.1	57	1.44	55.2	3.7	54	49.4	55.3	56.4	0.16
4	53.1	54.2	56.1	54	1.52	54	2	54	54	51.3	55.3	0.48
5	47	50.5	52.8	50	2.92	49.2	3.8	48	45.5	46.6	52.5	0.21
	Gingival											
5/max	77.6	83.4	87.2	83	4.83	81.2	6.2	80	75.1	76.9	86.7	

36000 mJ/cm²

	Occlusal											
	Axial			Avg.	stdev	avg	stdev	Avg	Proximal			t-test
1	58	58.1	59.6	59	0.9	57.7	4.1	57	52	59.7	58.5	0.5
2	55.3	56.6	57.5	56	1.1	56.9	2.1	57	55.8	59.8	56.8	0.46
3	55.8	58.1	59.5	58	1.9	57.3	2.1	57	54.7	57	58.8	0.02
4	53.1	57.7	56.4	56	2.4	55.2	1.1	55	54.4	55.9	53.7	0.48
5	47	51.7	54.6	51	3.8	50	5.4	49	46	45.7	55.2	0.4
	Gingival											
5/max	77.6	85.4	90.1	84	6.3	82.6	8.9	81	76	75.5	91.1	

48000 mJ/cm²

	Occlusal											
	Axial			Avg.	stdev	avg	stdev	Avg	Proximal			t-test
1	54	58.9	58.3	57	2.67	58	2.1	59	56.5	60.4	59.9	0.03
2	56.4	57.9	59.1	58	1.34	57.7	1.3	58	57.3	56.6	59.1	0.86
3	55	57.7	55.3	56	1.48	57.1	2	58	59.6	59.3	55.9	0.2
4	50.6	56.1	55.5	54	3.06	54.4	1.4	55	53.8	56.4	53.9	0.7
5	55	55.2	55.7	55	0.36	54.6	2.6	54	51	54.9	56	0.43
	Gingival											
5/max	90.8	91.1	92	91	0.62	90.2	4.3	89	84.2	90.6	92.5	

60000 mJ/cm²

	Occlusal											
	Axial			Avg.	stdev	avg	stdev	Avg	Proximal			t-test
1	58	60.7	58.3	59	1.5	58.9	2.4	59	56	59.9	60.3	0.84
2	58.3	59.1	57	58	1.1	57.3	2.7	56	58.9	56.8	53.5	0.3
3	57.3	60.7	57.2	58	2	58.1	2.6	58	57.7	60.3	55.1	0.42
4	60.7	58.6	56.1	58	2.3	57.8	2.2	57	56.7	59.5	55.1	0.44
5	54	54.5	54.9	54	0.5	54.7	1.8	55	53	55.3	56.6	0.59
	Gingival											
5/max	89.2	90	90.6	90	0.7	90.3	3	91	87.5	91.3	93.4	

KHN **n = 3** **Flattened template; Data collected directly on end**

4000 mJ/cm^2				avg	st dev		
top	68.8	71.8	67.3	69.3	2.3		
bottom	0.0	6.2	0.0	2.1	3.6	2.84	% of max

6000 mJ/cm^2				avg			
top	67.7	72.2	69.8	69.9	2.3		
bottom	16.0	17.3	15.9	16.4	0.8	22.6	% of max

8000 mJ/cm^2				avg			
top	65.5	71.2	70.5	69.1	3.1		
bottom	25.0	33.6	26.8	28.5	4.5	39.2	% of max

12000 mJ/cm^2				avg			
top	66.4	67.3	70.4	68.0	2.1		
bottom	39.2	39.7	39.1	39.3	0.3	54.1	% of max

24000 mJ/cm^2				avg			
top	69.3	66.9	70.1	68.8	1.7		
bottom	53.2	52.6	52.9	52.9	0.3	72.8	% of max

72000 mJ/cm^2		Control		avg			
top	72.7	70.6	71.9	71.7	1.1		
bottom	69.4	71.6	69.5	70.2	1.2	96.5	% of max

DC **n = 3** **Flattened template; Data collected directly on end**

	4000 mJ/cm^2			avg	st dev		
top	53.0	54.9	54.5	54.1	1.0		
bottom	9.8	13.2	19.8	14.3	5.1	24.5	% of max

	6000 mJ/cm^2			avg			
top	51.7	55.4	53.2	53.4	1.9		
bottom	21.9	30.7	25.9	26.2	4.4	45	% of max

	8000 mJ/cm^2			avg			
top	53.7	56.1	55.2	55.0	1.2		
bottom	33.2	33.4	33.5	33.4	0.2	57.3	% of max

	12000 mJ/cm^2			avg			
top	53.3	55.2	57.1	55.2	1.9		
bottom	41.8	39.0	37.3	39.4	2.3	67.6	% of max

	24000 mJ/cm^2			avg			
top	54.2	56.3	58.0	56.2	1.9		
bottom	47.2	45.5	46.9	46.5	0.9	80	% of max

	72000 mJ/cm^2		Control	avg			
top	57.3	56.8	58.2	57.4	0.7		
bottom	54.6	57.7	57.0	56.4	1.6	97	% of max

KNOOP HARDNESS TECHNIQUE STUDY

Purpose: To determine if the pre-operative use of graphite before Knoop hardness indentation can increase the readability and reduce the variability between evaluators of filar measurements.

Materials and Methods: Three evaluators were asked to determine the length of a Knoop hardness indentation at various occlusal-gingival increments in a specimen of Z250 resin composite. The 5 millimeter long resin composite specimens were created in a flattened tooth template (Figure 7) at 12000 mJ/cm^2 with Shade A-2 Z250, mounted in epoxy resin, sectioned and lightly polished as before. Graphite from a mechanical pencil was placed on one half of the increment. Two indentations were created side by side per increment using a 200 gram load with a 10 second dwell time. One indentation was made in graphite and one increment without. In addition, 5 indentations were made in the nearby mounting epoxy with and without graphite and evaluated by just one evaluator.

Results:

Z250: As can be seen in the tables on the following page, there was a significant increase in the average Knoop hardness number per increment between graphite and non-graphite coated surfaces. Also, there was a significant increase in the standard deviation without the use of graphite ($\alpha = 0.05$).

Epoxy: There was no significant difference in the average Knoop hardness numbers between graphite and non-graphite coated surfaces.

Discussion:

Z250: The use of graphite significantly reduced the variability between operators. The evaluators commented on the ease of readability of the graphite-coated surfaces. There was an apparent underestimation of the indentation without the use of graphite leading to a higher Knoop hardness number. Ideally a highly polished surface should be used to reduce the potential for measurement difficulties. The smoothest surface to is created against a milar strip or glass. However, after sectioning or sanding, it is much more difficult to produce a highly reflective surface. Care was taken in this study not to produce a high polish in the concern of possibly changing the mechanical properties.

Epoxy: Graphite did not have an effect on the actual measurements because it did not affect the Knoop hardness numbers in the highly reflective epoxy resin.

Z250

Knoop Hardness 3 evaluators

12000 mJ/cm^2

depth (mm)	1st Evaluator Graphite	1st Evaluator Non-graphite	2nd Evaluator Occlusal Graphite	2nd Evaluator Occlusal Non-graphite	3rd Evaluator Graphite	3rd Evaluator Non-graphite
1	73.6	81.4	70.6	86.5	76.7	95.4
2	68.2	73.6	67.1	81	69.2	107.8
3	70.3	73.6	68.2	70.3	68.2	92.1
4	62.7	75.5	60.7	70.3	64.3	88
5	57.4	59	56.3	66.5	59.5	81

Summary

	Graphite Avg	Graphite St Dev	Non-graphite Avg	Non-graphite St Dev
1	73.6	3.1	87.8	7.1
2	68.2	1.1	87.5	18.0
3	68.9	1.2	78.7	11.8
4	62.6	1.8	77.9	9.1
5	57.7	1.6	68.8	11.2

0.014158	t-tests treatment
0.000854	variance

Epoxy Resin

Knoop Hardness

	Graphite	Non-graphite
	11.8	12
	12.9	12.9
	12.3	12.3
	12.9	13.1
	12.6	12.6
avg	12.5	12.6
st dev	0.5	0.4

0.78755 t-test

2-Way ANOVA Energy or Location on DC

Tests of Between-Subjects Effects

Dependent Variable: FTIR

Source	Type III Sum of Squares	df	Mean Square	F	Sig.
Corrected Model	2529.834[a]	11	229.985	9.493	.000
Intercept	238290.422	1	238290.422	9835.648	.000
AXPROX	19.803	1	19.803	.817	.375
ENERGY	2455.989	5	491.198	20.275	.000
AXPROX * ENERGY	54.042	5	10.808	.446	.812
Error	581.453	24	24.227		
Total	241401.710	36			
Corrected Total	3111.287	35			

a. R Squared = .813 (Adjusted R Squared = .727)

Estimated Marginal Means

2. ENERGY

Dependent Variable: FTIR

ENERGY	Mean	Std. Error	95% Confidence Interval	
			Lower Bound	Upper Bound
6	65.967	2.009	61.819	70.114
12	77.883	2.009	73.736	82.031
24	81.150	2.009	77.003	85.297
36	82.617	2.009	78.469	86.764
48	90.200	2.009	86.053	94.347
60	90.333	2.009	86.186	94.481

Post Hoc Tests

ENERGY

Multiple Comparisons

Dependent Variable: FTIR
Tukey HSD

(I) ENERGY	(J) ENERGY	Mean Difference (I-J)	Std. Error	Sig.	95% Confidence Interval	
					Lower Bound	Upper Bound
6	12	-11.917*	2.842	.004	-20.703	-3.130
	24	-15.183*	2.842	.000	-23.970	-6.397
	36	-16.650*	2.842	.000	-25.437	-7.863
	48	-24.233*	2.842	.000	-33.020	-15.447
	60	-24.367*	2.842	.000	-33.153	-15.580
12	6	11.917*	2.842	.004	3.130	20.703
	24	-3.267	2.842	.856	-12.053	5.520
	36	-4.733	2.842	.566	-13.520	4.053
	48	-12.317*	2.842	.003	-21.103	-3.530
	60	-12.450*	2.842	.002	-21.237	-3.663
24	6	15.183*	2.842	.000	6.397	23.970
	12	3.267	2.842	.856	-5.520	12.053
	36	-1.467	2.842	.995	-10.253	7.320
	48	-9.050*	2.842	.041	-17.837	-.263
	60	-9.183*	2.842	.037	-17.970	-.397
36	6	16.650*	2.842	.000	7.863	25.437
	12	4.733	2.842	.566	-4.053	13.520
	24	1.467	2.842	.995	-7.320	10.253
	48	-7.583	2.842	.119	-16.370	1.203
	60	-7.717	2.842	.109	-16.503	1.070
48	6	24.233*	2.842	.000	15.447	33.020
	12	12.317*	2.842	.003	3.530	21.103
	24	9.050*	2.842	.041	.263	17.837
	36	7.583	2.842	.119	-1.203	16.370
	60	-.133	2.842	1.000	-8.920	8.653
60	6	24.367*	2.842	.000	15.580	33.153
	12	12.450*	2.842	.002	3.663	21.237
	24	9.183*	2.842	.037	.397	17.970
	36	7.717	2.842	.109	-1.070	16.503
	48	.133	2.842	1.000	-8.653	8.920

Based on observed means.

*. The mean difference is significant at the .05 level.

Homogeneous Subsets

FTIR

Tukey HSD[a,b]

ENERGY	N	Subset 1	Subset 2	Subset 3
6	6	65.967		
12	6		77.883	
24	6		81.150	
36	6		82.617	82.617
48	6			90.200
60	6			90.333
Sig.		1.000	.566	.109

Means for groups in homogeneous subsets are displayed.
Based on Type III Sum of Squares
The error term is Mean Square(Error) = 24.227.

a. Uses Harmonic Mean Sample Size = 6.000.

b. Alpha = .05.

2-Way ANOVA Energy or Location on KHN

Tests of Between-Subjects Effects

Dependent Variable: KNOOP

Source	Type III Sum of Squares	df	Mean Square	F	Sig.
Corrected Model	7023.334[a]	11	638.485	8.560	.000
Intercept	185890.323	1	185890.323	2492.310	.000
AXPROX	113.423	1	113.423	1.521	.229
ENERGY	6751.429	5	1350.286	18.104	.000
AXPROX * ENERGY	158.482	5	31.696	.425	.827
Error	1790.053	24	74.586		
Total	194703.710	36			
Corrected Total	8813.388	35			

a. R Squared = .797 (Adjusted R Squared = .704)

Estimated Marginal Means

2. ENERGY

Dependent Variable: KNOOP

ENERGY	Mean	Std. Error	95% Confidence Interval	
			Lower Bound	Upper Bound
6	46.367	3.526	39.090	53.643
12	65.300	3.526	58.023	72.577
24	71.483	3.526	64.207	78.760
36	77.317	3.526	70.040	84.593
48	80.933	3.526	73.657	88.210
60	89.750	3.526	82.473	97.027

Post Hoc Tests

ENERGY

Multiple Comparisons

Dependent Variable: KNOOP
Tukey HSD

(I) ENERGY	(J) ENERGY	Mean Difference (I-J)	Std. Error	Sig.	95% Confidence Interval	
					Lower Bound	Upper Bound
6	12	-18.933*	4.986	.010	-34.350	-3.516
	24	-25.117*	4.986	.000	-40.534	-9.700
	36	-30.950*	4.986	.000	-46.367	-15.533
	48	-34.567*	4.986	.000	-49.984	-19.150
	60	-43.383*	4.986	.000	-58.800	-27.966
12	6	18.933*	4.986	.010	3.516	34.350
	24	-6.183	4.986	.813	-21.600	9.234
	36	-12.017	4.986	.192	-27.434	3.400
	48	-15.633*	4.986	.046	-31.050	-.216
	60	-24.450*	4.986	.001	-39.867	-9.033
24	6	25.117*	4.986	.000	9.700	40.534
	12	6.183	4.986	.813	-9.234	21.600
	36	-5.833	4.986	.846	-21.250	9.584
	48	-9.450	4.986	.429	-24.867	5.967
	60	-18.267*	4.986	.014	-33.684	-2.850
36	6	30.950*	4.986	.000	15.533	46.367
	12	12.017	4.986	.192	-3.400	27.434
	24	5.833	4.986	.846	-9.584	21.250
	48	-3.617	4.986	.977	-19.034	11.800
	60	-12.433	4.986	.166	-27.850	2.984
48	6	34.567*	4.986	.000	19.150	49.984
	12	15.633*	4.986	.046	.216	31.050
	24	9.450	4.986	.429	-5.967	24.867
	36	3.617	4.986	.977	-11.800	19.034
	60	-8.817	4.986	.503	-24.234	6.600
60	6	43.383*	4.986	.000	27.966	58.800
	12	24.450*	4.986	.001	9.033	39.867
	24	18.267*	4.986	.014	2.850	33.684
	36	12.433	4.986	.166	-2.984	27.850
	48	8.817	4.986	.503	-6.600	24.234

Based on observed means.

*. The mean difference is significant at the .05 level.

Homogeneous Subsets

KNOOP

Tukey HSD[a,b]

ENERGY	N	Subset 1	2	3	4
6	6	46.367			
12	6		65.300		
24	6		71.483	71.483	
36	6		77.317	77.317	77.317
48	6			80.933	80.933
60	6				89.750
Sig.		1.000	.192	.429	.166

Means for groups in homogeneous subsets are displayed.
Based on Type III Sum of Squares
The error term is Mean Square(Error) = 74.586.

a. Uses Harmonic Mean Sample Size = 6.000.

b. Alpha = .05.

1-Way ANOVA; Energy vs KHN and Energy vs DC

Between-Subjects Factors

		N
ENERGY	12	3
	24	3
	4	3
	6	3
	8	3
	con	3

Descriptive Statistics

Dependent Variable: KHN

ENERGY	Mean	Std. Deviation	N
12	39.333	.321	3
24	52.900	.300	3
4	2.067	3.580	3
6	16.400	.781	3
8	28.467	4.536	3
con	70.167	1.242	3
Total	34.889	23.287	18

Tests of Between-Subjects Effects

Dependent Variable: KHN

Source	Type III Sum of Squares	df	Mean Square	F	Sig.
Corrected Model	9147.171[a]	5	1829.434	307.181	.000
Intercept	21910.222	1	21910.222	3678.955	.000
ENERGY	9147.171	5	1829.434	307.181	.000
Error	71.467	12	5.956		
Total	31128.860	18			
Corrected Total	9218.638	17			

a. R Squared = .992 (Adjusted R Squared = .989)

Post Hoc Tests

ENERGY

Multiple Comparisons

Dependent Variable: KHN
Tukey HSD

(I) ENERGY	(J) ENERGY	Mean Difference (I-J)	Std. Error	Sig.	95% Confidence Interval	
					Lower Bound	Upper Bound
12	24	-13.567*	1.993	.000	-20.260	-6.874
	4	37.267*	1.993	.000	30.574	43.960
	6	22.933*	1.993	.000	16.240	29.626
	8	10.867*	1.993	.002	4.174	17.560
	con	-30.833*	1.993	.000	-37.526	-24.140
24	12	13.567*	1.993	.000	6.874	20.260
	4	50.833*	1.993	.000	44.140	57.526
	6	36.500*	1.993	.000	29.807	43.193
	8	24.433*	1.993	.000	17.740	31.126
	con	-17.267*	1.993	.000	-23.960	-10.574
4	12	-37.267*	1.993	.000	-43.960	-30.574
	24	-50.833*	1.993	.000	-57.526	-44.140
	6	-14.333*	1.993	.000	-21.026	-7.640
	8	-26.400*	1.993	.000	-33.093	-19.707
	con	-68.100*	1.993	.000	-74.793	-61.407
6	12	-22.933*	1.993	.000	-29.626	-16.240
	24	-36.500*	1.993	.000	-43.193	-29.807
	4	14.333*	1.993	.000	7.640	21.026
	8	-12.067*	1.993	.001	-18.760	-5.374
	con	-53.767*	1.993	.000	-60.460	-47.074
8	12	-10.867*	1.993	.002	-17.560	-4.174
	24	-24.433*	1.993	.000	-31.126	-17.740
	4	26.400*	1.993	.000	19.707	33.093
	6	12.067*	1.993	.001	5.374	18.760
	con	-41.700*	1.993	.000	-48.393	-35.007
con	12	30.833*	1.993	.000	24.140	37.526
	24	17.267*	1.993	.000	10.574	23.960
	4	68.100*	1.993	.000	61.407	74.793
	6	53.767*	1.993	.000	47.074	60.460
	8	41.700*	1.993	.000	35.007	48.393

Based on observed means.

*. The mean difference is significant at the .05 level.

Homogeneous Subsets

KHN

Tukey HSD[a,b]

ENERGY	N	Subset					
		1	2	3	4	5	6
4	3	2.067					
6	3		16.400				
8	3			28.467			
12	3				39.333		
24	3					52.900	
con	3						70.167
Sig.		1.000	1.000	1.000	1.000	1.000	1.000

Means for groups in homogeneous subsets are displayed.
Based on Type III Sum of Squares
The error term is Mean Square(Error) = 5.956.

a. Uses Harmonic Mean Sample Size = 3.000.

b. Alpha = .05.

Univariate Analysis of Variance

Between-Subjects Factors

		N
ENERGY	12	3
	24	3
	4	3
	6	3
	8	3
	con	3

Descriptive Statistics

Dependent Variable: DC

ENERGY	Mean	Std. Deviation	N
12	39.367	2.272	3
24	46.533	.907	3
4	14.267	5.085	3
6	26.167	4.406	3
8	33.367	.153	3
con	56.433	1.626	3
Total	36.022	14.256	18

Tests of Between-Subjects Effects

Dependent Variable: DC

Source	Type III Sum of Squares	df	Mean Square	F	Sig.
Corrected Model	3347.311[a]	5	669.462	74.495	.000
Intercept	23356.809	1	23356.809	2599.051	.000
ENERGY	3347.311	5	669.462	74.495	.000
Error	107.840	12	8.987		
Total	26811.960	18			
Corrected Total	3455.151	17			

a. R Squared = .969 (Adjusted R Squared = .956)

Post Hoc Tests

ENERGY

Multiple Comparisons

Dependent Variable: DC
Tukey HSD

(I) ENERGY	(J) ENERGY	Mean Difference (I-J)	Std. Error	Sig.	95% Confidence Interval	
					Lower Bound	Upper Bound
12	24	-7.167	2.448	.102	-15.388	1.055
	4	25.100*	2.448	.000	16.878	33.322
	6	13.200*	2.448	.002	4.978	21.422
	8	6.000	2.448	.213	-2.222	14.222
	con	-17.067*	2.448	.000	-25.288	-8.845
24	12	7.167	2.448	.102	-1.055	15.388
	4	32.267*	2.448	.000	24.045	40.488
	6	20.367*	2.448	.000	12.145	28.588
	8	13.167*	2.448	.002	4.945	21.388
	con	-9.900*	2.448	.016	-18.122	-1.678
4	12	-25.100*	2.448	.000	-33.322	-16.878
	24	-32.267*	2.448	.000	-40.488	-24.045
	6	-11.900*	2.448	.004	-20.122	-3.678
	8	-19.100*	2.448	.000	-27.322	-10.878
	con	-42.167*	2.448	.000	-50.388	-33.945
6	12	-13.200*	2.448	.002	-21.422	-4.978
	24	-20.367*	2.448	.000	-28.588	-12.145
	4	11.900*	2.448	.004	3.678	20.122
	8	-7.200	2.448	.100	-15.422	1.022
	con	-30.267*	2.448	.000	-38.488	-22.045
8	12	-6.000	2.448	.213	-14.222	2.222
	24	-13.167*	2.448	.002	-21.388	-4.945
	4	19.100*	2.448	.000	10.878	27.322
	6	7.200	2.448	.100	-1.022	15.422
	con	-23.067*	2.448	.000	-31.288	-14.845
con	12	17.067*	2.448	.000	8.845	25.288
	24	9.900*	2.448	.016	1.678	18.122
	4	42.167*	2.448	.000	33.945	50.388
	6	30.267*	2.448	.000	22.045	38.488
	8	23.067*	2.448	.000	14.845	31.288

Based on observed means.

*. The mean difference is significant at the .05 level.

Homogeneous Subsets

DC

Tukey HSD[a,b]

ENERGY	N	Subset 1	2	3	4	5
4	3	14.267				
6	3		26.167			
8	3		33.367	33.367		
12	3			39.367	39.367	
24	3				46.533	
con	3					56.433
Sig.		1.000	.100	.213	.102	1.000

Means for groups in homogeneous subsets are displayed.
Based on Type III Sum of Squares
The error term is Mean Square(Error) = 8.987.

a. Uses Harmonic Mean Sample Size = 3.000.

b. Alpha = .05.

PART TWO
FIRST PILOT

First Pilot Study

- 5 mm prep - dentin cervical margin

- 4000 mJ/cm^2 - 60% of max cure

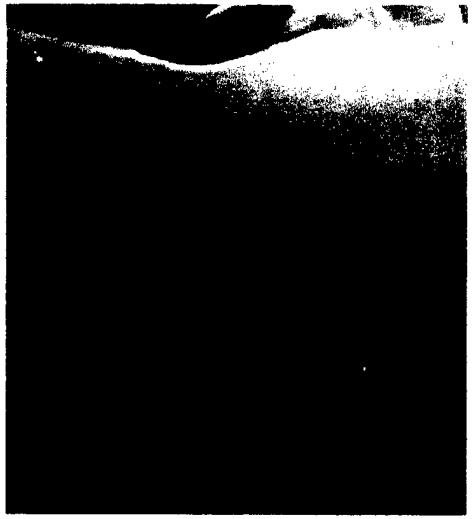

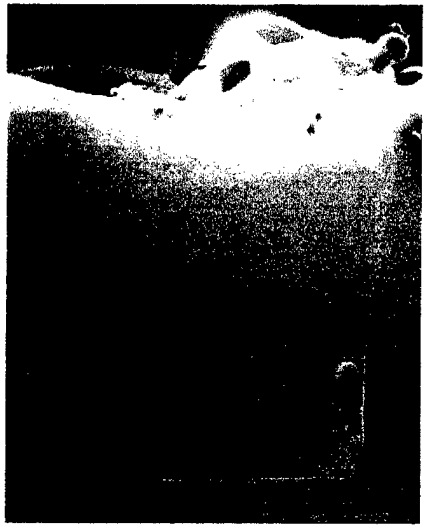

- 5 mm prep - dentin cervical margin

- 4000 mJ/cm^2 - 60% of max cure

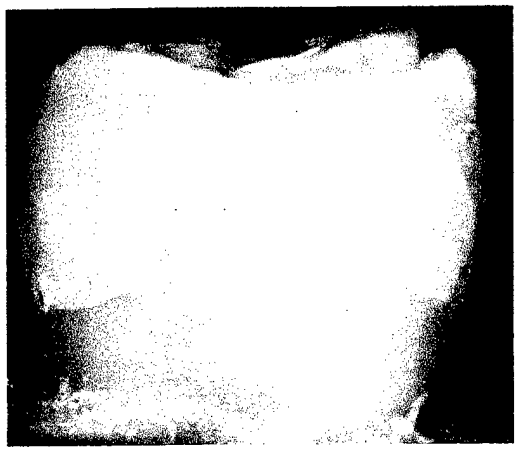

Pre-operative

Post-thermal

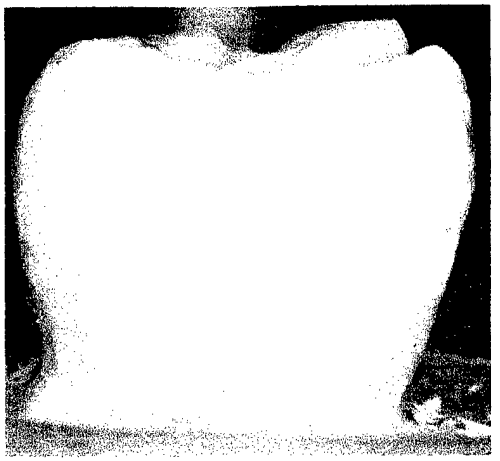

Post-fatigue

- 5 mm prep
- dentin cervical margin
- 4000 mJ/cm^2
- 60% of max cure

	Pre-op	Post-thermal	Post-fatigue
1	bubble	49.24	16.17
2	0	19.08	34.26
3	0	23.49	0
4	23	31.8	0
5	15.76	40.62	0
6	0	17.13	0
7	3.43	14.19	0
8	0	13.9	0
9	0	15.19	3.43
10	0	22.51	0
11	0	75.37	0
12	0	2.45	0
13	0	87.09	0
14	bubble	bubble	0
15	bubble	bubble	0
16	bubble	bubble	0
17	0	bubble	0
18	0	bubble	0
19	0	11.74	0
20	0	13.7	2.16
21	0	16.15	9.3
22	0	34.3	11.74
23	0	17.13	0
24	0	14.68	0
25	0	17.15	0
avg.	2.0	26.8	3.1
std dev	5.9	21.6	7.7
% gapped	10	100	24

- 5 mm prep - dentin margins

- 12000 mJ/cm^2 - 80% of max cure

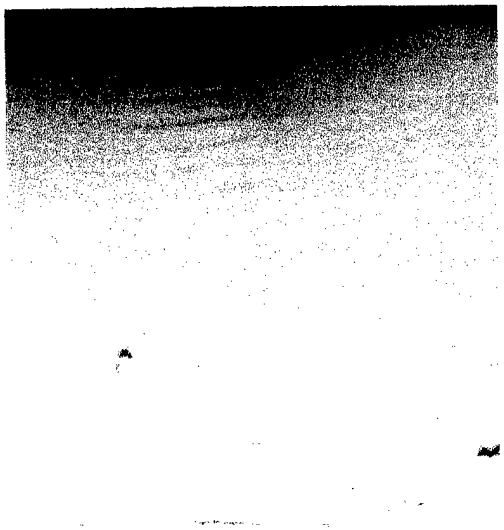

Pre-operative 12X

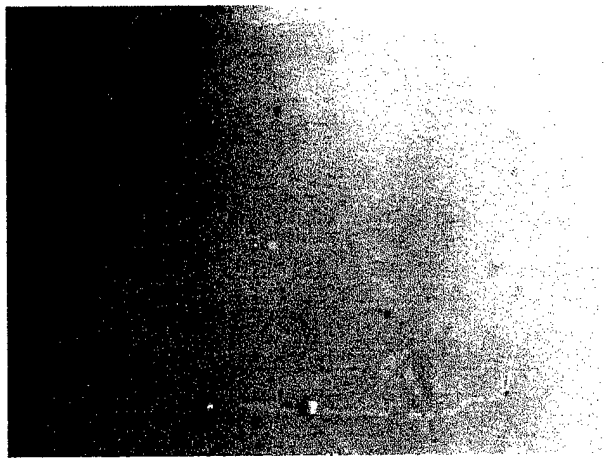

Post-thermal 12X

Post-fatigue 12X

- 5 mm prep - dentin margins
- 12000 mJ/cm^2 - 80% of max cure

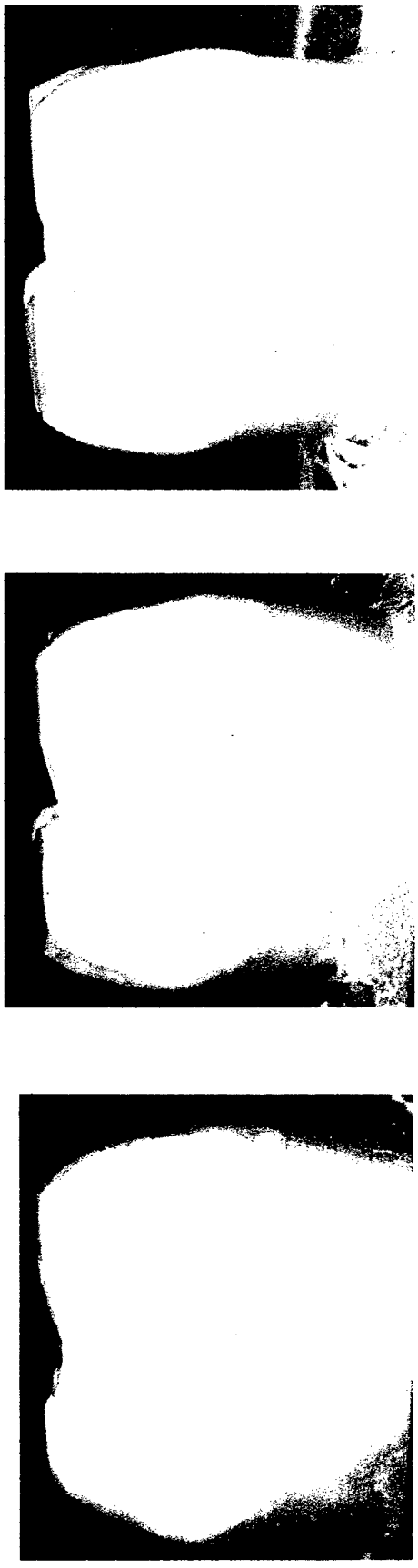

- 5 mm prep
- dentin margins
- 12000 mJ/cm^2
- 80% of max cure

	Pre-op	Post-thermal	Post-fatigue
1	7.4	2.5	10.2
2	8.9	7.6	7.0
3	9.3	5.1	2.6
4	2.7	2.3	2.2
5	0.0	0.0	6.3
6	7.9	0.0	8.9
7	10.6	11.8	6.8
8	17.5	8.9	0.0
9	4.5	0.7	1.9
10	1.4	0.0	1.3
11	5.1	2.5	8.9
12	5.5	1.7	10.1
13	8.2	10.8	9.5
14	10.0	4.4	12.0
15	0.0	1.3	1.3
16	1.5	0.0	10.8
17	2.7	6.3	4.6
18	0.0	3.8	0.0
19	3.2	1.9	2.2
20	1.0	0.0	4.4
21	12.7	3.2	14.8
22	2.1	4.4	3.9
23	3.4	0.9	5.7
24	1.4	0.0	0.0
25	1.4	4.4	2.6
avg.	5.1	3.4	5.5
std dev	4.6	3.4	4.2
% gapped	88.0	76.0	88.0

- 5 mm prep - dentin margins

- 48000 mJ/cm^2 - 90% of max cure

Pre-operative 12X

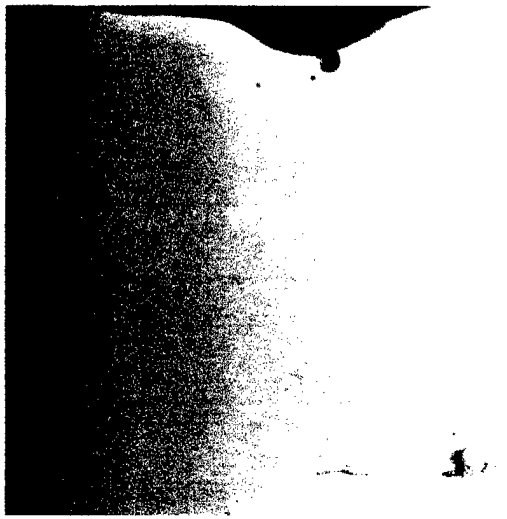

Post-thermal 12X

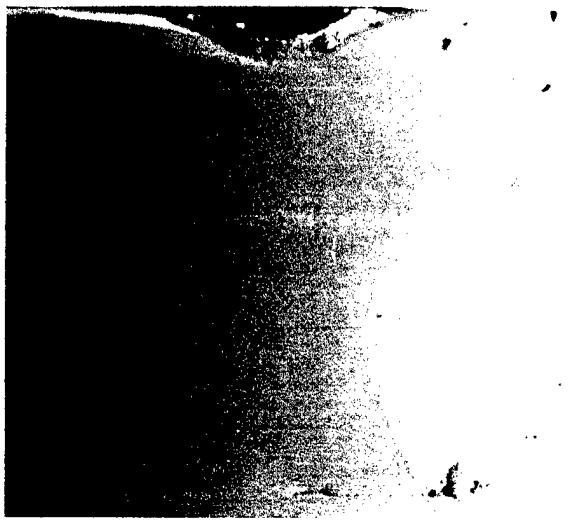

Post-fatigue 12X

- 5 mm prep - dentin margins

- 48000 mJ/cm^2 - 90% of max cure

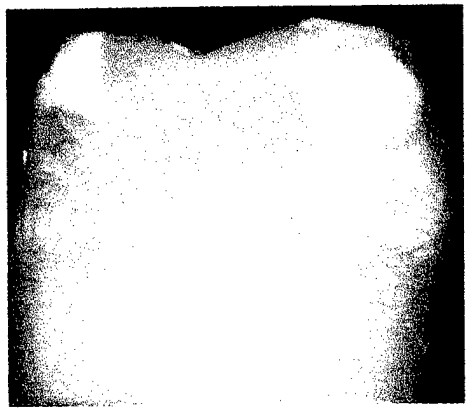

Pre-operative 12X

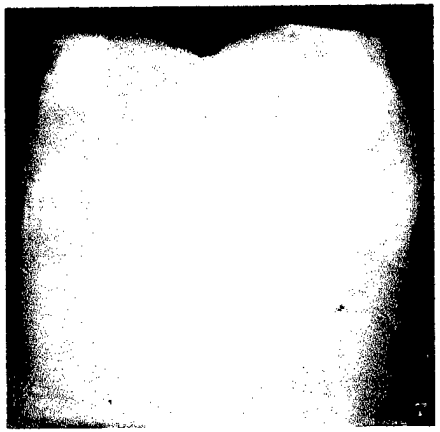

Post-thermal 12X

Post-fatigue 12X

- 5 mm prep
- dentin margins
- 48000 mJ/cm^2
- 90% of max cure

	Pre-op	Post-thermal	Post-fatigue
1	7.5	2.8	4.8
2	bubble	bubble	bubble
3	bubble	bubble	bubble
4	bubble	bubble	bubble
5	5.1	59.6	56.3
6	27.9	19.6	24.2
7	0.0	3.2	7.0
8	5.1	17.0	0.0
9	8.2	7.0	6.7
10	5.7	4.4	7.6
11	13.9	13.8	13.7
12	24.0	34.9	11.4
13	3.8	20.3	22.8
14	14.5	22.2	19.0
15	0.0	7.0	12.7
16	1.9	4.4	0.0
17	0.0	4.4	3.8
18	1.9	0.0	3.8
19	0.0	3.8	0.0
20	4.4	0.7	7.6
21	0.0	0.9	0.0
22	1.3	0.0	0.0
23	0.0	0.0	0.0
24	0.0	1.3	0.0
25	0.0	3.8	6.3
avg.	5.7	10.5	9.4
std dev	7.9	14.3	12.8
% gapped	63.0	86.0	68.0

PART TWO
SECOND PILOT

Second Pilot

4000 mJ/cm2 5mm dentin 20% of max

pre-op

post-therm

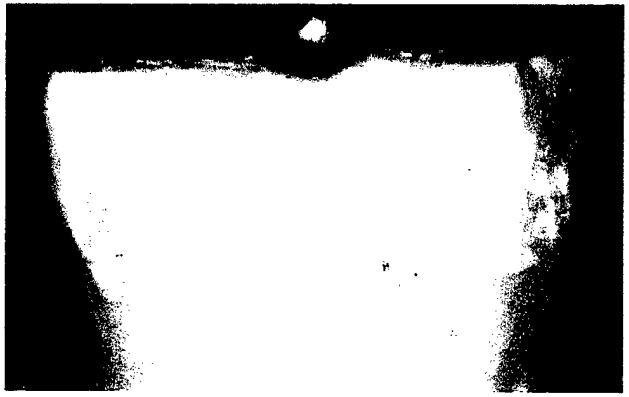

50k cycles

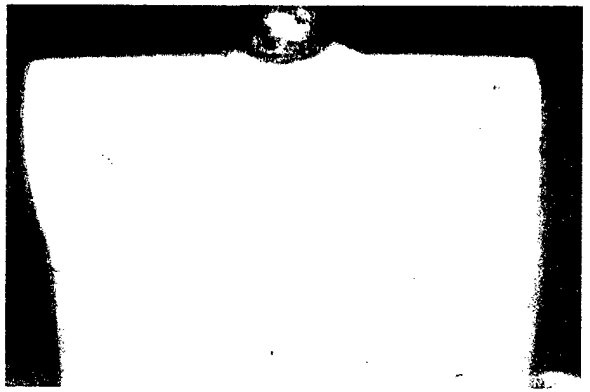

250k cycles

4000 mJ/cm2 5mm dentin 20% of max

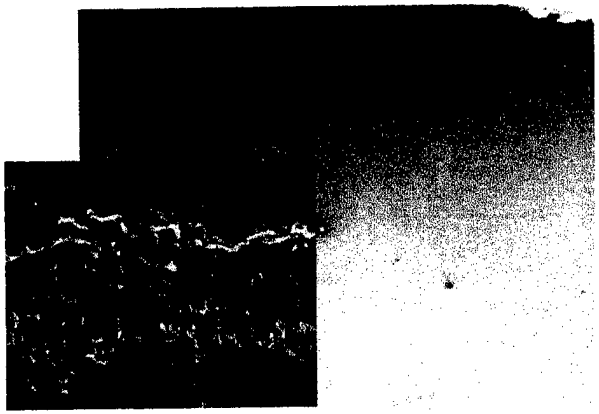

pre-op

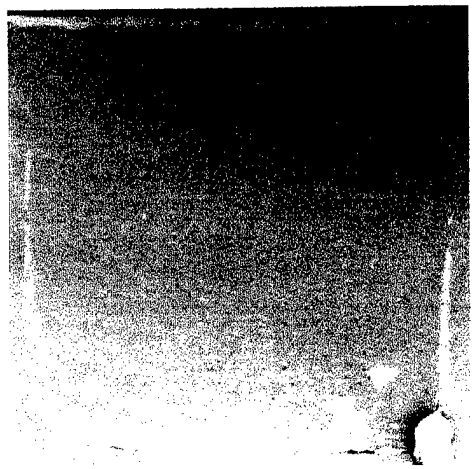

post-therm

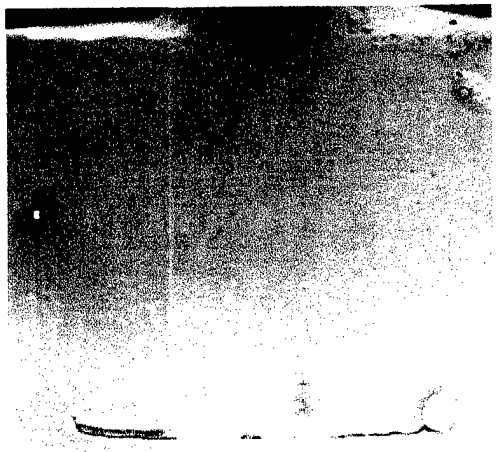

50k cycles

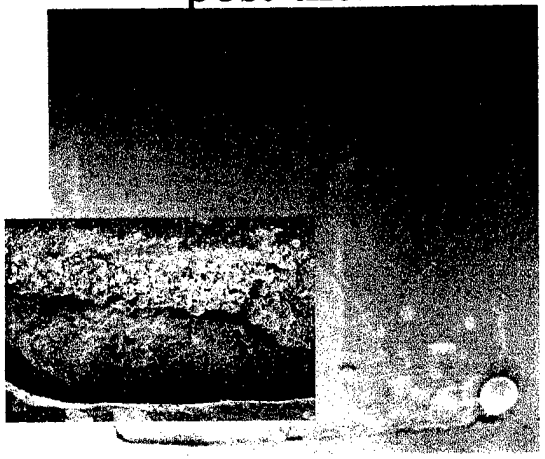

250k cycles

4000 mJ/cm2 5mm dentin 20% of max

	Pre-op	Post-thermal	50K cyc	250K cyc
1	bubble	bubble	bubble	80.1
2	0.0	bubble	17.9	40.8
3	0.0	22.8	14.1	5.1
4	0.0	0.0	20.9	3.0
5	0.0	20.7	19.6	9.7
6	0.0	16.0	24.1	0.0
7	0.0	13.1	21.7	0.0
8	0.0	5.9	21.4	0.0
9	0.0	2.5	0.0	0.0
10	0.0	16.2	6.3	0.0
11	0.0	0.0	14.1	9.3
12	0.0	0.0	0.0	4.6
13	0.0	0.5	27.2	35.5
14	0.0	9.7	27.2	0.0
15	0.0	0.0	0.0	0.0
16	0.0	0.0	0.0	0.0
17	0.0	0.7	0.0	0.0
18	3.8	4.4	0.0	0.0
19	0.0	0.0	17.1	6.2
20	0.0	22.3	15.7	9.5
21	0.0	22.8	15.5	10.1
22	0.0	16.0	18.2	6.1
23	0.0	0.0	19.3	5.2
24	0.0	0.0	13.5	24.5
25	0.0	0.0	22.6	17.7
avg.	0.2	7.5	14.0	10.7
std dev	0.8	8.9	9.4	18.2
% gapped	4.0	64.0	76.0	60

6000 mJ/cm2 5mm dentin 45% of max

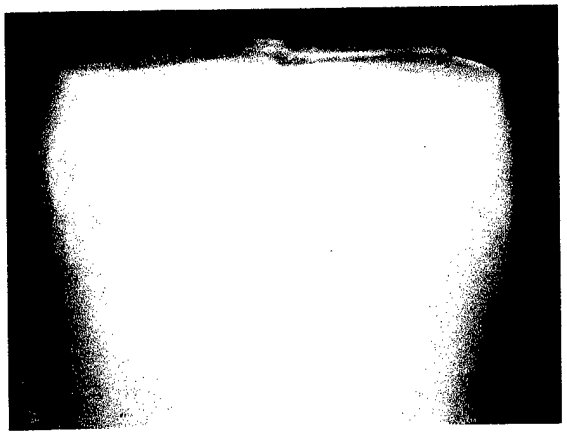

pre-op

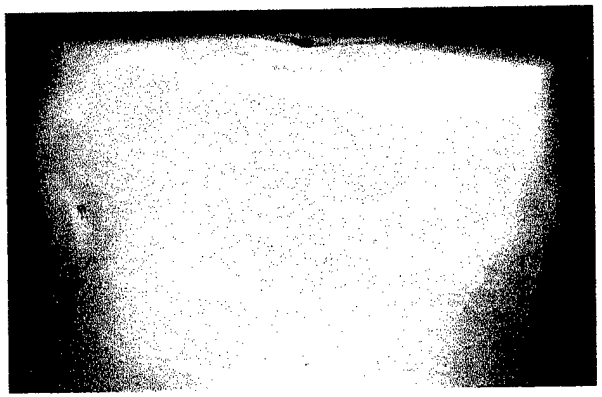

post-therm

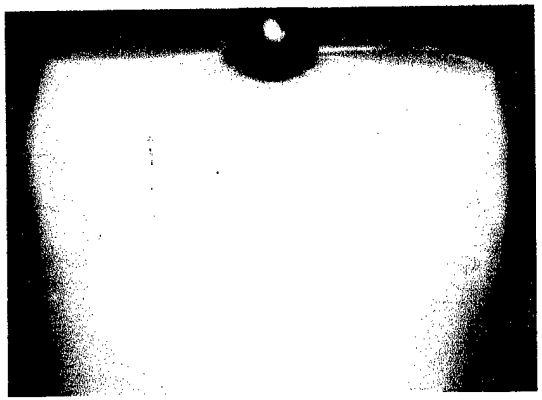

50k cycles

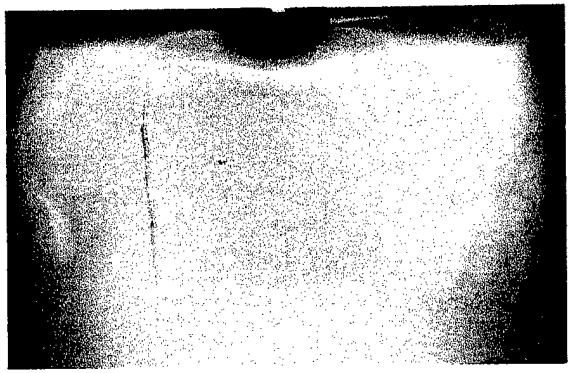

250k cycles

6000 mJ/cm2 5mm dentin 45% of max

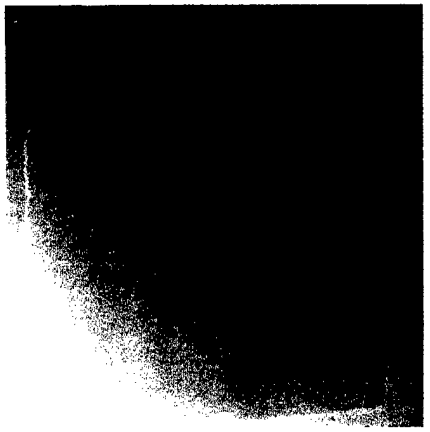

pre-op

post-

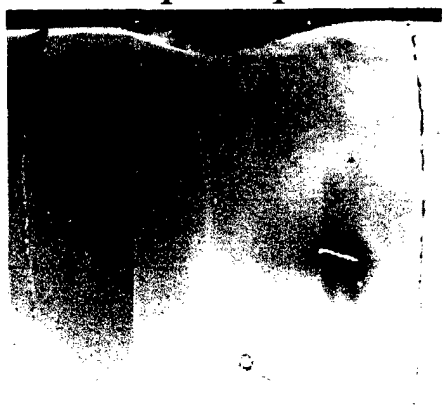

50k cycles

250k cycles

6000 mJ/cm2 5mm dentin 45% of max

	Pre-op	Post-thermal	50K cyc	250K cyc
1	0.0	0.0	0.0	0.0
2	0.0	0.0	0.0	0.0
3	0.0	0.0	0.0	0.0
4	0.0	0.0	8.2	12.4
5	0.0	0.0	0.0	0.0
6	0.0	0.0	0.0	0.0
7	0.0	0.0	0.0	0.0
8	1.0	0.0	0.0	0.0
9	3.6	3.6	0.0	4.8
10	0.0	3.2	0.0	2.9
11	0.0	0.0	0.0	0.0
12	0.0	0.0	0.0	0.0
13	0.0	0.0	3.5	7.3
14	0.0	0.0	0.0	0.0
15	0.0	0.0	2.9	0.0
16	0.0	0.0	2.9	0.0
17	0.0	0.0	6.3	0.0
18	3.8	0.0	0.0	0.0
19	1.0	4.8	11.4	0.0
20	0.0	6.0	0.0	0.0
21	0.0	0.0	0.0	0.0
22	0.0	0.0	0.0	0.0
23	0.0	0.0	0.0	5.4
24	0.0	0.0	0.0	4.4
25	0.0	0.0	25.3	15.6
avg.	0.4	0.7	2.5	2.1
std dev	1.0	1.7	5.7	4.2
% gapped	16.0	16.0	28.0	28.0

8000 mJ/cm2 5mm dentin 58% of max

pre-op

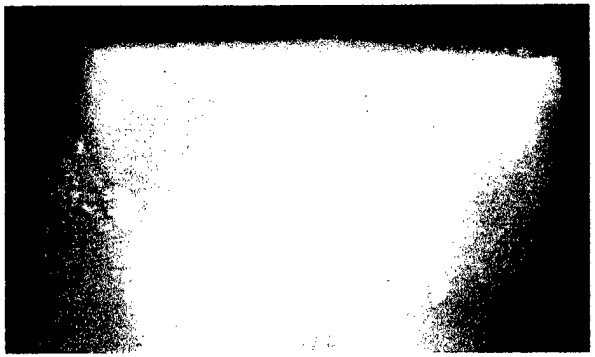

post-therm

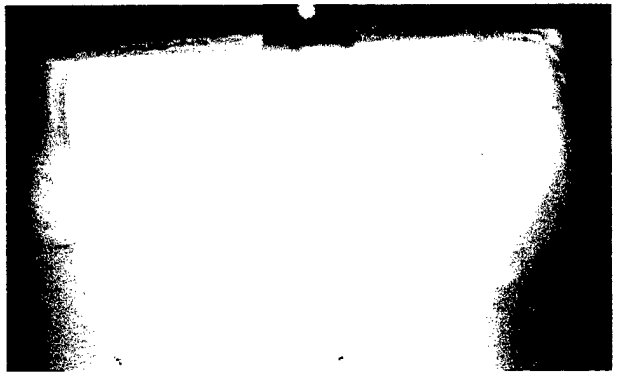

50k cycles

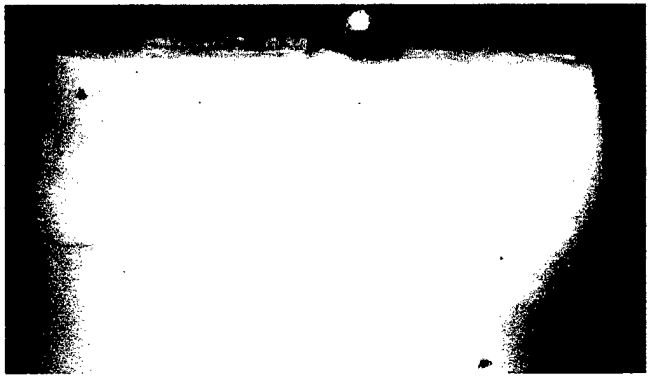

250k cycles

8000 mJ/cm2 5mm dentin 58% of max

pre-op

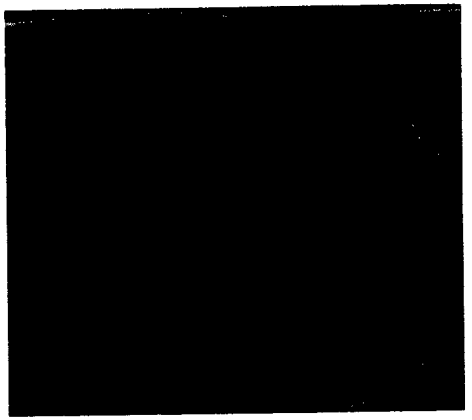

post-therm

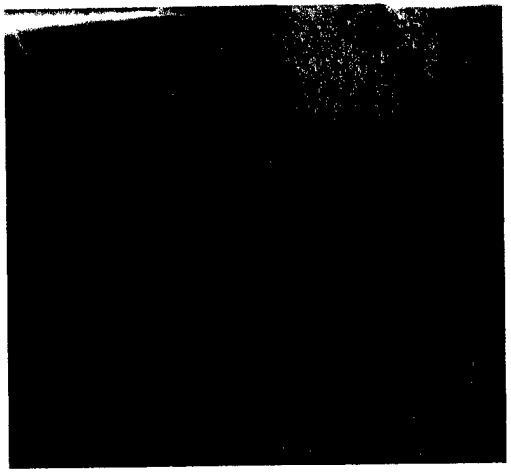

50k cycles

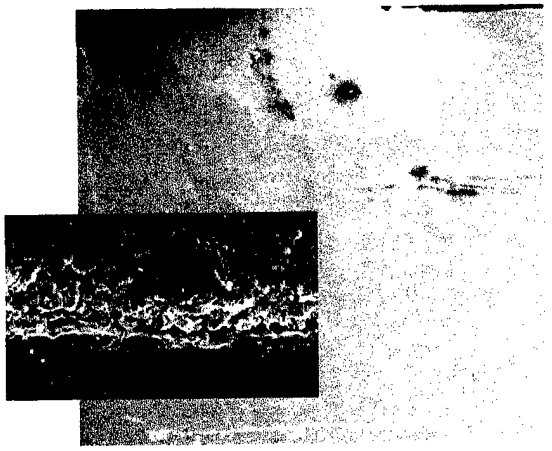

250k cycles

8000 mJ/cm2 5mm dentin 58% of max

	Pre-op	Post-thermal	50K cyc	250K cyc
1	0.0	0.0	0.0	3.8
2	0.0	0.0	0.0	0.0
3	0.0	0.0	0.0	0.0
4	0.0	0.0	2.2	7.3
5	0.0	0.0	0.0	6.8
6	0.0	0.0	8.6	0.0
7	0.0	0.0	0.0	0.0
8	0.0	0.0	0.0	0.0
9	0.0	0.0	0.0	0.0
10	0.0	0.0	0.0	0.0
11	0.0	6.7	0.0	2.5
12	1.5	0.0	0.0	0.0
13	0.0	0.0	0.0	0.0
14	0.0	0.0	0.0	0.0
15	0.0	0.0	0.0	0.0
16	0.0	0.0	0.0	0.0
17	0.0	0.0	0.0	4.1
18	0.0	0.0	0.0	0.0
19	0.0	0.0	0.0	0.0
20	0.0	0.0	0.0	0.0
21	0.0	0.0	0.0	0.0
22	0.0	0.0	0.0	0.0
23	0.0	0.0	0.0	0.0
24	0.0	0.0	0.0	0.0
25	0.0	0.0	0.0	0.0
avg.	0.1	0.3	0.5	1.0
std dev	0.3	1.3	1.8	2.2
% gapped	4.0	4.0	8.0	16.0

10000 mJ/cm2 5mm dentin 68% of max

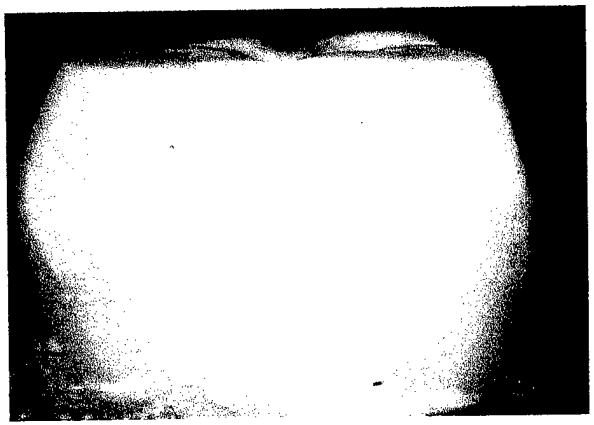

pre-op

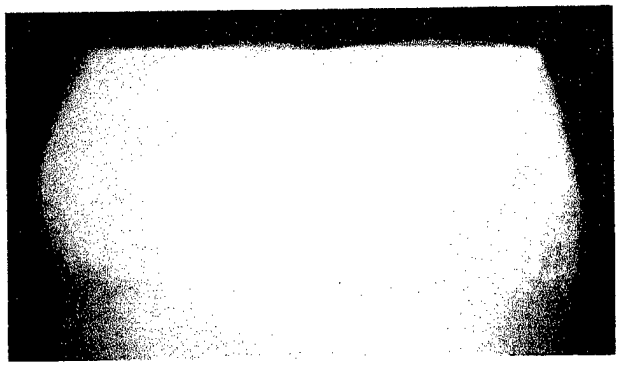

post-therm

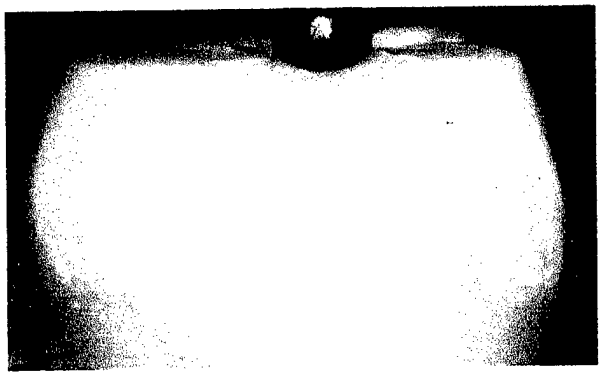

50k cycles

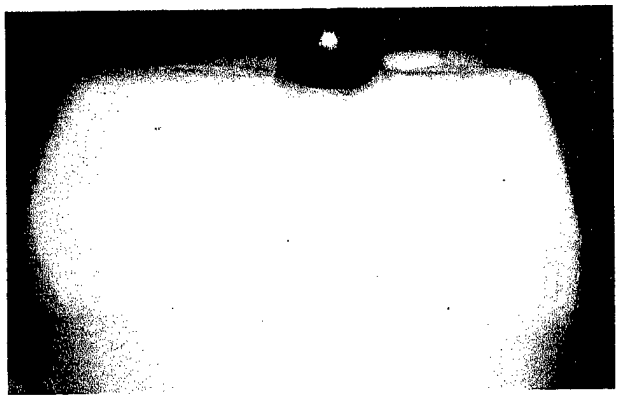

250k cycles

10000 mJ/cm2 5mm dentin 68% of max

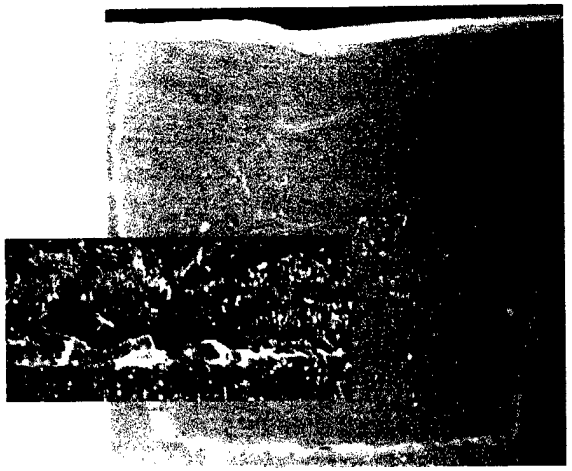

pre-op

post-therm

50k cycles

250k cycles

10000 mJ/cm2 5mm dentin 68% of max

	Pre-op	Post-thermal	50K cyc	250K cyc
1	7.2	16.5	68.0	68.0
2	0.0	0.0	53.8	53.8
3	8.2	3.8	0.0	0.0
4	0.0	0.0	0.0	6.6
5	0.0	0.0	5.1	0.0
6	0.0	2.2	bubble	0.0
7	0.0	3.5	0.0	0.0
8	0.0	0.0	0.0	0.0
9	0.0	7.6	0.0	0.0
10	1.8	0.0	0.0	5.5
11	0.0	0.0	0.0	1.1
12	25.7	9.5	0.0	0.0
13	0.0	3.2	0.0	0.0
14	0.0	0.0	0.0	0.0
15	0.0	0.0	0.0	0.0
16	0.0	0.0	0.0	2.1
17	8.6	5.7	0.0	7.4
18	0.0	4.8	0.0	0.0
19	0.0	0.0	0.0	4.3
20	0.0	0.0	0.0	0.0
21	0.0	0.0	3.9	0.0
22	0.0	11.4	0.0	3.5
23	0.0	0.0	0.0	0.0
24	0.0	0.0	18.2	0.0
25	0.0	11.8	20.9	20.9
avg.	2.1	3.2	4.4	6.9
std dev	5.6	4.7	12.2	17.0
% gapped	20.0	44.0	24.0	40.0

12000 mJ/cm2 5mm dentin 71% of max

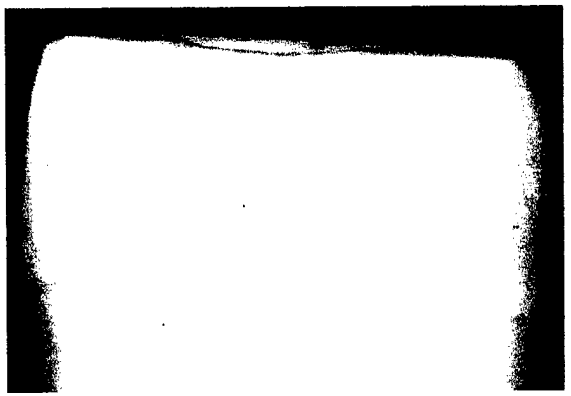

pre-op

post-therm

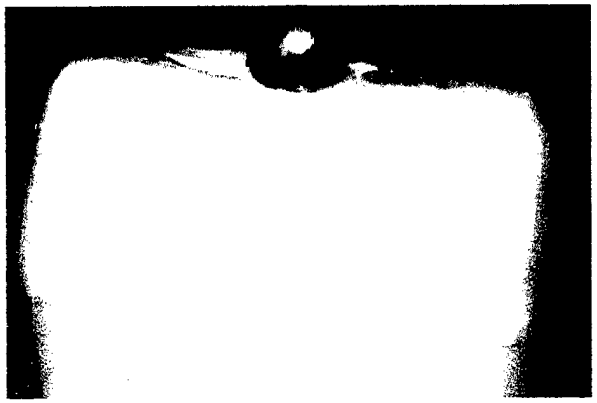

50k cycles

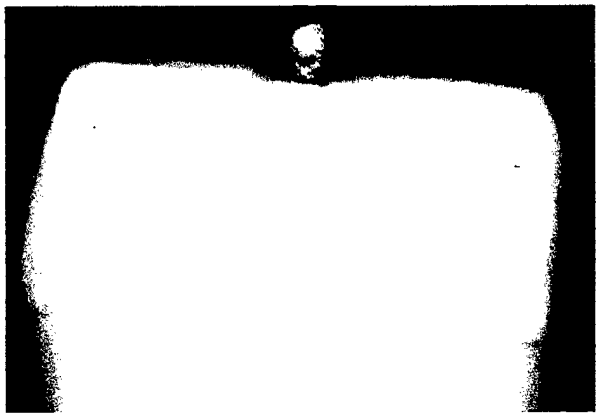

250k cycles

12000 mJ/cm2 5mm dentin 71% of max

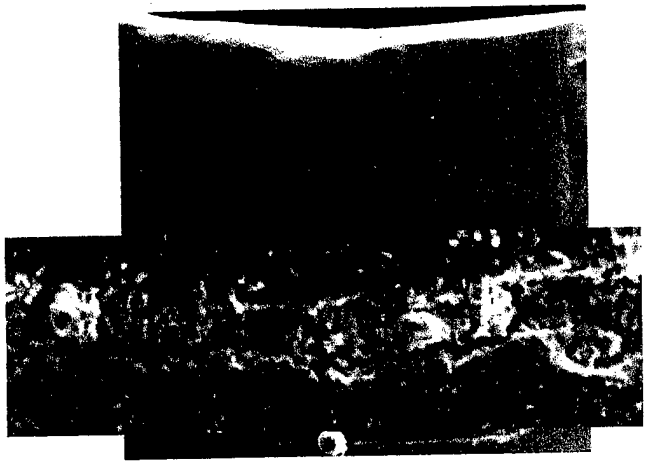

pre-op

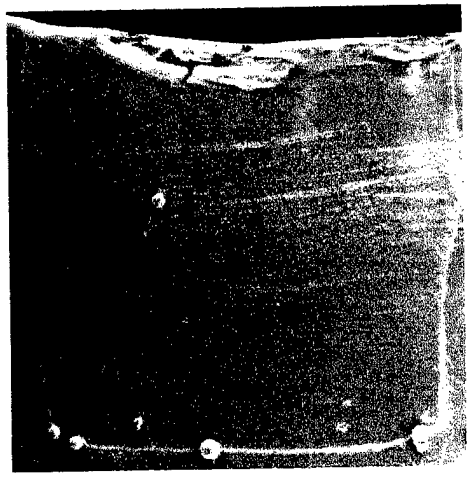

post-therm

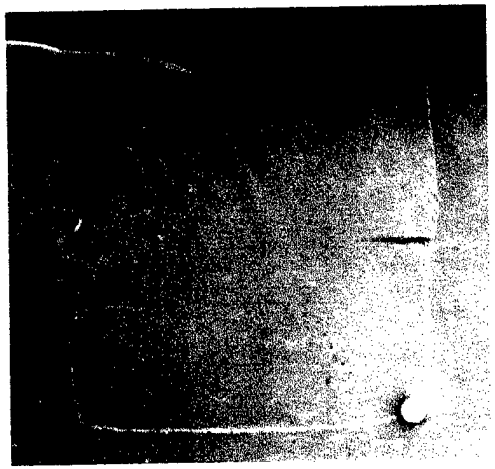

50k cycles

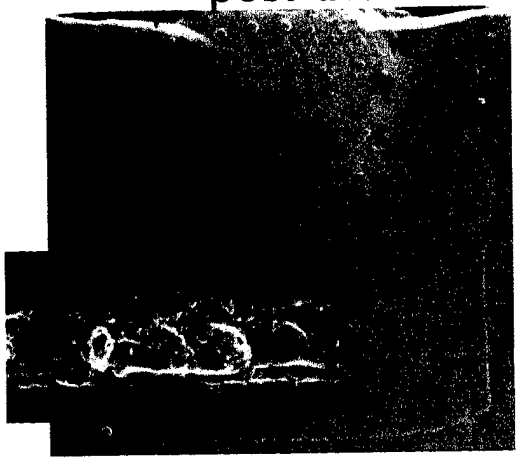

250k cycles

12000 mJ/cm2 5mm dentin 71% of max

	Pre-op	Post-thermal	50K cyc	250K cyc
1	3.5	0.0	0.0	0.0
2	8.2	0.0	bubble	0.0
3	2.1	0.0	0.0	0.0
4	0.0	0.0	0.0	0.0
5	0.0	0.0	5.1	0.0
6	0.0	0.0	bubble	0.0
7	0.0	0.0	0.0	0.0
8	2.1	0.0	0.0	0.0
9	0.0	0.0	0.0	1.2
10	1.7	0.0	0.0	0.0
11	0.0	0.0	0.0	0.0
12	0.0	0.0	0.0	0.0
13	3.6	0.0	0.0	0.0
14	1.2	0.0	0.0	0.0
15	0.0	0.0	0.0	0.0
16	2.2	0.0	0.0	0.0
17	bubble	0.0	0.0	0.0
18	bubble	0.0	0.0	0.0
19	16.1	0.0	0.0	0.0
20	4.1	0.0	0.0	0.0
21	0.0	0.0	0.0	0.0
22	0.0	0.0	0.0	0.0
23	0.0	3.8	0.0	0.0
24	17.4	0.0	0.0	0.0
25	1.4	0.0	0.0	bubble
avg.	2.8	0.2	0.2	0.1
std dev	4.8	0.8	1.1	0.2
% gapped	48.0	4.0	4.0	4.0

PART TWO
THIRD PILOT

Third Pilot

4000-1 mJ/cm2 Water Only 5mm dentin 20% of

pre-op

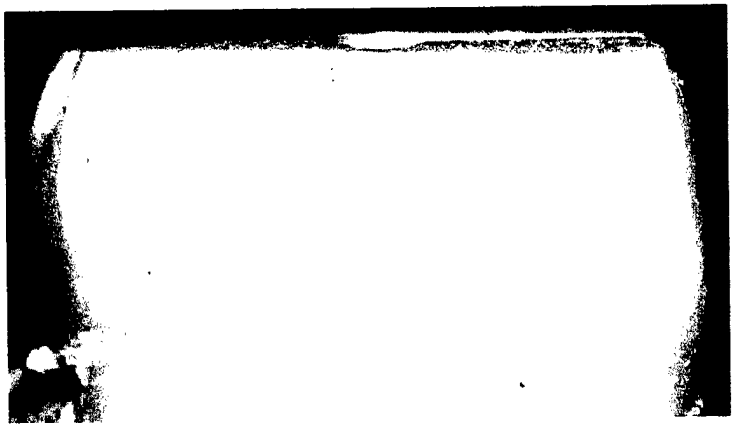

(48 hrs)

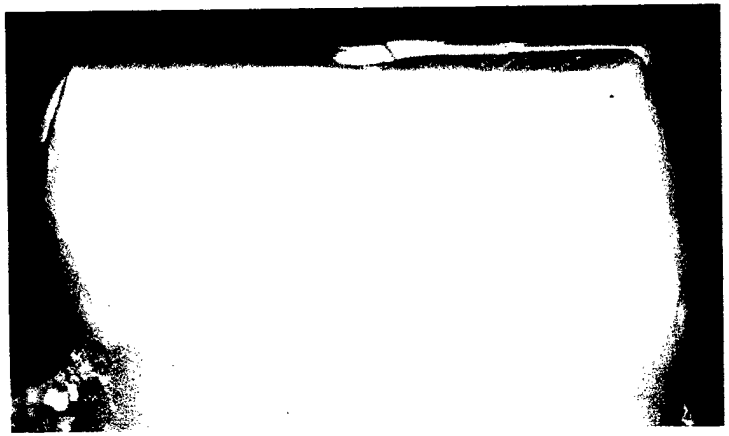

(72 hrs)

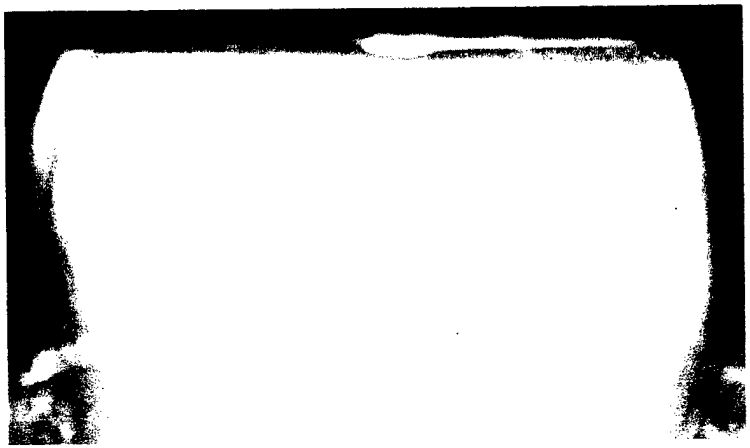

(1 wk)

4000-1 mJ/cm2 Water Only 5mm dentin 20% of

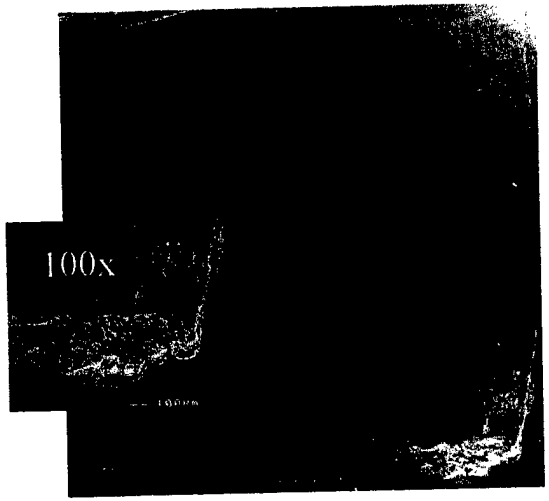

147.6 um

100%

pre-op

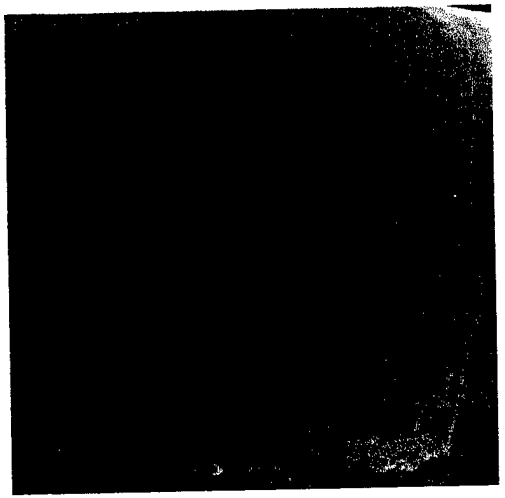

142.6um

100 %

(48 hrs)

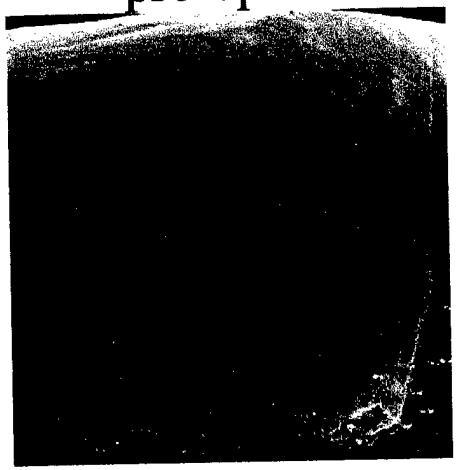

146.2 um

100%

(72 hrs)

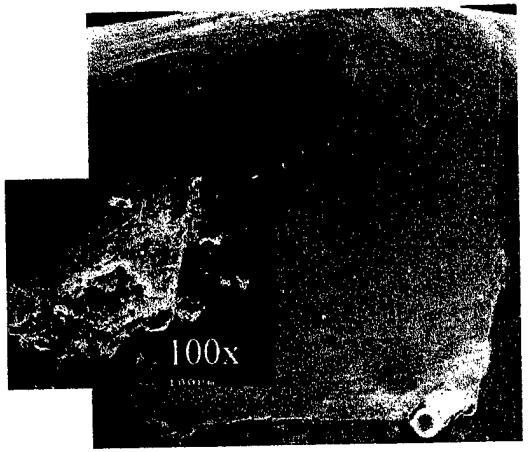

144.9 um

100%

(1 wk)

4000-2 mJ/cm2 5mm dentin 20% of max

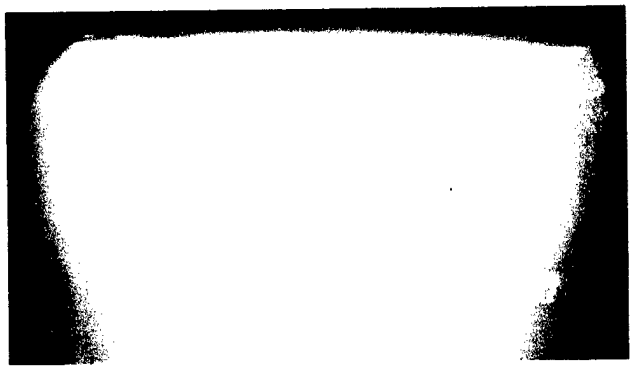

pre-op

post-therm

100k cycles

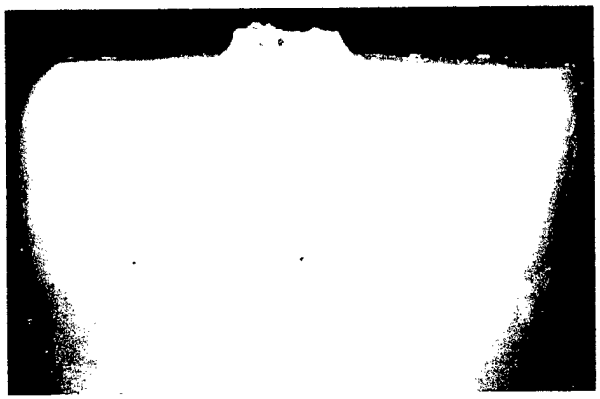

500k cycles

4000-2 mJ/cm2 5mm dentin 20% of max

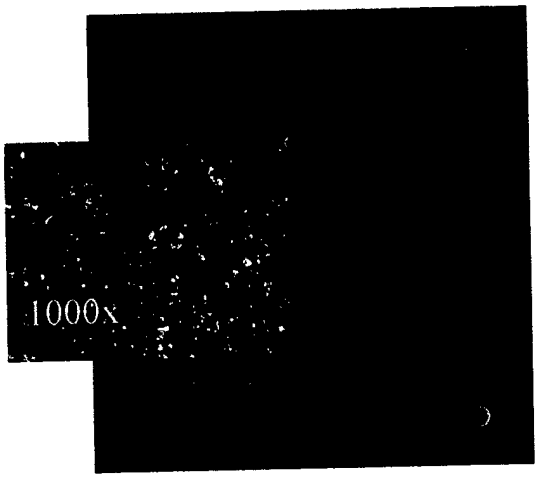

298 um

100%

pre-op

303 um

100%

post-therm

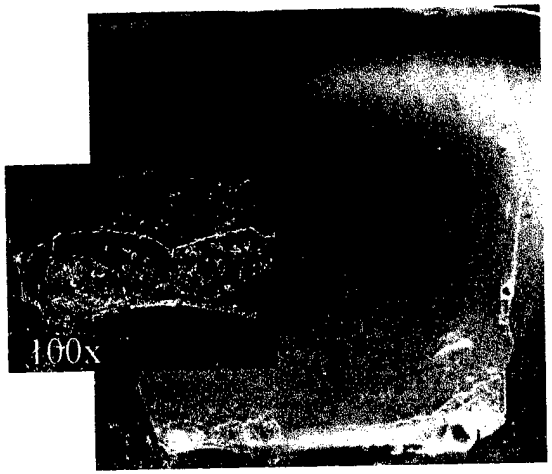

308 um

100%

100k cycles

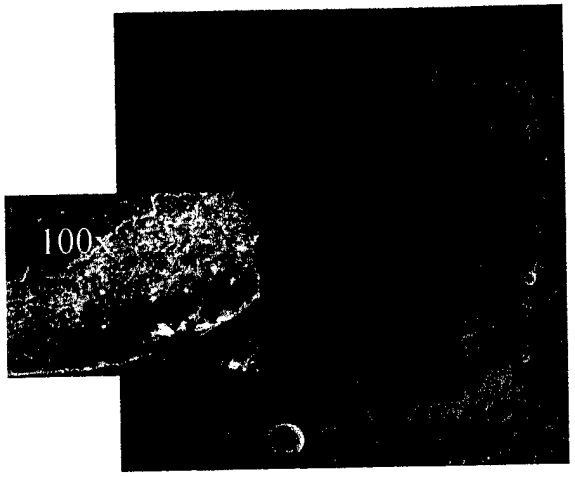

327um

100%

500k cycles

6000-1 mJ/cm2 5mm dentin 45% of max

pre-op

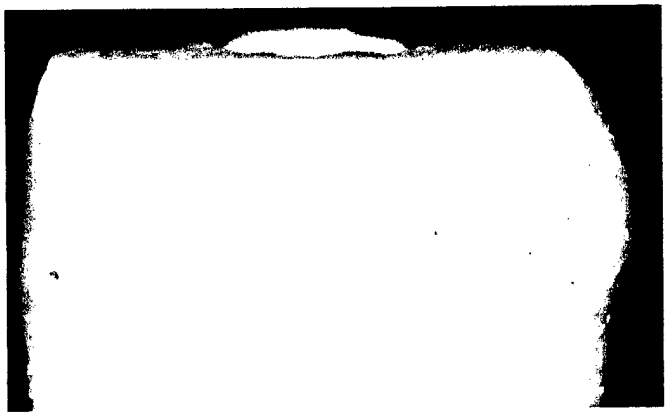

post-therm

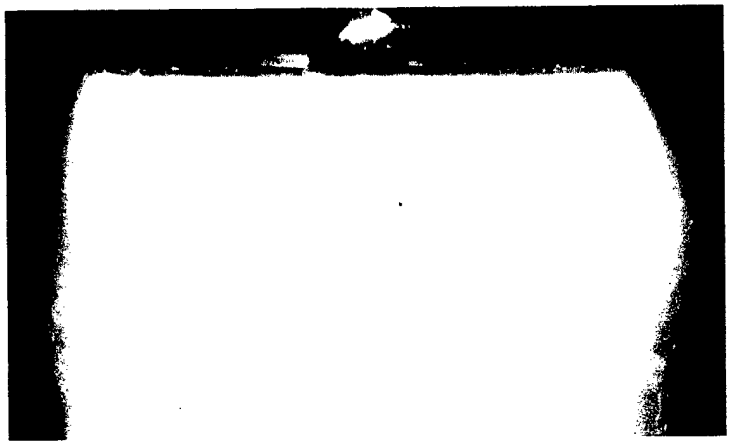

100k cycles

500k cycles

6000-1 mJ/cm2 5mm dentin 45% of max

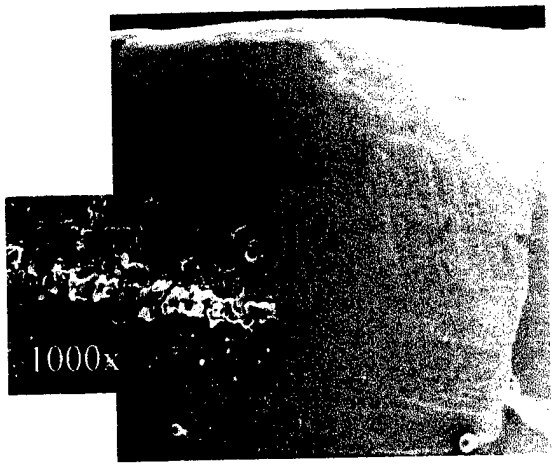

5.3 um

17 %

pre-op

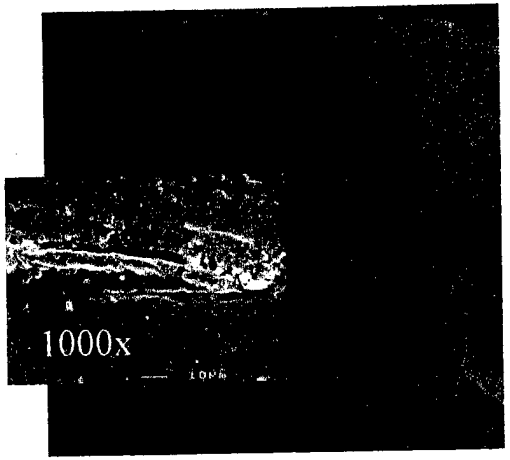

9.6 um

92 %

post-

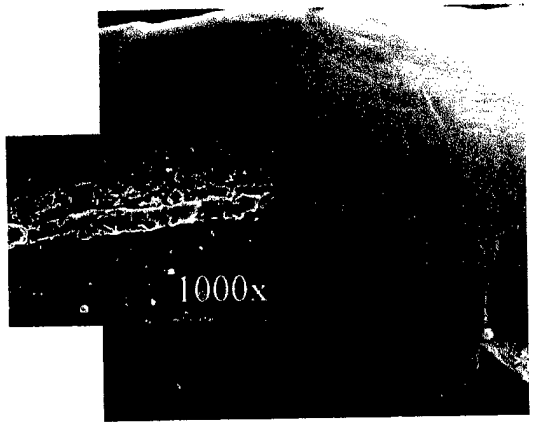

4.0 um

75 %

100k cycles

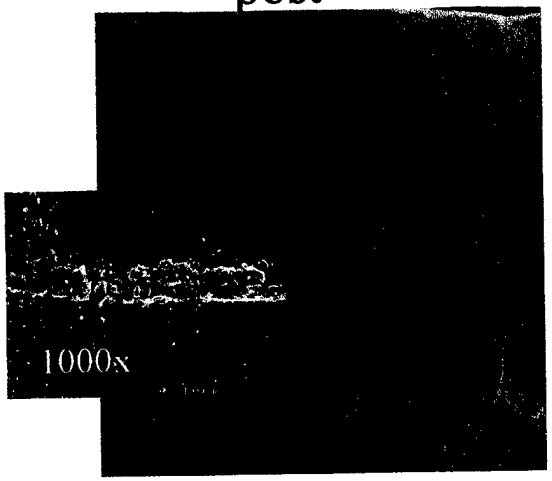

7.1 um

48%

500k cycles

8000-2 mJ/cm2 5mm dentin 57% of max

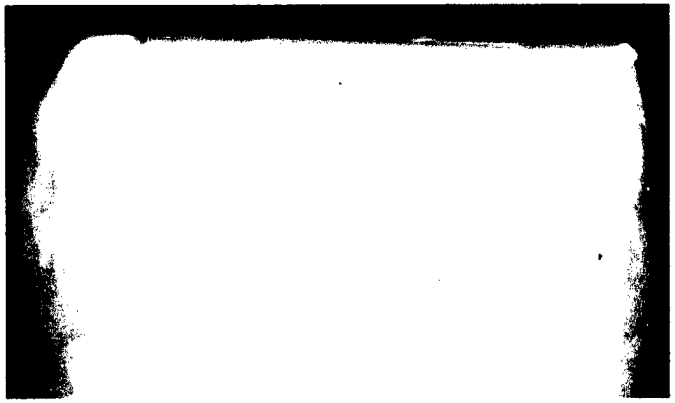

pre-op

post-therm

100k cycles

500k cycles

8000-2 mJ/cm2 5mm dentin 58 % of max

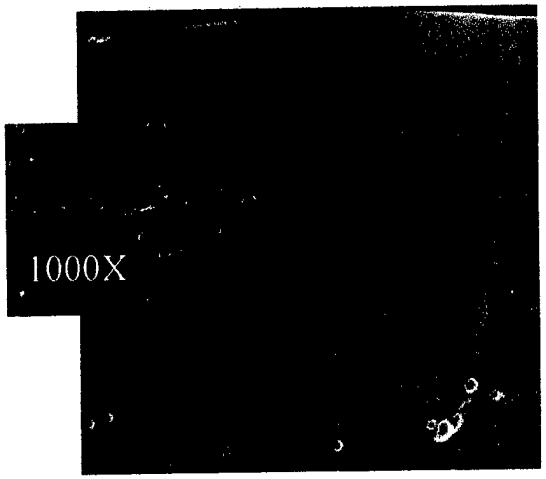

15.6 um

8%

pre-op

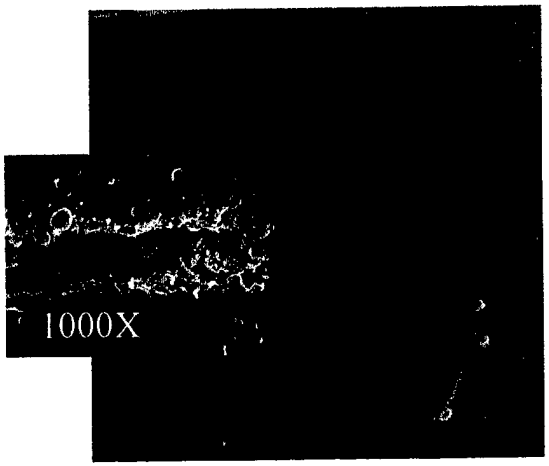

34.9 um

100%

post-therm

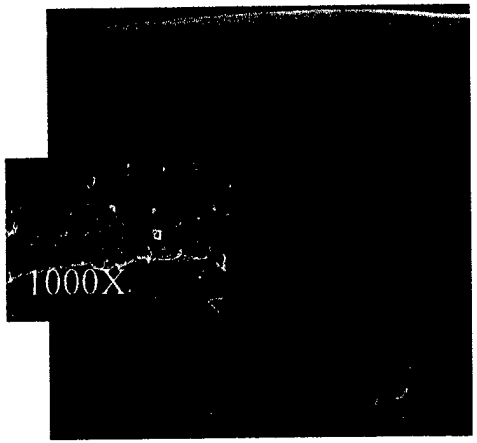

31.2 um

70%

100k cycles

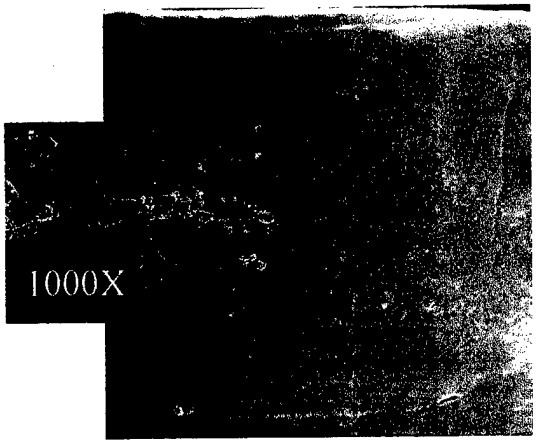

31.3 um

80%

500k cycles

10000-2 mJ/cm2 5mm dentin 68 % of max

pre-op

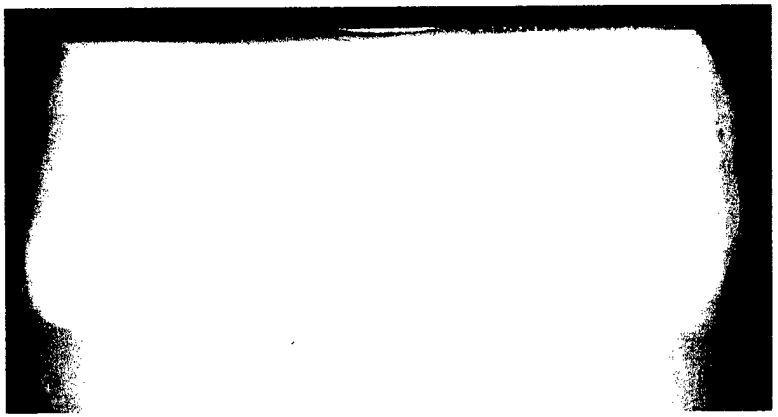

post-therm

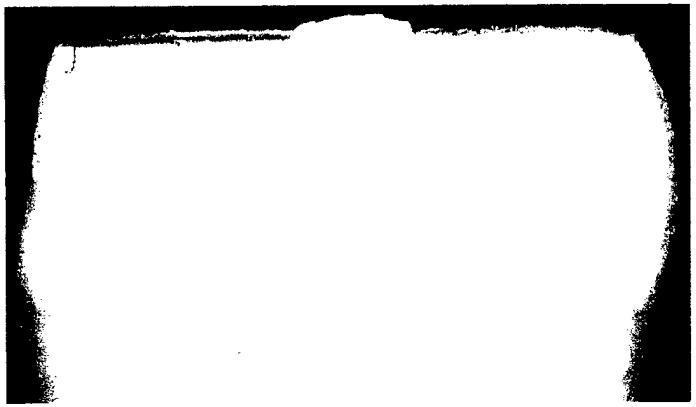

100k cycles

500k cycles

10000-2 mJ/cm2 5mm dentin 68% of max

1.4 um

9%

pre-op

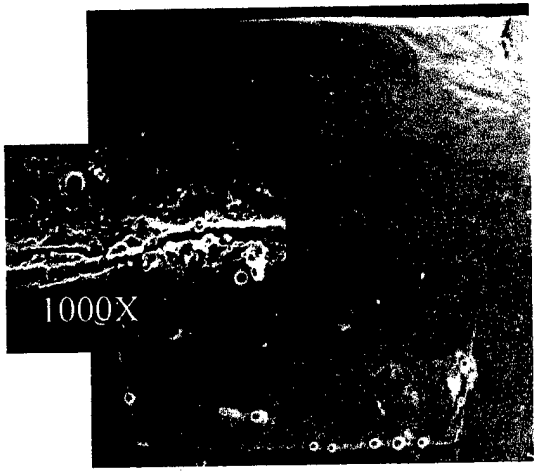

12.0 um

100%

post-therm

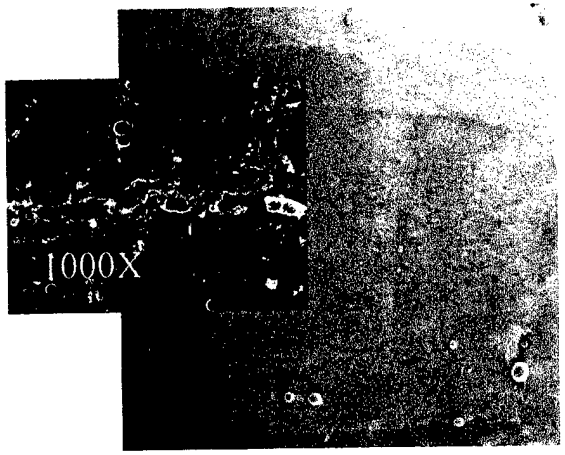

15.5 um

96%

100k cycles

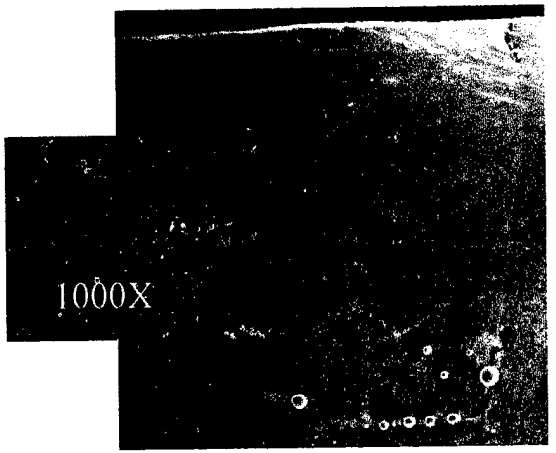

15.8 um

91%

500k cycles

12000-2 mJ/cm2 5mm dentin 71% of max

pre-op

post-therm

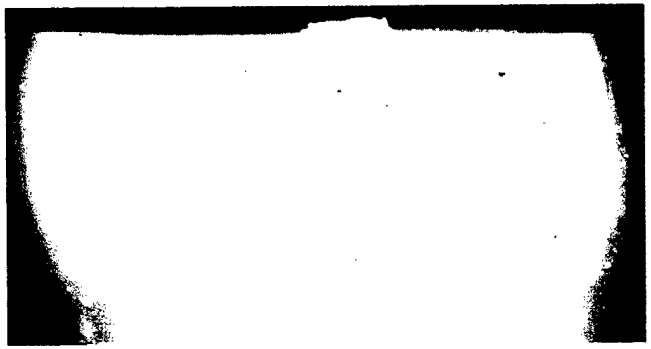

100k cycles

500k cycles

12000-2 mJ/cm2 5mm dentin 71% of max

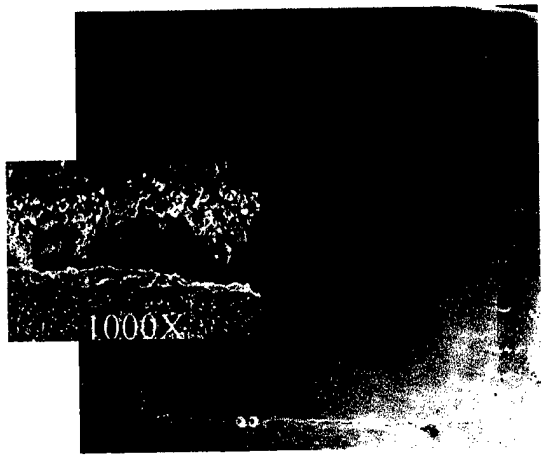

29.2 um

83%

pre-op

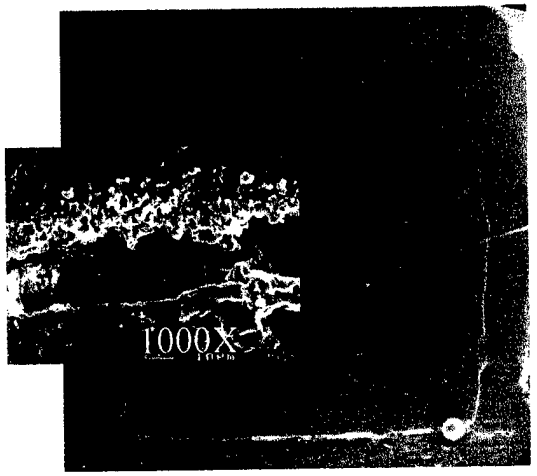

32.9 um

100%

post-therm

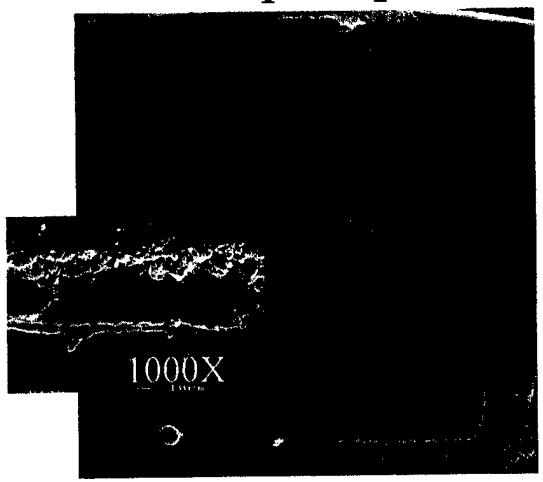

31.0 um

100%

100k cycles

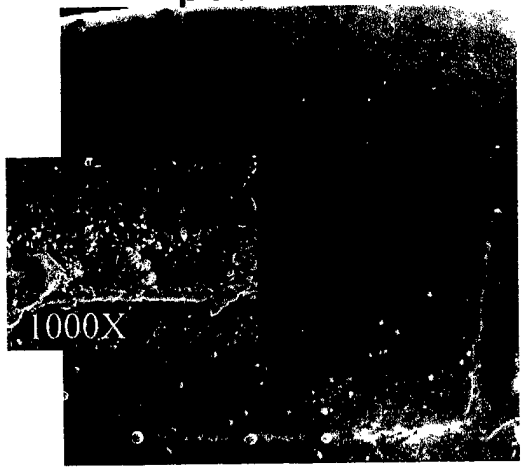

36.0 um

100 %

500k cycles

Control-2 Incremental (24000 mJ/cm2 x3) 5mm dentin 98% of max

pre-op

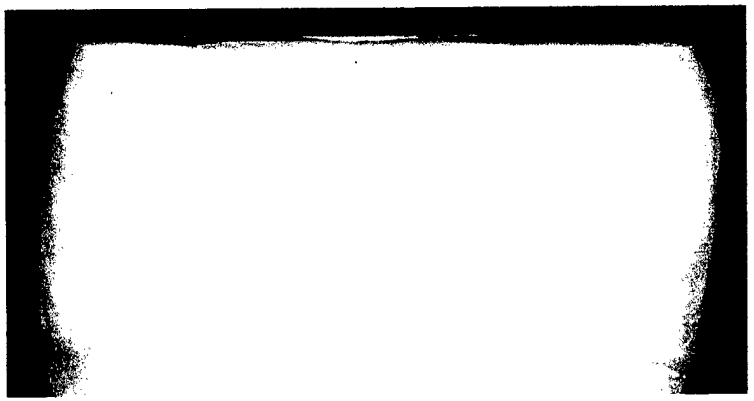

post-therm

100k cycles

500k cycles

Control-2 Incremental (24000 mJ/cm2 x3) 5mm dentin 98% of max

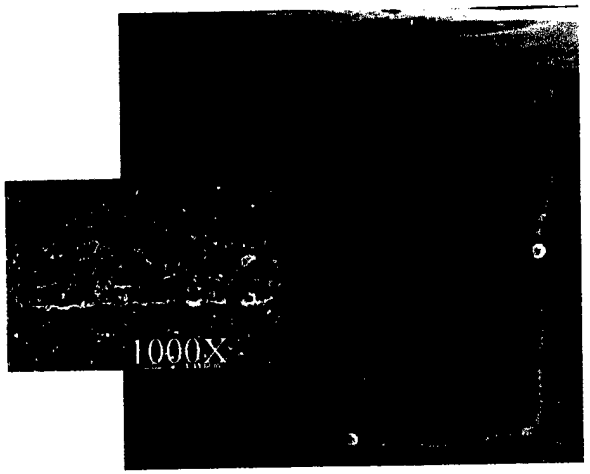

2.6 um

10%

pre-op

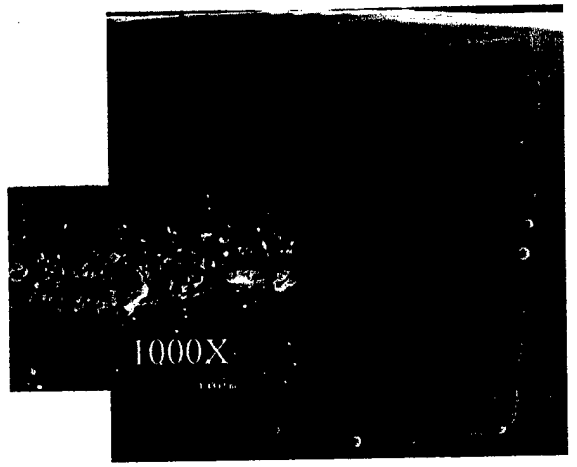

5.1um

89%

post-therm

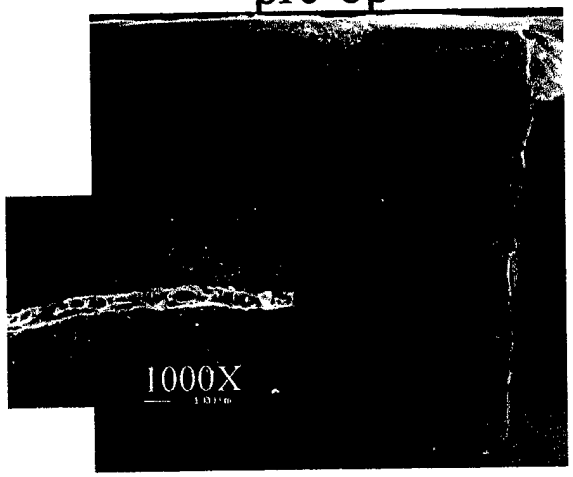

4.8 um

81%

100k cycles

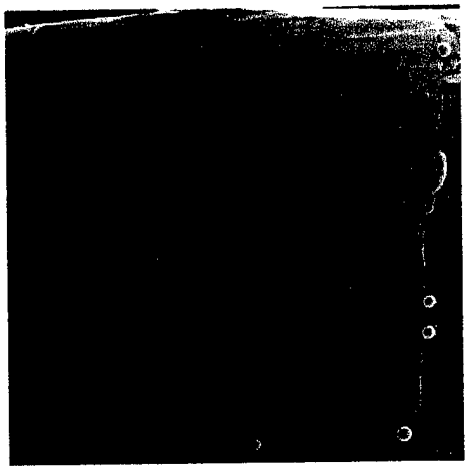

3.1 um

60%

500k cycles

Third Pilot Defect Width (microns)

4000 mJ/cm2	4W-1				4W-2				4W-3				4W-4			
	Pre-op	48 hrs	72 hrs	1 wk	Pre-op	48 hrs	72 hrs	1 wk	Pre-op	48 hrs	72 hrs	1 wk	Pre-op	48 hrs	72 hrs	1 wk
1	480.0	518.0	520.0	515.0	168.0	132.0	128.0	133.0	48.2	40.0	41.0	42.6	1275.0	1160.0	1150.3	1213.0
2	516.0	490.0	495.0	480.0	57.6	63.1	54.3	64.0	104.0	100.1	98.2	105.5	1129.5	1130.0	1143.2	1131.2
3	427.0	422.0	428.0	430.0	0.0	0.0	0.0	0.0	0.0	0.0	0.0	0.0	1112.0	1100.0	1110.0	1111.3
4	323.0	300.0	317.0	312.0	0.0	0.0	0.0	0.0	0.0	0.0	0.0	0.0	1079.3	1083.0	1095.3	1075.6
5	237.0	230.0	245.0	235.0	0.0	0.0	0.0	0.0	0.0	0.0	0.0	0.0	1040.6	1043.0	1035.2	1044.2
6	193.0	210.0	207.0	210.0	0.0	0.0	0.0	0.0	0.0	0.0	0.0	0.0	1020.3	1022.0	1023.3	1023.0
7	191.0	191.0	183.0	193.0	0.0	0.0	0.0	0.0	0.0	0.0	0.0	0.0	1010.6	1000.0	989.3	998.0
8	234.0	183.0	215.0	210.0	0.0	4.8	0.0	0.0	0.0	0.0	0.0	0.0	946.3	947.0	953.2	933.0
9	206.0	175.0	204.0	200.0	0.0	0.0	0.0	0.0	0.0	0.0	0.0	0.0	900.6	899.0	906.5	900.0
10	25.5	10.1	12.7	20.1	0.0	0.0	0.0	0.0	0.0	0.0	0.0	0.0	846.9	853.0	863.2	847.0
11	28.5	25.2	28.9	26.4	0.0	0.0	0.0	0.0	0.0	0.0	0.0	0.0	800.2	801.3	786.3	800.0
12	76.0	50.3	60.3	63.1	0.0	0.0	0.0	0.0	0.0	0.0	0.0	0.0	770.5	760.0	760.0	750.0
13	53.8	78.4	63.4	70.4	0.0	0.0	0.0	0.0	0.0	0.0	0.0	0.0	713.5	715.9	723.6	723.2
14	47.5	60.3	50.4	53.4	0.0	0.0	0.0	0.0	0.0	0.0	0.0	0.0	670.6	669.0	665.3	650.2
15	57.1	51.7	51.4	54.1	0.0	0.0	0.0	0.0	0.0	0.0	0.0	0.0	628.3	623.0	624.3	638.2
16	43.2	40.2	42.3	41.4	0.0	0.0	0.0	0.0	0.0	0.0	0.0	0.0	590.3	583.2	593.5	586.5
17	47.8	53.6	50.9	53.2	0.0	0.0	0.0	0.0	0.0	0.0	0.0	0.0	544.6	536.1	526.5	530.6
18	53.4	52.1	49.1	49.2	0.0	0.0	0.0	0.0	0.0	0.0	0.0	0.0	497.2	491.7	490.2	480.2
19	57.2	53.4	40.3	54.4	0.0	0.0	0.0	0.0	0.0	0.0	0.0	0.0	435.6	440.0	438.5	452.3
20	48.1	45.8	48.4	40.1	100.0	94.2	105.1	100.0	0.0	0.0	0.0	0.0	440.3	436.0	435.5	444.6
21	40.5	40.1	40.2	39.8	bubble	162.0	145.6	150.0	0.0	0.0	0.0	0.0	428.6	429.5	430.5	436.9
22	20.1	20.2	21.2	19.0	120.3	120.1	bubble	120.0	0.0	0.0	0.0	0.0	420.3	422.3	420.3	410.5
23	115.2	93.4	100.1	95.1	110.0	119.2	121.9	110.0	0.0	0.0	0.0	0.0	418.2	416.8	415.2	410.2
24	97.0	90.7	90.2	90.1	100.0	109.6	110.0	100.0	0.0	0.0	0.0	0.0	409.3	410.9	405.3	410.9
25	72.0	80.3	90.1	68.2	bubble	bubble	0.0	0.0	0.0	0.0	0.0	0.0	385.3	400.0	375.2	400.0
avg.	147.6	142.6	146.2	144.9	28.5	33.5	27.7	31.1	6.1	5.6	5.6	5.9	740.6	734.9	734.4	736.0
std dev	147.8	147.1	150.3	147.8	52.0	55.2	51.1	52.7	22.6	21.2	21.0	22.4	279.6	270.4	273.5	273.9
% def	100	100	100	100	26	33	25	28	8	8	8	8	100	100	100	100

Avg	230.7	229.2	228.5	229.5
Std dev	345.5	342.3	342.9	343.1
% def	58.5	60.3	58.3	59.0
Std dev	48.5	47.0	48.7	48.0

Third Pilot Defect Width (microns)

4000 mJ/cm2	4-1				4-2				4-3				4-4			
	Pre-op	Post Therm	100K	500K	Pre-op	Post Therm	100K	500K	Pre-op	Post Therm	100K	500K	Pre-op	Post Therm	100K	500K
1	750.0	749.3	763.2	765.3	bubble	394.0	507.4	501.0			broke		195.3	200.5	225.3	235.8
2	728.3	730.2	728.6	745.2	395.6	386.5	456.3	465.2					200.3	236.5	240.0	235.8
3	738.0	744.5	748.0	753.6	387.5	385.6	413.2	425.3					212.4	210.5	200.1	225.5
4	752.3	742.3	732.5	745.2	402.3	398.9	458.3	445.3					196.3	175.5	189.6	198.5
5	718.9	720.1	736.9	744.3	375.2	405.2	386.5	358.0					215.8	235.6	225.6	215.4
6	732.4	737.5	745.8	756.2	372.4	386.5	396.5	375.2					235.6	248.9	247.6	237.7
7	746.1	755.6	758.2	762.3	364.2	375.6	356.2	365.8					270.6	286.5	280.0	281.4
8	775.3	780.3	790.5	801.2	343.5	352.3	345.2	351.2					265.3	277..2	286.5	234.6
9	762.9	770.3	783.5	802.3	325.4	333.9	330.2	382.5					278.2	272.3	284.6	289.9
10	750.0	751.3	745.3	768.3	300.4	303.9	272.4	414.7					298.6	289.4	296.4	285.6
11	767.7	770.3	786.3	785.0	275.6	281.2	292.3	398.5					315.2	325.6	330.2	345.2
12	777.4	780.8	775.6	765.0	289.3	293.2	278.2	385.2					345.6	333.3	345.4	333.4
13	775.3	790.3	801.6	803.2	288.5	291.5	288.5	275.2					389.5	378.5	386.5	375.2
14	762.3	778.4	802.6	795.3	254.8	261.3	255.3	265.3					395.8	410.6	400.0	398.2
15	754.3	764.3	795.3	789.3	245.4	237.5	250.0	297.9					412.3	411.5	421.5	415.6
16	730.2	745.2	756.8	765.3	232.5	235.6	256.3	275.3					423.6	452.3	467.2	455.7
17	742.8	743.2	735.2	745.8	256.4	265.3	263.0	255.3					445.5	438.2	444.2	456.6
18	733.2	728.4	732.5	730.9	247.8	253.4	247.5	233.5					475.3	487.2	496.8	486.5
19	715.8	735.5	735.5	745.2	254.2	255.8	244.3	241.3					478.9	489.6	478.8	489.7
20	745.8	750.0	754.2	755.6	244.3	237.5	203.0	215.2					489.2	495.3	500.0	499.6
21	738.2	740.5	745.2	789.3	238.5	232.1	213.3	210.2					475.0	489.5	506.3	475.5
22	756.2	760.1	770.9	785.3	245.6	241.3	213.2	200.2					468.8	475.2	487.5	500.0
23	775.3	789.3	798.6	802.3	256.3	215.3	223.3	235.3					456.8	469.5	475.6	512.3
24	780.2	798.3	806.3	807.3	275.6	289.6	275.3	345.9					435.6	444.7	454.6	498.5
25	745.2	751.2	789.3	775.3	250.4	258.0	285.5	252.6					412.6	450.3	463.5	489.6
avg.	750.2	756.3	764.7	771.4	296.7	302.8	308.4	326.8					351.5	362.8	365.4	366.9
std dev	18.5	21.1	26.1	23.1	57.7	63.8	84.8	87.9					105.8	109.1	109.5	113.8
% def	100	100	100	100	100	100	100	100					100	100	100	100

Avg	466.1	474.0	479.5	488.4
Std dev	247.5	246.3	248.6	245.9
% def	100.0	100.0	100.0	100.0
Std dev	0.0	0.0	0.0	0.0

Third Pilot Defect Width (microns)

6000 mJ/cm2

	6-1				6-2				6-3			
	Pre-op	Post Therm	100K	500K	Pre-op	Post Therm	100K	500K	Pre-op	Post Therm	100K	500K
1	22.7	22.3	22.4	22.2	7.4	9.9	11.0	6.1	95.0	85.0	90.0	89.0
2	0.0	12.4	12.3	11.3	0.0	0.0	0.0	7.6	115.0	100.0	110.0	107.0
3	bubble	15.0	bubble	6.5	0.0	0.0	14.9	14.6	0.0	0.0	0.0	0.0
4	0.0	7.9	8.8	12.5	0.0	17.7	14.9	15.5	0.0	0.0	0.0	14.9
5	0.0	0.0	3.5	4.1	0.0	14.6	14.6	15.2	0.0	0.0	0.0	12.1
6	0.0	0.0	0.0	0.0	0.0	10.1	10.8	11.4	0.0	7.3	0.0	0.0
7	0.0	2.9	10.1	0.0	0.0	15.2	12.0	16.1	7.6	10.5	0.0	12.3
8	0.0	13.5	2.4	0.0	0.0	13.3	11.1	11.1	0.0	0.0	8.4	33.5
9	0.0	3.2	4.0	0.0	0.0	16.1	14.6	12.0	flash	flash	flash	flash
10	0.0	6.3	0.0	0.0	0.0	8.9	13.9	10.8	flash	flash	flash	flash
11	0.0	4.1	1.5	0.0	0.0	0.0	9.5	12.3	flash	flash	flash	flash
12	0.0	3.5	10.5	0.0	0.0	13.3	8.2	8.6	flash	flash	flash	flash
13	0.0	6.7	8.3	4.7	0.0	14.6	11.4	15.2	flash	flash	flash	flash
14	0.0	1.9	2.9	0.0	0.0	11.7	9.8	9.5	flash	flash	flash	flash
15	0.0	2.9	1.6	3.5	0.0	10.8	10.7	9.5	0.0	0.0	0.0	0.0
16	0.0	3.5	1.0	4.3	0.0	14.9	11.7	12.0	2.2	0.0	10.4	12.0
17	0.0	2.5	1.5	0.0	0.0	10.7	9.8	6.7	10.4	10.5	20.2	13.9
18	0.0	2.8	2.2	0.0	0.0	10.7	10.1	12.7	0.0	bubble	bubble	20.6
19	0.0	11.7	0.9	7.7	0.0	8.2	12.0	12.3	0.0	0.0	5.4	6.0
20	0.0	4.4	1.9	0.0	0.0	7.6	6.9	11.4	0.0	14.2	12.2	16.5
21	0.0	4.1	0.0	0.0	0.0	6.3	9.2	9.4	0.0	0.0	bubble	32.7
22	0.0	2.5	0.5	0.0	0.0	25.9	24.8	23.1	0.0	0.0	0.0	0.0
23	14.4	14.5	14.0	10.7	0.0	8.6	7.9	8.4	0.0	0.0	0.0	13.9
24	21.4	22.4	20.8	22.7	0.0	11.2	10.4	10.4	0.0	0.0	0.0	11.1
25	68.1	70.0	71.3	68.0	0.0	10.7	11.5	10.3	0.0	0.0	0.0	0.0
avg.	5.3	9.6	8.4	7.1	0.3	10.8	11.3	11.7	12.1	12.6	15.1	20.8
std dev	15.0	14.1	14.9	14.3	1.5	5.7	4.2	3.6	33.0	29.5	32.7	29.1
% def	17	92	75	48	4	88	96	100	26	33	41	74

Avg	5.9	11.0	11.6	13.2
Std dev	5.9	1.5	3.3	7.0
% def	15.7	71.0	70.7	74.0
Std dev	11.1	33.0	27.8	26.0

Third Pilot Defect Width (microns)

8000 mJ/cm2

	8-1				8-2				8-3			
	Pre-op	Post Therm	100K	500K	Pre-op	Post Therm	100K	500K	Pre-op	Post Therm	100K	500K
1	0	16.3	23.7	12.2	90.2	152.0	172.0	160.1	0	18.3	5.8	9.4
2	0.0	0.0	6.3	0.0	150.0	161.6	142.2	162.8	0.0	60.2	bubble	72.4
3	0.0	4.1	6.0	10.2	121.0	133.0	128.0	130.0	bubble	bubble	72.6	82.3
4	0.0	0.0	0.0	11.1	0.0	6.7	0.0	0.0	10.3	27.4	17.9	15.9
5	0.0	3.8	30.4	41.4	0.0	12.7	5.1	6.7	7.3	6.7	0.0	0.0
6	0.0	6.9	30.4	57.9	0.0	18.0	0.0	14.9	5.4	13.0	0.0	0.0
7	0.0	5.4	10.2	6.1	0.0	12.7	0.0	9.2	4.8	10.1	0.0	0.0
8	0.0	10.2	28.0	16.5	bubble	17.7	bubble	15.5	0.0	9.5	0.0	13.6
9	80.0	76.3	64.0	51.0	0.0	13.3	0.0	13.0	5.1	8.9	0.0	0.0
10	67.7	67.0	60.1	bubble	0.0	17.1	0.0	0.0	0.0	12.7	0.0	0.0
11	82.3	91.2	90.5	93.6	0.0	13.3	10.5	15.2	8.6	16.5	0.0	9.8
12	0.0	3.2	90.6	86.1	0.0	18.0	12.7	13.3	0.0	12.0	0.0	8.2
13	0.0	8.6	8.2	14.2	0.0	8.6	16.1	13.9	12.7	13.3	0.0	11.7
14	0.0	13.0	11.7	6.8	12.7	12.7	0.0	21.2	6.3	12.7	0.0	7.9
15	0.0	15.2	7.9	12.2	0.0	23.8	17.7	13.3	11.7	12.0	0.0	0.0
16	0.0	9.8	18.0	10.8	0.0	24.1	0.0	0.0	8.2	12.7	0.0	17.2
17	0.0	15.5	24.4	12.1	0.0	27.9	bubble	22.2	9.2	11.4	0.0	17.2
18	0.0	13.3	12.7	10.2	0.0	46.9	10.5	20.0	8.9	10.1	0.0	16.5
19	20.6	2.1	9.5	10.4	0.0	34.8	44.0	52.8	7.0	10.1	0.0	12.1
20	24.4	bubble	22.8	14.9	0.0	37.0	47.5	30.7	0.0	17.7	0.0	22.2
21	bubble	13.0	43.0	65.8	0.0	32.0	33.2	26.6	17.1	17.7	0.0	17.4
22	bubble	17.1	67.4	55.6	0.0	12.1	32.0	0.0	6.7	12.1	0.0	7.6
23	5.7	bubble	bubble	18.7	0.0	5.1	24.7	0.0	6.1	67.1	0.0	0.0
24	3.2	bubble	4.2	4.5	0.0	16.9	8.2	26.6	bubble	89.0	44.3	60.4
25	31.2	32.8	35.4	39.3	0.0	15.6	13.3	14.0	bubble	bubble	bubble	bubble
avg.	13.7	19.3	29.4	27.6	15.6	34.9	31.2	31.3	6.2	20.9	6.1	16.7
std dev	26.5	25.3	26.7	27.0	41.5	44.3	48.6	46.9	4.7	21.2	17.5	22.5
% def	34	91	96	96	8	100	70	80	68	100	17	71

Avg	11.8	25.1	22.2	25.2
Std dev	5.0	8.6	14.0	7.6
% def	36.7	97.0	61.0	82.3
Std dev	30.1	5.2	40.3	12.7

Third Pilot Defect Width (microns)

	10000 mJ/cm2	10-1			10-2				10-3			
	Pre-op	Post Therm	100K	500K	Pre-op	Post Therm	100K	500K	Pre-op	Post Therm	100K	500K
1	bubble	67.8	36.2	40.9	30.8	22.7	22.1	18.9	142.5	166.5	164.8	162.8
2	26.6	26.4	16.7	0.0	0.0	10.5	10.8	7.3	147.0	65.0	47.0	45.0
3	11.7	23.6	19.6	17.5	0.0	8.9	10.1	2.2	bubble	150.8	bubble	bubble
4	9.5	39.2	30.1	29.5	0.0	83.0	87.4	85.6	140.5	bubble	142.6	126.6
5	flash	flash	flash	flash	0.0	bubble	18.1	28.2	140.0	110.2	130.9	109.2
6	flash	flash	flash	flash	0.0	1.1	63.3	69.0	71.3	84.5	72.8	70.4
7	6.6	15.8	23.2	10.1	bubble	bubble	bubble	bubble	45.2	25.7	38.1	24.5
8	0.0	10.7	10.7	9.8	0.0	8.2	10.1	37.3	0.0	24.1	21.2	20.7
9	6.6	4.1	7.2	9.2	0.0	4.4	3.8	0.0	0.0	32.3	33.9	bubble
10	0.0	0.0	13.6	8.6	0.0	11.7	2.0	bubble	0.0	17.1	bubble	36.1
11	flash	flash	3.2	flash	bubble	bubble	9.2	12.4	0.0	20.6	25.3	17.4
12	flash	flash	flash	flash	0.0	5.4	5.1	7.6	0.0	19.0	25.6	21.5
13	flash	flash	flash	flash	0.0	5.4	5.3	8.2	0.0	14.9	0.0	9.2
14	flash	flash	flash	flash	2.1	3.5	6.4	5.4	0.0	25.1	23.4	15.5
15	flash	flash	flash	flash	0.0	2.1	11.7	6.3	0.0	14.8	0.0	0.0
16	flash	flash	flash	7.3	0.0	5.1	6.3	5.4	0.0	0.0	0.0	0.0
17	23.1	1.1	8.2	38.6	0.0	5.1	5.0	4.3	0.0	1.8	0.9	0.0
18	57.6	28.1	52.5	47.2	0.0	5.2	5.1	1.2	0.0	2.0	0.5	0.0
19	59.5	43.9	43.2	53.5	0.0	5.0	3.5	3.1	0.0	0.0	2.0	0.0
20	66.8	51.5	54.4	62.8	0.0	4.1	2.6	1.9	0.0	6.9	7.0	0.0
21	63.9	bubble	66.4	66.8	0.0	2.2	0.0	2.1	0.0	9.8	0.0	0.0
22	63.4	bubble	bubble	70.2	0.0	4.1	2.5	1.3	0.0	0.0	4.5	0.0
23	bubble	63.2	bubble	84.5	0.0	bubble	2.4	1.7	0.0	15.5	11.7	16.1
24	bubble	bubble	bubble	bubble	0.0	4.2	28.2	0.0	0.0	51.6	51.9	33.2
25	49.4	61.7	94.6	bubble	0.0	50.9	50.0	53.0	0.0	10.8	11.4	10.4
avg.	31.8	31.2	32.0	34.8	1.4	12.0	15.5	15.8	28.6	36.2	35.5	31.2
std dev	26.7	23.7	26.0	27.0	6.4	19.5	21.7	23.6	54.7	46.7	48.2	44.7
% def	86	93	100	94	9	100	96	91	25	88	87	65

Avg	20.6	26.5	27.6	27.3
Std dev	16.7	12.8	10.7	10.1
% def	40.0	93.7	94.3	83.3
Std dev	40.6	6.0	6.7	15.9

Third Pilot Defect Width (microns)

12000 mJ/cm2

	12-1				12-2				12-3			
	Pre-op	Post Therm	100K	500K	Pre-op	Post Therm	100K	500K	Pre-op	Post Therm	100K	500K
1	52.5	56.2	58.5	56.6	62.6	66.4	60.5	65.6	38.7	81.6	33.7	23.9
2	33.5	38.5	51.2	40.7	42.1	bubble	43.9	55.8	15.2	10.8	6.1	0.0
3	50.6	37.2	42.2	38.6	44.0	53.8	51.3	69.0	11.7	16.5	12.4	0.0
4	28.4	44.6	28.4	27.0	9.1	36.1	30.4	32.6	10.8	26.0	19.0	20.3
5	bubble	34.4	bubble	bubble	93.6	35.8	37.0	44.7	bubble	36.4	21.6	16.8
6	32.5	31.9	30.1	26.8	28.6	31.3	34.8	41.5	33.6	39.9	bubble	20.3
7	26.8	15.7	28.7	28.2	22.1	17.1	20.6	22.8	40.2	47.5	26.9	15.2
8	21.7	22.7	27.5	32.5	30.2	38.4	29.2	35.8	63.3	50.3	bubble	19.6
9	33.8	22.1	32.2	37.9	37.7	50.6	39.6	32.6	bubble	43.7	40.5	44.6
10	19.2	36.3	27.5	27.8	40.8	27.2	30.7	35.2	bubble	48.1	50.9	29.8
11	26.2	28.1	17.7	36.3	22.2	31.3	32.9	bubble	47.0	51.3	36.1	0.0
12	6.7	23.0	22.4	10.1	30.8	30.1	27.2	25.9	44.2	37.1	29.1	0.0
13	flash	bubble	flash	flash	24.6	28.8	14.8	22.8	31.4	17.4	14.5	0.0
14	flash	bubble	flash	flash	0.0	29.4	36.1	30.1	15.8	15.2	3.2	0.0
15	flash	flash	flash	flash	31.3	42.1	bubble	32.0	bubble	32.0	29.4	8.2
16	flash	flash	flash	flash	29.9	32.9	30.1	bubble	20.6	32.9	17.5	13.0
17	0.0	2.4	9.5	4.5	24.3	25.6	27.1	28.5	40.2	25.0	bubble	10.1
18	3.6	3.1	4.5	4.7	bubble	23.7	24.2	23.2	21.5	23.7	11.1	0.0
19	flash	11.1	flash	flash	16.5	22.5	22.1	30.7	20.3	14.2	9.5	0.0
20	15.7	20.5	8.1	8.5	0.0	22.5	25.8	20.6	11.4	14.6	15.2	0.0
21	30.4	19.0	13.2	8.5	0.0	25.1	23.9	24.4	21.2	27.5	19.3	0.0
22	41.1	24.0	31.7	24.6	0.0	51.9	43.7	23.9	10.8	bubble	10.1	0.0
23	bubble	35.4	33.1	bubble	15.6	36.4	bubble	44.6	bubble	bubble	8.4	17.8
24	0.0	32.3	28.2	17.2	61.4	22.5	15.4	49.4	27.9	15.2	bubble	bubble
25	0.0	5.0	0.0	11.6	33.6	8.0	12.3	bubble	34.9	47.9	26.2	32.4
avg.	23.5	25.9	26.0	24.6	29.2	32.9	31.0	36.0	28.0	32.8	21.0	11.3
std dev	16.6	13.9	15.1	14.6	22.1	12.9	11.6	13.8	14.5	17.1	12.4	12.8
% def	83	100	95	100	83	100	100	100	100	100	100	54

Avg	26.9	30.5	26.0	24.0
Std dev	3.0	4.0	5.0	12.3
% def	88.7	100.0	98.3	84.7
Std dev	9.8	0.0	2.9	26.6

Third Pilot Defect Width (microns)

24000 mJ/cm2	24-1				24-2				24-3			
	Pre-op	Post Therm	100K	500K	Pre-op	Post Therm	100K	500K	Pre-op	Post Therm	100K	500K
1	100	102.2	103.2	105.7	0	27.8	28.2	32.8	6.2	5.8	bubble	9.4
2	0.0	0.0	0.0	0.0	17.7	27.2	51.9	45.6	45.1	45.6	bubble	41.5
3	0.0	0.0	0.0	41.5	0.0	0.0	0.0	1.5	48.1	45.6	45.8	51.6
4	0.0	16.5	0.0	0.0	0.0	0.0	0.0	0	10.8	9.2	0.0	8.2
5	bubble	4.8	0.0	16.1	16.2	0.0	0.0	0	10.1	9.5	12.0	10.7
6	0.0	5.4	0.0	0.0	0.0	0.0	5.7	5.8	48.5	31.4	42.7	26.9
7	0.0	13.0	25.9	0.0	7.6	9.5	12.0	0	bubble	37.4	38.0	35.1
8	0.0	5.7	29.2	0.0	10.5	9.5	10.1	9.2	49.4	38.0	bubble	31.7
9	0.0	16.5	0.0	11.1	16.2	19.9	10.8	16.2	34.5	32.0	32.6	26.3
10	0.0	0.0	0.0	5.7	10.8	72.1	bubble	10.8	19.6	20.0	19.3	18.7
11	0.0	0.0	0.0	0.0	9.5	bubble	15.2	4.7	37.1	40.2	40.5	31.9
12	0.0	0.0	0.0	4.1	8.9	21.8	3.5	11.4	26.6	26.3	27.9	37.7
13	0.0	0.0	0.0	0.0	9.2	18.1	9.8	7.9	10.5	10.8	7.9	9.5
14	0.0	0.0	0.0	0.0	9.5	16.5	6.9	3.2	8.0	7.1	7.6	17.1
15	0.0	0.0	0.0	0.0	26.9	32.3	12.0	8.6	8.2	9.4	8.8	8.2
16	0.0	5.7	8.9	0.0	23.4	36.1	29.8	27.8	11.1	22.2	10.1	10.2
17	0.0	14.3	bubble	0.0	24.4	29.1	24.1	17.1	10.4	11.4	14.2	8.7
18	0.0	29.5	26.3	39.3	8.2	12.9	19.3	9.8	8.3	8.9	12.9	10.2
19	0.0	11.4	22.5	0.0	14.6	10.8	6.0	1.2	0.0	8.9	16.1	8.4
20	42.4	50.9	51.3	40.8	34.8	19.6	29.8	54.7	6.0	5.1	15.2	10.1
21	0.0	14.6	17.1	12.7	bubble	20.2	38.6	bubble	10.1	10.2	bubble	10.1
22	71.0	56.0	13.6	32.1	12.4	43.0	34.5	33.6	8.2	15.5	9.8	9.8
23	0.0	8.6	27.2	31.7	24.1	82.3	bubble	65.1	12.0	15.5	13.7	8.3
24	7.9	46.8	44.2	bubble	12.4	bubble	41.5	bubble	27.9	52.0	bubble	17.1
25	0.0	0.0	27.1	36.4	bubble	bubble	50.1	bubble	8.0	bubble	bubble	12.2
avg.	9.2	16.1	16.5	15.7	12.9	23.1	19.1	16.7	19.4	21.6	19.7	18.8
std dev	25.4	24.3	24.2	24.8	9.2	21.3	16.1	18.7	15.9	14.9	13.7	12.7
% def	13	64	50	50	82	82	87	86	96	96	94	100

Avg	13.8	20.3	18.5	17.1
Std dev	5.1	3.7	1.7	1.6
% def	63.7	80.7	77.0	78.7
Std dev	44.4	16.0	23.6	25.8

Third Pilot Defect Width (microns)

72000 mJ/cm2

	c-1				c-2				c-3				c-4			
	Pre-op	Post Therm	100K	500K	Pre-op	Post Therm	100K	500K	Pre-op	Post Therm	100K	500K	Pre-op	Post Therm	100K	500K
1	flash	flash	flash	flash	47.0	47.0	47.0	47.0	0.0	14.9	4.9	11.3	0.0	5.2	5.6	6.2
2	flash	flash	flash	flash	4.4	bubble	2.9	bubble	0.0	9.8	5.1	6.7	0.0	6.0	6.2	6.4
3	flash	flash	flash	flash	0.0	2.2	0.0	1.6	0.0	11.7	7.6	6.0	0.0	4.7	4.7	5.4
4	flash	flash	flash	flash	0.0	2.5	3.2	0.0	0.0	10.1	0.0	0.0	0.0	6.0	6.5	7.3
5	flash	flash	flash	flash	0.0	4.3	4.0	3.2	0.0	2.9	11.7	0.0	0.0	6.1	6.7	6.2
6	flash	flash	flash	flash	flash	flash	flash	flash	0.0	3.2	8.3	0.0	0.0	4.9	4.8	4.6
7	flash	flash	flash	flash	flash	flash	flash	flash	0.0	5.4	0.0	0.0	0.0	3.5	2.7	2.7
8	flash	flash	flash	flash	flash	flash	flash	flash	0.0	7.9	0.0	0.0	0.0	4.9	4.9	4.2
9	flash	flash	flash	flash	flash	flash	flash	flash	0.0	8.5	0.0	0.0	0.0	3.5	4.5	4.2
10	flash	flash	flash	flash	0.0	2.1	11.1	0.5	0.0	11.1	1.8	0.0	0.0	2.8	2.8	4.1
11	flash	flash	flash	flash	0.0	bubble	5.3	0.6	0.0	3.0	0.0	0.0	0.0	2.6	2.9	2.7
12	flash	flash	flash	flash	0.0	2.9	0.0	1.0	0.0	4.7	0.0	0.0	0.0	3.0	3.5	3.7
13	flash	flash	flash	flash	bubble	2.3	5.1	0.4	0.0	3.5	0.0	5.7	0.0	1.6	1.5	1.8
14	flash	flash	flash	flash	0.0	1.8	2.9	1.0	0.0	7.3	0.0	0.0	0.0	1.8	1.8	1.7
15	0.0	1.3	0.0	1.6	0.0	2.9	0.0	1.1	0.0	4.4	0.0	0.0	0.0	1.9	1.6	1.9
16	0.0	0.0	0.0	0.3	0.0	4.4	2.9	1.2	0.0	8.6	0.0	0.0	0.0	1.8	1.5	1.5
17	0.0	0.0	0.0	0.0	0.0	1.9	5.4	0.0	0.0	4.4	0.0	0.0	0.0	1.3	1.8	1.1
18	0.0	0.0	0.0	0.2	0.0	2.0	2.2	1.0	0.0	7.2	0.0	0.0	0.0	1.6	1.4	1.3
19	0.0	0.0	0.0	0.0	0.0	1.5	2.2	0.0	14.9	44.9	0.0	63.3	0.0	4.9	2.9	3.5
20	0.0	0.0	0.0	2.4	0.0	2.4	0.0	0.0	42.8	44.7	60.0	57.0	0.0	3.8	4.5	4.4
21	0.0	9.8	0.0	0.0	0.0	0.0	1.9	0.0	46.2	42.3	54.4	41.2	0.0	3.7	5.2	6.8
22	0.0	0.3	0.0	0.0	0.0	1.7	0.6	0.0	bubble	42.7	55.8	0.0	0.0	2.6	3.4	3.4
23	0.0	5.1	0.0	2.3	0.0	10.7	0.5	0.0	31.2	70.9	34.5	0.0	0.0	6.4	8.7	5.2
24	0.0	0.0	0.0	0.0	0.0	0.0	1.0	0.0	47.6	66.5	80.0	80.7	0.0	5.2	5.4	4.2
25	0.0	0.0	0.0	0.0	0.0	4.5	2.3	3.5	84.1	96.3	85.1	86.4	0.0	8.4	9.6	8.5
avg.	0.0	1.5	0.0	0.6	2.6	5.1	4.8	3.1	11.1	21.5	16.4	14.3	0.0	3.9	4.2	4.1
std dev	0.0	3.1	0.0	1.0	10.5	10.4	2.7	10.4	22.4	25.8	28.0	27.4	0.0	1.9	2.3	2.0
% def	0	36	0	45	10	89	81	60	21	100	48	36	0	100	100	100

Avg	3.4	8.0	6.3	5.5
Std dev	5.3	9.1	7.0	6.0
% def	7.8	81.3	57.3	60.3
Std dev	10.0	30.6	43.8	28.3

Ridit Analysis

	Pre-op	Post-thm	100k	500k	Pre-op	Post-thm	100k	500k	Pre-op	Post-thm	100k	500k	Pre-op	Post-thm	100k	500k
									3 evaluators				Avg. Total			
4000-1-W mJ/cm^2	7	7	7	7	6	7	6	6	4	6	6	6	5.7	6.7	6.3	6.3
2	4	5	5	6	3	4	5	6	5	4	4	6	4.0	4.3	4.7	6.0
3	2	2	3	3	2	2	3	3	2	2	2	2	2.0	2.0	2.7	2.7
4	7	8	10	11	8	8	10	10	7	8	10	11	7.3	8.0	10.0	10.7
avg	5.0	5.5	6.3	6.8	4.8	5.3	6.0	6.3	4.5	5.0	5.5	6.3	4.8	5.3	5.9	6.4
st dev													2.3	2.6	3.1	3.3
4000-1 mJ/cm^2	8	8	9	11	8	8	9	11	9	8	9	11	8.3	8.0	9.0	11.0
2	7	9	10	11	8	8	9	11	7	8	10	11	7.3	8.3	9.7	11.0
3	fell	out			fell	out			fell	out						
4	7	8	9	9	6	8	8	9	7	8	9	9	6.7	8.0	8.7	9.0
avg	7.3	8.3	9.3	10.3	7.3	8.0	8.7	10.3	7.7	8.0	9.3	10.3	7.4	8.1	9.1	10.3
st dev													0.8	0.2	0.5	1.2
6000-1 mJ/cm2	1	2	2	2	1	2	1	2	2	2	2	2	1.3	2.0	1.7	2.0
2	1	2	2	2	1	2	1.5	2	2.5	2	2	2	1.5	2.0	1.8	2.0
3	4	4	3	4	4	5	3	4	3	3	2.5	3.5	3.7	4.0	2.8	3.8
avg	2.0	2.7	2.3	2.7	2.0	3.0	1.8	2.7	2.5	2.3	2.2	2.5	2.2	2.7	2.1	2.6
st dev													1.3	1.6	1.0	1.1
8000-1 mJ/cm2	3	5	6	5	3	6	5	6	2	4	6	4	2.7	5.0	5.7	5.0
2	2	3	3	3	2	2	2	2	2	2	2	2	2.0	2.3	2.3	2.3
3	1	5	2	4	1	3	2	4	4	4	2	3.5	2.0	4.0	2.0	3.8
avg	2.0	4.3	3.7	4.0	2.0	3.7	3.0	4.0	2.7	3.3	3.3	3.2	2.2	3.8	3.3	3.7
st dev													0.6	1.6	2.0	1.7
12000-1 mJ/cm2	4	4	4	4	3	5	4	5	3	3.5	4	3.5	3.3	4.2	4.0	4.2
2	5	5	5	5	4	4	4	4	4	4	5	4	4.3	4.3	4.7	4.3
3	4	5	4	3	3	4	3	2	3	4	3	2	3.3	4.3	3.3	2.3
avg	4.3	4.7	4.3	4.0	3.3	4.3	3.7	3.7	3.3	3.8	4.0	3.2	3.7	4.3	4.0	3.6
st dev													0.6	0.1	0.7	1.1
24000-1 mJ/cm2	2	3	3	3	5	3	3	4	2	3	3	4	3.0	3.0	3.0	3.7
2	2	2	3	4	4	3	3	4	2	2	4	3	2.7	2.3	3.3	3.7
3	2	3	3	2	4	4	4	4	3	4	3	3	3.0	3.7	3.3	3.0
avg	2.0	2.7	3.0	3.0	4.3	3.3	3.3	4.0	2.3	3.0	3.3	3.3	2.9	3.0	3.2	3.4
st dev													0.2	0.7	0.2	0.4
Control-1	2	1	1	1	1	1	1	1	1	1	1	1	1.3	1.0	1.0	1.0
2	1	1	1	1	2	2	2	2	2	2	2	2	1.7	1.7	1.7	1.7
3	5	5	5	5	5	5	4.5	5	4.5	5	5	5	4.8	5.0	4.8	5.0
4	1	1	1	1	1	1.5	1.5	1.5	1	2	2	2	1.0	1.5	1.5	1.5
avg	2.3	2.0	2.0	2.0	2.3	2.4	2.3	2.4	2.1	2.7	2.5	2.5	2.2	2.3	2.3	2.3
st dev													1.8	1.8	1.7	1.8

PART TWO
FINAL METHOD

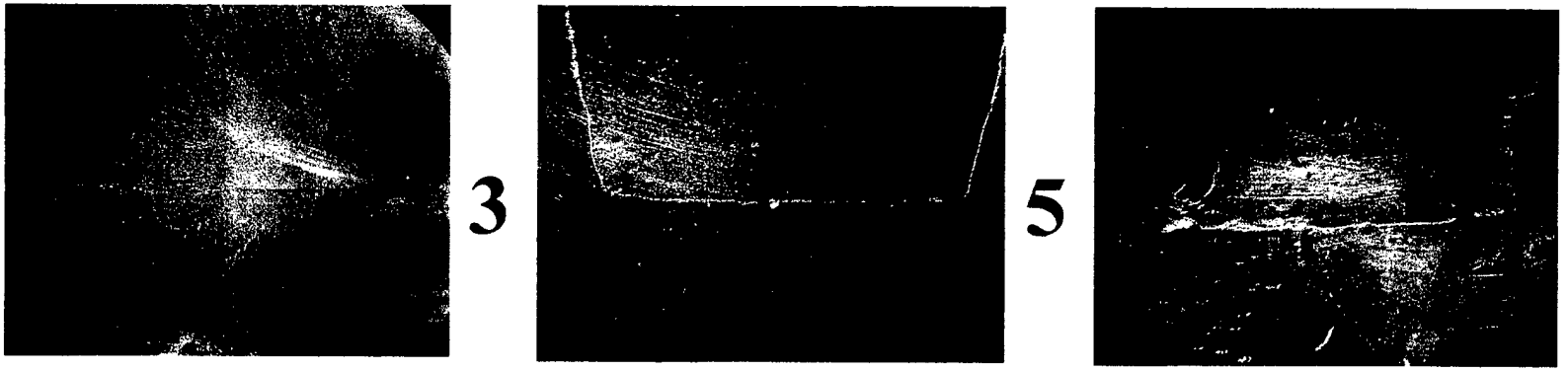

Ridit Scale

Ridit Analysis n = 8 3 evaluators

	Pre-op	Post-thm	100k	500k	Pre-op	Post-thm	100k	500k	Pre-op	Post-thm	100k	500k	Avg. Total Pre-op	Post-thm	100k	500k	T-tests
4000-1-W mJ/cm^2	7	7	7	7	6	6	7	7	6	6	7	7	6.3	6.3	7.0	7.0	pre-500k
2	4	5	5	6	3	3	4	5	3	3	4	4	3.3	3.7	4.3	5.0	
3	2	2	3	3	2	2	3	4	2	2	2	2	2.0	2.0	2.7	3.0	
4	7	8	10	11	7	9	9	11	7	7	9	11	7.0	8.0	9.3	11.0	
5	2	1	3	4	2	3	5	5	2	3	4	4	2.0	2.3	4.0	4.3	
6	6	6	6	7	3	4	3	5	6	6	7	7	5.0	5.3	5.3	6.3	
7	6	7	7	8	2	3	7	7	1	2	5	7	3.0	4.0	6.3	7.3	
8	2	5	6	6	5	5	4	5	3	3	7	7	3.3	4.3	5.7	6.0	
avg	4.5	5.1	5.9	6.5	3.8	4.4	5.3	6.1	3.8	4.0	5.6	6.1	4.0	4.5	5.6	6.3	0.0022083
st dev													1.9	2.0	2.0	2.4	
4000-1 mJ/cm^2	8	8	9	11	9	8	10	11	9	9	9	11	8.7	8.3	9.3	11.0	
2	7	9	10	11	7	7	9	11	7	8	9	10	7.0	8.0	9.3	10.7	
3	fell	out											fell	out			
4	7	8	9	9	7	8	9	9	7	8	8	9	7.0	8.0	8.7	9.0	
5	1	1	2	2	2	2	3	2	1	1	2	1	1.3	1.3	2.3	1.7	
6	6	6	6	6	4	2	3	4	4	4	4	3	4.7	4.0	4.3	4.3	
7	1	1	1	1	2	1	2	2	1	1	1	1	1.3	1.0	1.3	1.3	
8	3	4	4	4	3	3	3	5	3	4	3	4	3.0	3.7	3.3	4.3	
9	5	5	5	5	5	4	5	5	4	4	4	6	4.7	4.3	4.7	5.3	
avg	4.8	5.3	5.8	6.1	4.9	4.4	5.5	6.1	4.5	4.9	5.0	5.6	4.7	4.8	5.4	6.0	0.0348542
st dev													2.7	3.0	3.2	3.8	
6000-1 mJ/cm2	1	2	2	2	2	5	3	3	1	3	2	2	1.3	3.3	2.3	2.3	
2	2	2	2	2	3	4	3	3	1	3	4	3	2.0	3.0	3.0	2.7	
3	5	5	4	5	5	6	6	6	4	4	4	4	4.7	5.0	4.7	5.0	
4	2	2	2	2	3	2	2	4	1	2	2	2	2.0	2.0	2.0	2.7	
5	fell	out											fell	out			
6	3	3	3	2	4	2	2	3	4	3	4	2	3.7	2.7	3.0	2.3	
7	4	4	3	5	3	4	4	5	3	4	3	3	3.3	4.0	3.3	4.3	
8	1	1	1	1	2	2	2	2	2	2	2	1	1.7	1.7	1.7	1.3	
9	1	1	1	1	3	2	2	2	1	2	2	2	1.7	1.7	1.7	1.7	
avg	2.4	2.5	2.3	2.5	3.1	3.4	3.0	3.5	2.1	2.9	2.9	2.4	2.5	2.9	2.7	2.8	0.4015076
st dev													1.2	1.2	1.0	1.3	
8000-1 mJ/cm2	3	5	6	5	3	5	5	5	2	5	6	5	2.7	5.0	5.7	5.0	
2	2	3	3	3	2	6	3	5	1	3	3	3	1.7	4.0	3.0	3.7	
3	2	5	3	4	2	6	5	7	1	4	3	4	1.7	5.0	3.7	5.0	

4	4	4	4	4	5	5	5	5	3	3	4	4	4.0	4.0	4.3	4.3	
5	6	6	6	6	7	5	6	6	5	4	5	5	6.0	5.0	5.7	5.7	
6	2	2	2	2	4	3	4	3	2	3	2	2	2.7	2.7	2.7	2.3	
7	3	5	4	3	5	5	6	5	3	3	3	4	3.7	4.3	4.3	4.0	
8	4	4	4	3	4	6	5	5	4	4	4	3	4.0	4.7	4.3	3.7	
avg	3.3	4.3	4.0	3.8	4.0	5.1	4.9	5.1	2.6	3.6	3.8	3.8	3.3	4.3	4.2	4.2	0.1134822
st dev													1.4	0.8	1.1	1.0	
12000-1 mJ/cm2	4	4	4	4	4	5	4	4	3	5	4	4	3.7	4.7	4.0	4.0	
2	5	5	5	5	5	5	5	5	5	6	4	5	5.0	5.3	4.7	5.0	
3	4	5	4	3	4	5	4	4	3	4	4	4	3.7	4.7	4.0	3.7	
4	1	1	1	1	3	1	3	4	2	1	2	3	2.0	1.0	2.0	2.7	
5	4	4	4	4	5	5	5	5	3	5	4	5	4.0	4.7	4.3	4.7	
6	5	5	5	5	6	7	5	5	3	3	5	5	4.7	5.0	5.0	5.0	
7	3	3	3	3	5	5	5	5	3	3	4	4	3.7	3.7	4.0	4.0	
8	5	4	4	4	5	5	5	4	4	2	4	3	4.7	3.7	4.3	3.7	
avg	3.9	3.9	3.8	3.6	4.6	4.8	4.5	4.5	3.3	3.6	3.9	4.1	3.9	4.1	4.0	4.1	0.4070838
st dev													0.9	1.4	0.9	0.8	
24000-1 mJ/cm2	2	3	3	3	5	3	3	4	2	3	3	4	3.0	3.0	3.0	3.7	
2	2	2	3	4	4	3	3	4	2	2	4	3	2.7	2.3	3.3	3.7	
3	2	3	3	2	4	4	4	4	3	4	3	3	3.0	3.7	3.3	3.0	
4	4	4	3	4	5	4	4	3	4	5	4	4	4.3	4.3	3.7	3.7	
5	2	3	3	2	3	3	4	4	3	4	3	3	2.7	3.3	3.3	3.0	
6	3	3	2	2	3	3	3	2	3	3	2	2	3.0	3.0	2.3	2.0	
7	2	3	3	3	3	3	5	3	2	4	3	3	2.3	3.3	3.7	3.0	
8	2	3	4	3	5	4	4	4	2	4	4	3	3.0	3.7	4.0	3.3	
avg	2.4	3.0	3.0	2.9	4.0	3.4	3.8	3.5	2.6	3.6	3.3	3.1	3.0	3.3	3.3	3.2	0.5164896
st dev													0.6	0.6	0.5	0.6	
Control-1	2	2	2	2	2	3	3	3	1	2	2	2	1.7	2.3	2.3	2.3	
2	2	2	2	2	3	3	2	2	2	2	3	2	2.3	2.3	2.3	2.0	
3	5	5	5	5	6	3	4	3	5	4	4	4	5.3	4.0	4.3	4.0	
4	1	1	1	1	2	1	2	2	2	2	2	2	1.7	1.3	1.7	1.7	
5	2	2	2	2	3	2	2	2	3	2	3	3	2.7	2.0	2.3	2.3	
6	3	2	2	2	2	1	1	1	1	2	1	1	2.0	1.7	1.3	1.3	
7	2	1	1	2	2	2	2	3	2	3	2	2	2.0	2.0	1.7	2.3	
8	2	1	1	2	2	2	2	2	1	2	3	2	1.7	1.7	2.0	2.0	
avg	2.4	2.0	2.0	2.3	2.8	2.1	2.3	2.3	2.1	2.4	2.5	2.3	2.4	2.2	2.3	2.3	0.4869154
st dev													1.2	0.8	0.9	0.8	

Microleakage Raw Scores and Summary

Group	% pre	% post
4w-1	38	41
4w-2	100	38
4w-3	100	74
4w-4	52	65
4w-5	28	45
4w-6	20	90
4w-7	51	30
4w-8	35	35
4-1	38	52
4-2	100	38
4-3	broke	broke
4-4	100	100
4-5	52	52
4-6	28	45
4-7	20	38
4-8	51	95
4-9	35	25
6-1	20	44
6-2	76	100
6-3	100	100
6-4	42	64
6-5	broke	broke
6-6	89	33
6-7	32	23
6-8	59	42
6-9	43	33
8-1	100	100
8-2	79	39
8-3	76	39
8-4	25	31
8-5	50	61
8-6	39	43
8-7	41	24
8-8	45	40
12-1	50	43
12-2	73	100
12-3	82	100
12-4	48	70
12-5	82	28
12-6	41	21
12-7	36	34
12-8	56	51

Group	Avg Pre	St dev	Avg Post	St Dev	T-test	ANOVA
4w	53	31	52	21	0.96	a
4	53	31	56	27	0.86	a
6	58	28	55	30	0.85	a
8	57	25	47	24	0.44	a
12	59	18	56	31	0.84	a
24	38	14	30	5	0.15	a
C	68	25	41	32	0.11	a

Group	% pre	% post
24-1	30	27
24-2	15	37
24-3	36	27
24-4	36	30
24-5	49	26
24-6	38	24
24-7	39	34
24-8	64	37
C-1	100	13
C-2	65	39
C-3	68	100
C-4	62	100
C-5	19	14
C-6	52	20
C-7	91	20
C-8	85	21

Microleakage 4000 mJ/cm^2 (water only)

Pre-operative

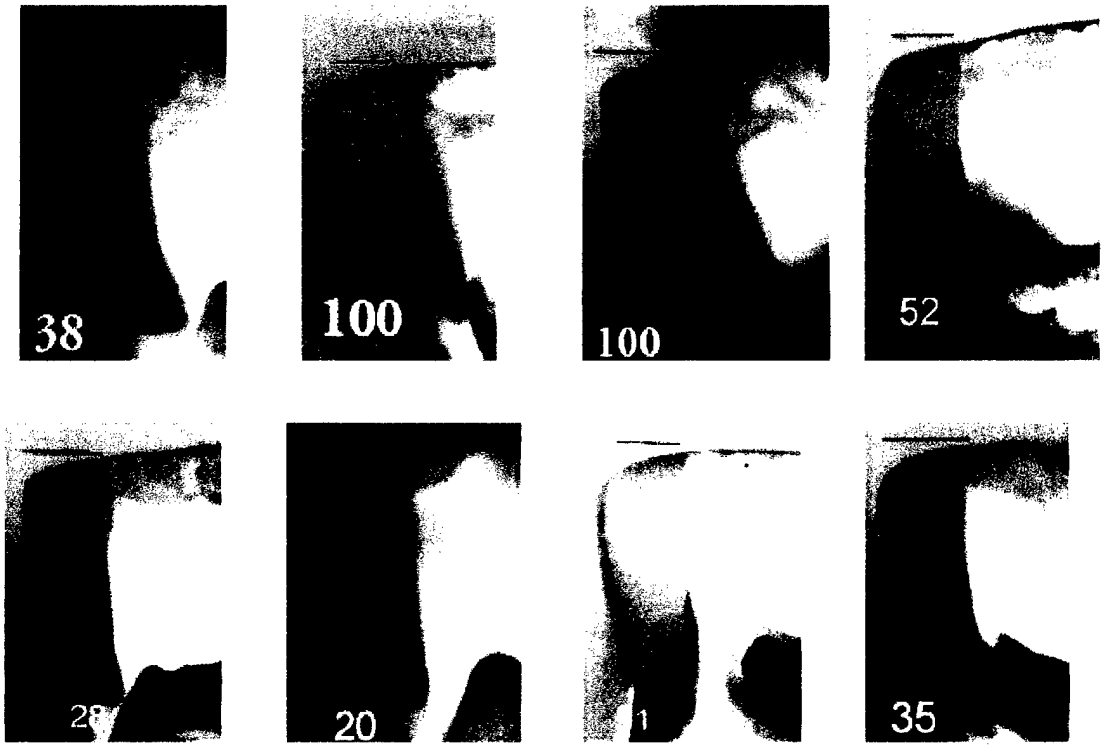

Post thermal-mechanical

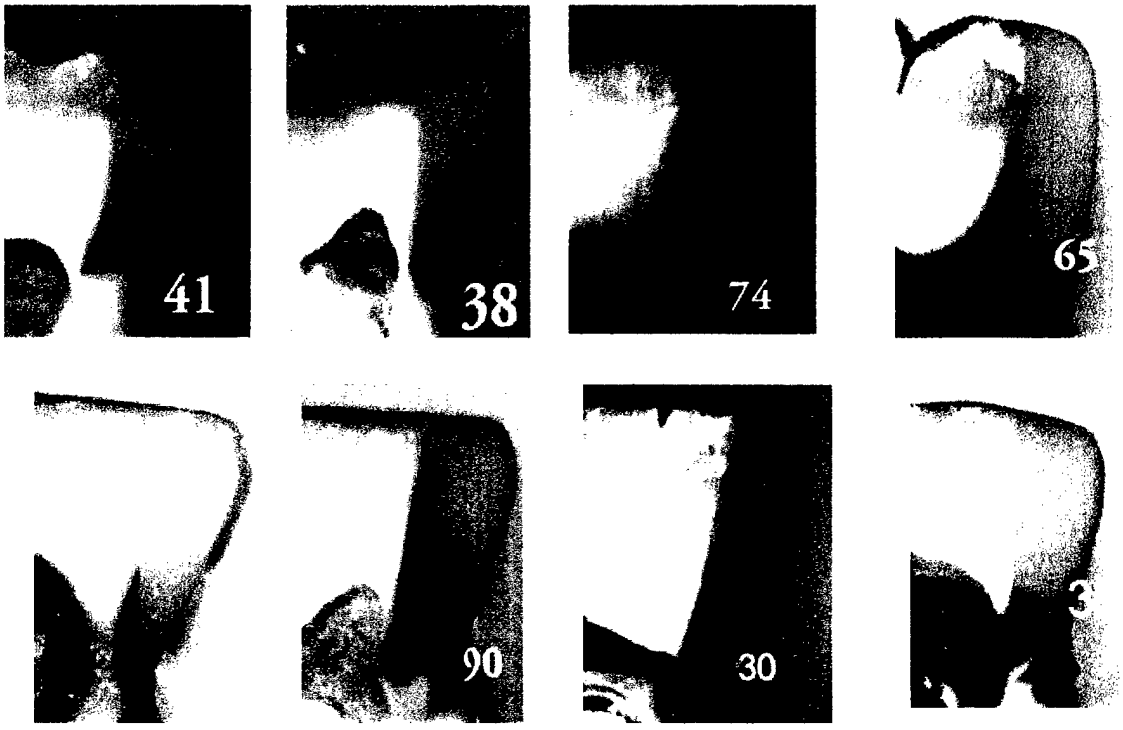

Microleakage 4000 mJ/cm^2

Pre-operative

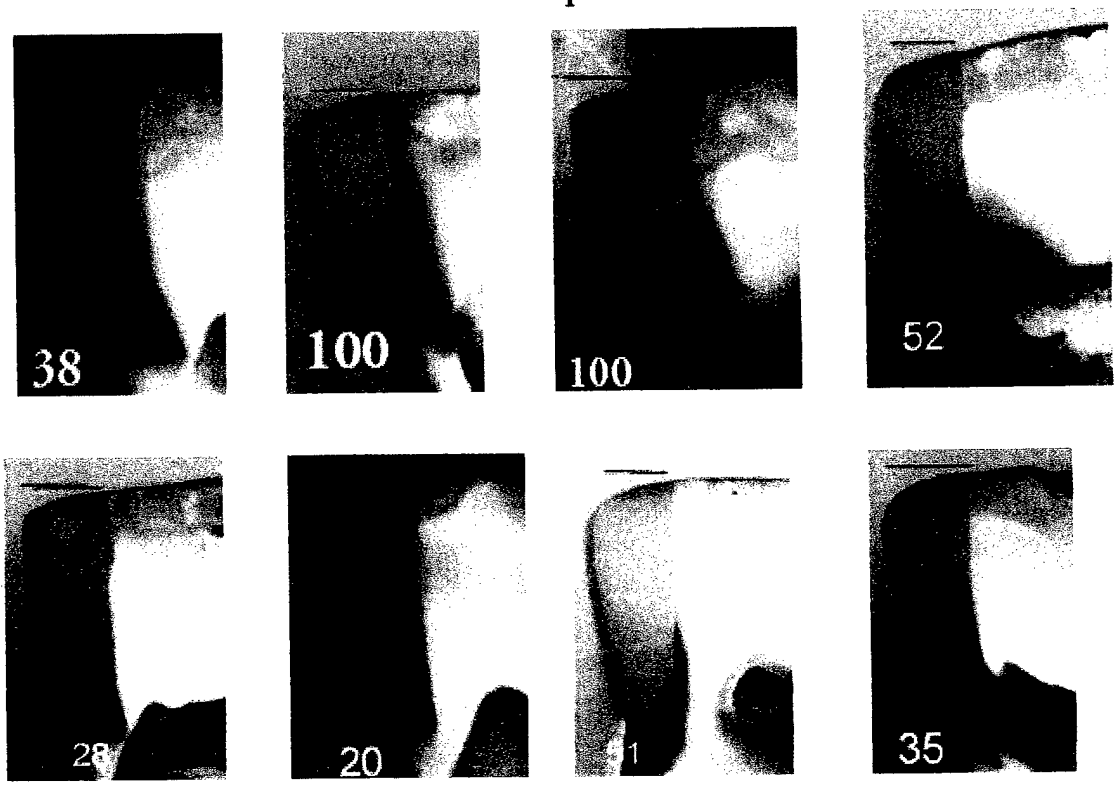

Post thermal-mechanical

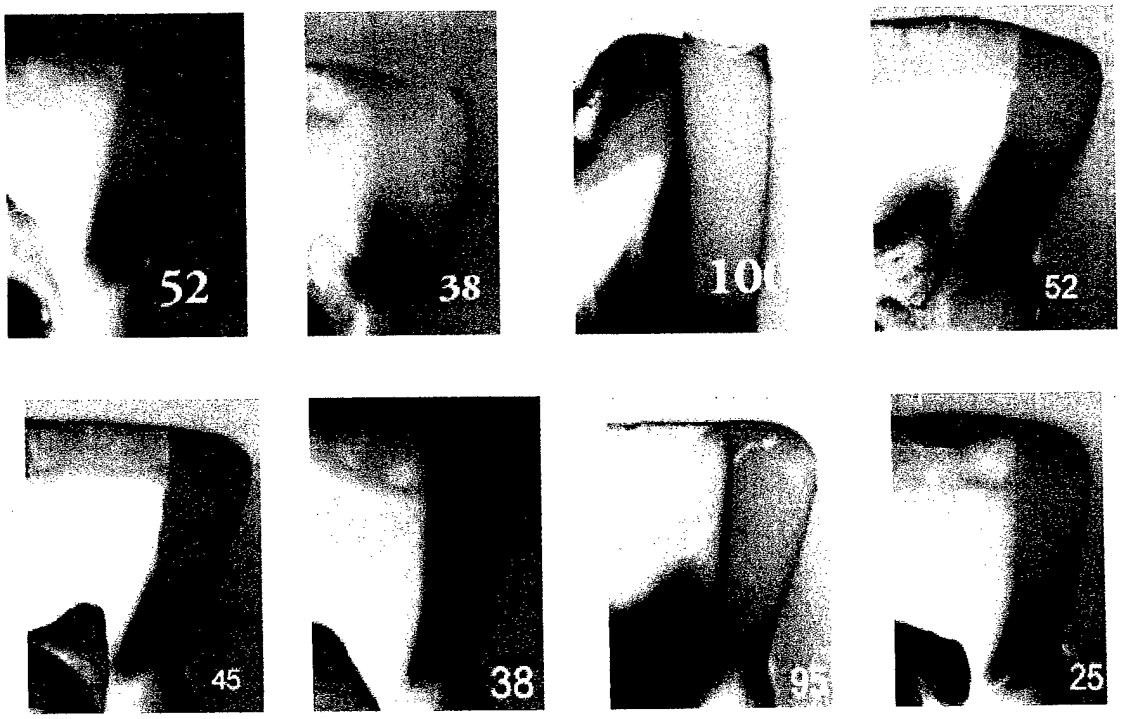

Microleakage 6000 mJ/cm^2

Pre-operative

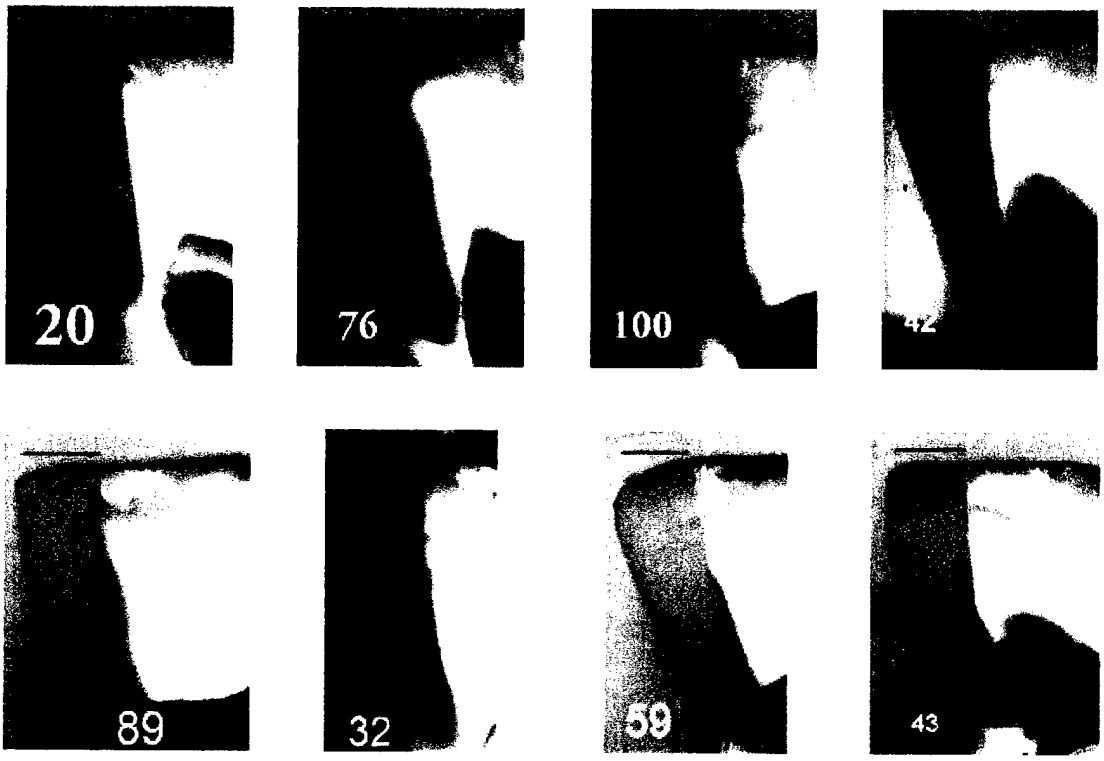

Post thermal-mechanical

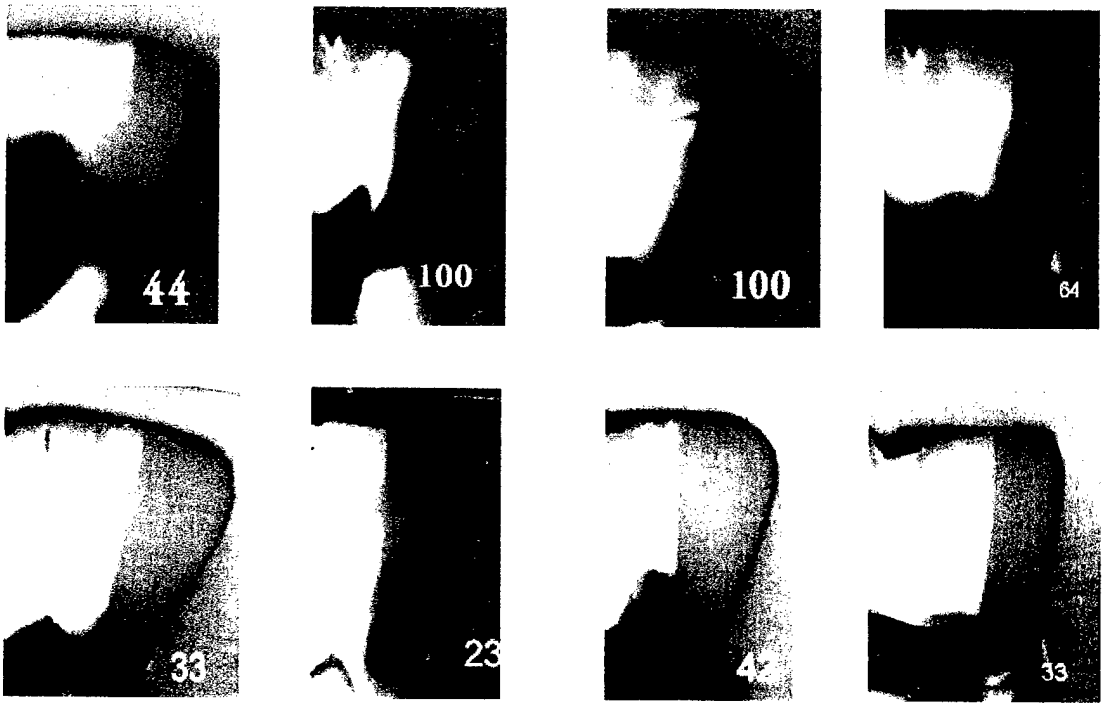

Microleakage 8000 mJ/cm^2

Pre-operative

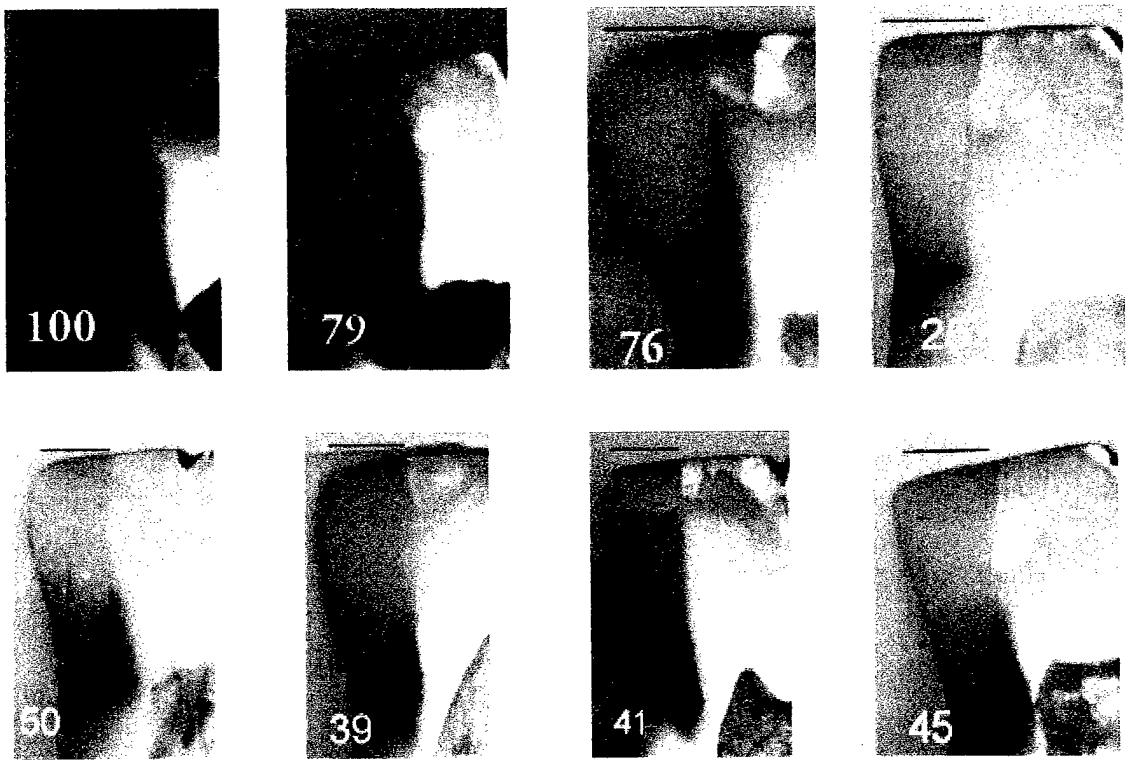

Post thermal-mechanical

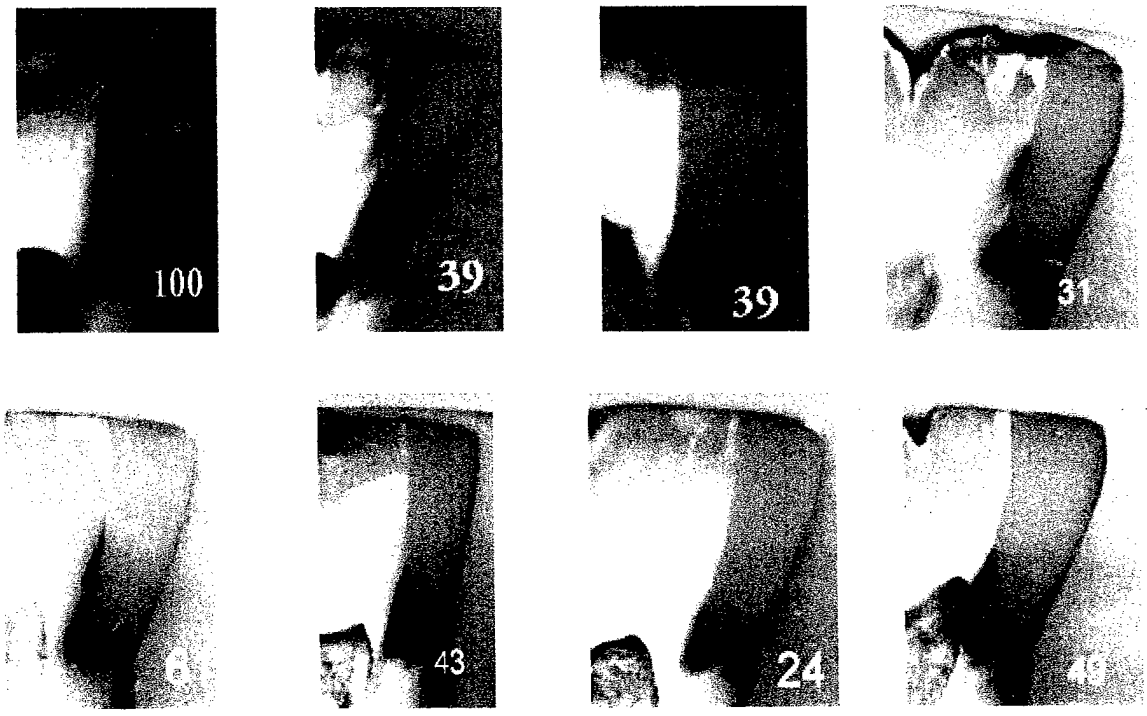

Microleakage 12000 mJ/cm^2

Pre-operative

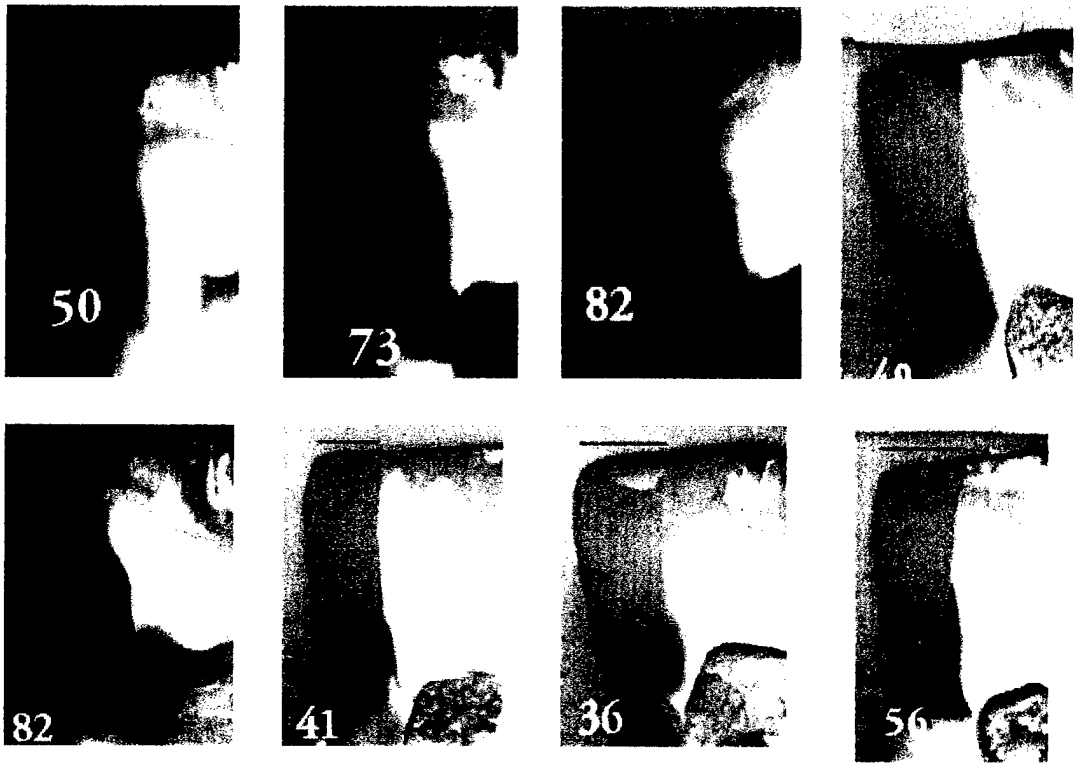

Post thermal-mechanical

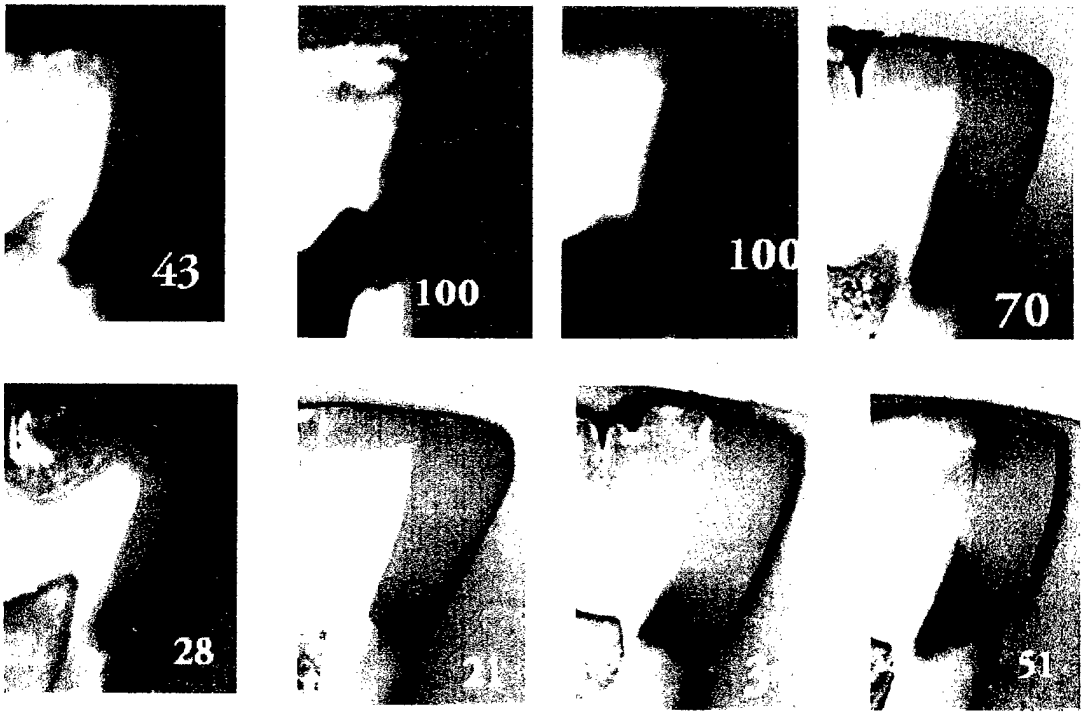

Microleakage 24000 mJ/cm^2

Pre-operative

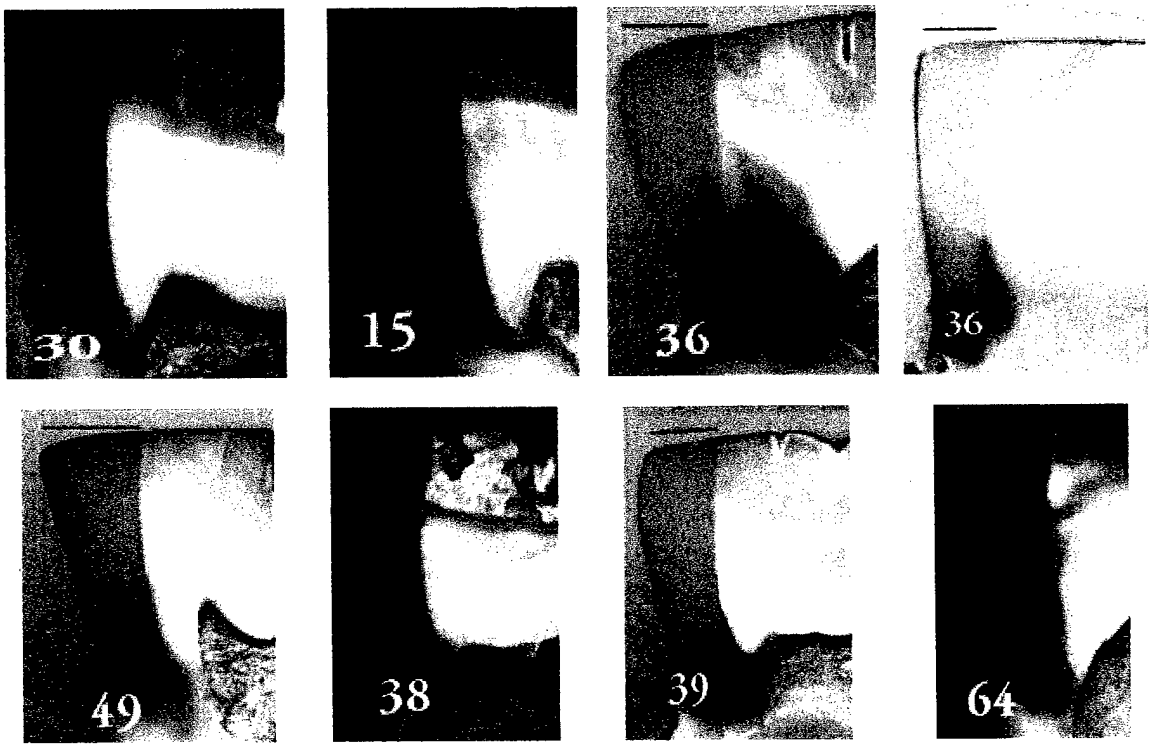

Post thermal-mechanical

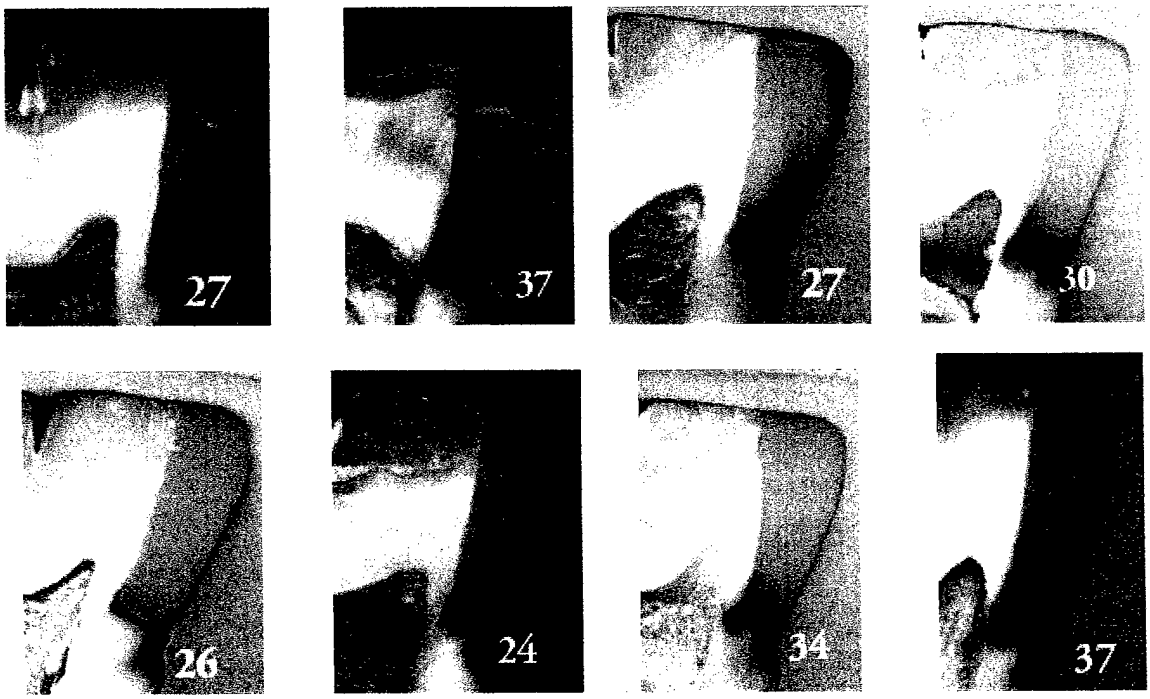

Microleakage 72000 mJ/cm^2 (Control)

Pre-operative

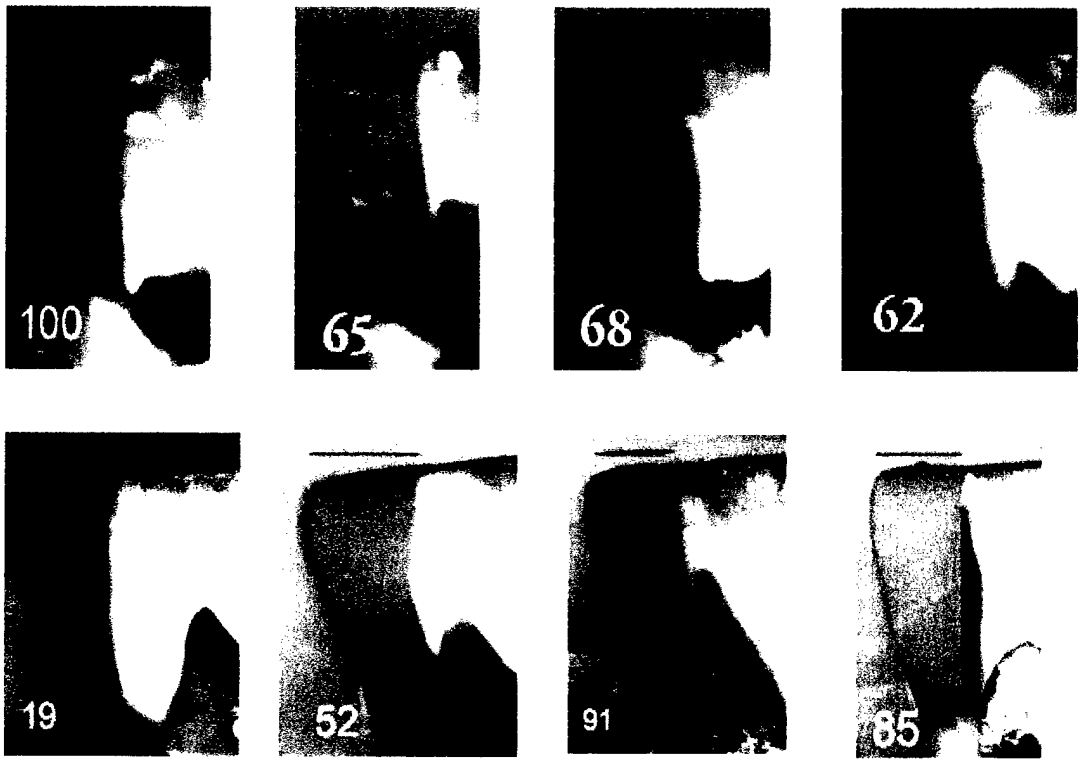

Post thermal-mechanical

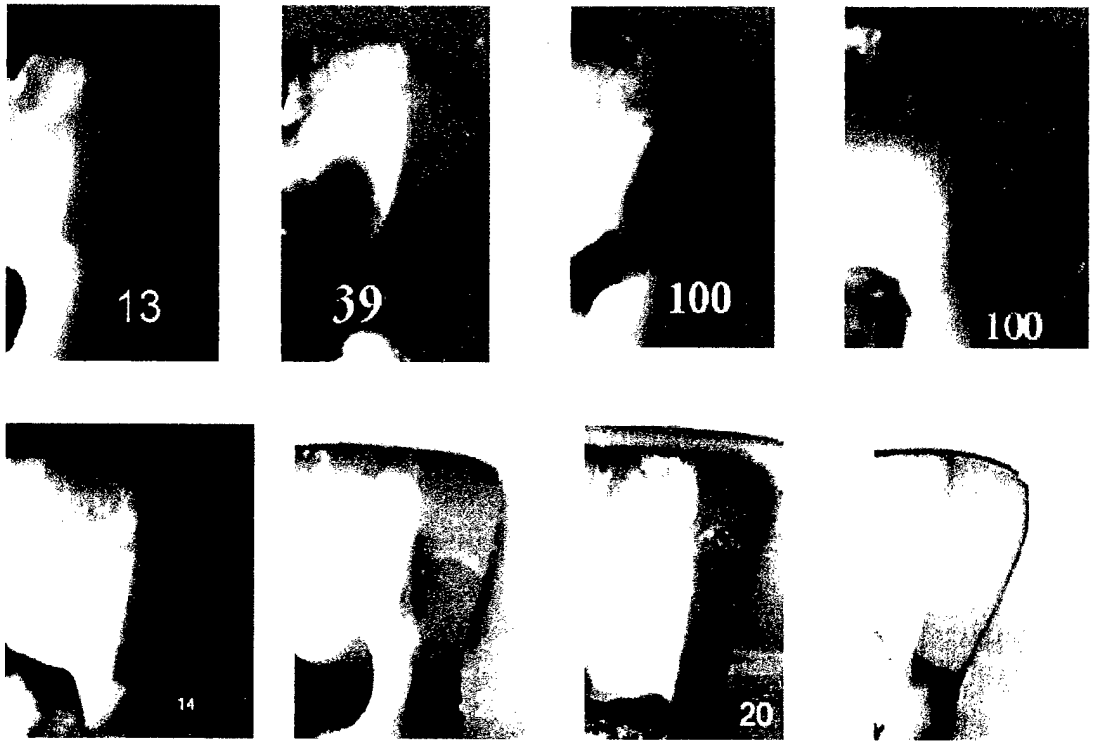

Ridit 2 - WAY ANOVA

Descriptive Statistics

Dependent Variable: RIDIT

ENERGY	STRESS	Mean	Std. Deviation	N
12	100k	4.037	.899	8
	500k	4.100	.782	8
	postherm	4.100	1.376	8
	preop	3.938	.943	8
	Total	4.044	.976	32
24	100k	3.325	.520	8
	500k	3.175	.575	8
	postherm	3.325	.597	8
	preop	3.000	.581	8
	Total	3.206	.558	32
4	100k	5.400	3.248	8
	500k	5.950	3.834	8
	postherm	4.825	2.964	8
	preop	4.713	2.741	8
	Total	5.222	3.104	32
4w	100k	5.575	2.032	8
	500k	6.238	2.397	8
	postherm	4.488	2.005	8
	preop	3.988	1.900	8
	Total	5.072	2.182	32
6	100k	2.713	1.013	8
	500k	2.788	1.257	8
	postherm	2.925	1.166	8
	preop	2.550	1.202	8
	Total	2.744	1.114	32
8	100k	4.212	1.100	8
	500k	4.213	1.048	8
	postherm	4.338	.789	8
	preop	3.313	1.428	8
	Total	4.019	1.139	32
Con	100k	2.238	.909	8
	500k	2.238	.793	8
	postherm	2.163	.814	8
	preop	2.425	1.213	8
	Total	2.266	.905	32
Total	100k	3.929	1.950	56
	500k	4.100	2.278	56
	postherm	3.737	1.749	56
	preop	3.418	1.677	56
	Total	3.796	1.931	224

Tests of Between-Subjects Effects

Dependent Variable: RIDIT

Source	Type III Sum of Squares	df	Mean Square	F	Sig.
Corrected Model	282.080[a]	27	10.447	3.725	.000
Intercept	3227.724	1	3227.724	1150.942	.000
ENERGY	242.210	6	40.368	14.395	.000
STRESS	14.359	3	4.786	1.707	.167
ENERGY * STRESS	25.512	18	1.417	.505	.954
Error	549.666	196	2.804		
Total	4059.470	224			
Corrected Total	831.746	223			

a. R Squared = .339 (Adjusted R Squared = .248)

Post Hoc Tests

ENERGY

Multiple Comparisons

Dependent Variable: RIDIT
Tukey HSD

(I) ENERGY	(J) ENERGY	Mean Difference (I-J)	Std. Error	Sig.	95% Confidence Interval	
					Lower Bound	Upper Bound
12	24	.838	.419	.414	-.397	2.072
	4	-1.178	.419	.073	-2.412	5.622E-02
	4w	-1.028	.419	.176	-2.262	.206
	6	1.300*	.419	.031	6.565E-02	2.534
	8	2.500E-02	.419	1.000	-1.209	1.259
	Con	1.778*	.419	.000	.544	3.012
24	12	-.838	.419	.414	-2.072	.397
	4	-2.016*	.419	.000	-3.250	-.781
	4w	-1.866*	.419	.000	-3.100	-.631
	6	.463	.419	.927	-.772	1.697
	8	-.813	.419	.453	-2.047	.422
	Con	.941	.419	.271	-.294	2.175
4	12	1.178	.419	.073	-5.622E-02	2.412
	24	2.016*	.419	.000	.781	3.250
	4w	.150	.419	1.000	-1.084	1.384
	6	2.478*	.419	.000	1.244	3.712
	8	1.203	.419	.062	-3.122E-02	2.437
	Con	2.956*	.419	.000	1.722	4.191
4w	12	1.028	.419	.176	-.206	2.262
	24	1.866*	.419	.000	.631	3.100
	4	-.150	.419	1.000	-1.384	1.084
	6	2.328*	.419	.000	1.094	3.562
	8	1.053	.419	.154	-.181	2.287
	Con	2.806*	.419	.000	1.572	4.041
6	12	-1.300*	.419	.031	-2.534	-6.565E-02
	24	-.463	.419	.927	-1.697	.772
	4	-2.478*	.419	.000	-3.712	-1.244
	4w	-2.328*	.419	.000	-3.562	-1.094
	8	-1.275*	.419	.038	-2.509	-4.065E-02
	Con	.478	.419	.915	-.756	1.712
8	12	-2.500E-02	.419	1.000	-1.259	1.209
	24	.813	.419	.453	-.422	2.047
	4	-1.203	.419	.062	-2.437	3.122E-02
	4w	-1.053	.419	.154	-2.287	.181
	6	1.275*	.419	.038	4.065E-02	2.509
	Con	1.753*	.419	.001	.519	2.987
Con	12	-1.778*	.419	.000	-3.012	-.544
	24	-.941	.419	.271	-2.175	.294
	4	-2.956*	.419	.000	-4.191	-1.722
	4w	-2.806*	.419	.000	-4.041	-1.572
	6	-.478	.419	.915	-1.712	.756
	8	-1.753*	.419	.001	-2.987	-.519

Based on observed means.

*. The mean difference is significant at the .05 level.

Homogeneous Subsets

RIDIT

Tukey HSD[a,b]

ENERGY	N	Subset 1	Subset 2	Subset 3
Con	32	2.266		
6	32	2.744		
24	32	3.206	3.206	
8	32		4.019	4.019
12	32		4.044	4.044
4w	32			5.072
4	32			5.222
Sig.		.271	.414	.062

Means for groups in homogeneous subsets are displayed.
Based on Type III Sum of Squares
The error term is Mean Square(Error) = 2.804.

a. Uses Harmonic Mean Sample Size = 32.000.

b. Alpha = .05.

STRESS

Multiple Comparisons

Dependent Variable: RIDIT
Tukey HSD

(I) STRESS	(J) STRESS	Mean Difference (I-J)	Std. Error	Sig.	95% Confidence Interval Lower Bound	95% Confidence Interval Upper Bound
100k	500k	-.171	.316	.949	-.984	.642
	postherm	.191	.316	.931	-.622	1.004
	preop	.511	.316	.371	-.302	1.324
500k	100k	.171	.316	.949	-.642	.984
	postherm	.363	.316	.661	-.451	1.176
	preop	.682	.316	.136	-.131	1.495
postherm	100k	-.191	.316	.931	-1.004	.622
	500k	-.363	.316	.661	-1.176	.451
	preop	.320	.316	.744	-.493	1.133
preop	100k	-.511	.316	.371	-1.324	.302
	500k	-.682	.316	.136	-1.495	.131
	postherm	-.320	.316	.744	-1.133	.493

Based on observed means.

Homogeneous Subsets

RIDIT

Tukey HSD[a,b]

STRESS	N	Subset 1
preop	56	3.418
postherm	56	3.737
100k	56	3.929
500k	56	4.100
Sig.		.136

Means for groups in homogeneous subsets are displayed.
Based on Type III Sum of Squares
The error term is Mean Square(Error) = 2.804.

a. Uses Harmonic Mean Sample Size = 56.000.

b. Alpha = .05.

Microleakage 2-way ANOVA

Between-Subjects Factors

		N
ENERGY	12	16
	24	16
	4	16
	4w	16
	6	16
	8	16
	con	16
STRESS	post	56
	pre	56

Descriptive Statistics

Dependent Variable: PERCENT

ENERGY	STRESS	Mean	Std. Deviation	N
12	post	55.88	31.06	8
	pre	58.50	18.19	8
	Total	57.19	24.63	16
24	post	30.25	5.12	8
	pre	38.38	14.13	8
	Total	34.31	11.09	16
4	post	55.63	27.30	8
	pre	53.00	30.91	8
	Total	54.31	28.20	16
4w	post	52.25	21.50	8
	pre	53.00	30.91	8
	Total	52.63	25.72	16
6	post	54.88	30.27	8
	pre	57.63	28.41	8
	Total	56.25	28.39	16
8	post	47.13	23.85	8
	pre	56.88	25.33	8
	Total	52.00	24.30	16
con	post	40.88	37.34	8
	pre	67.75	25.48	8
	Total	54.31	33.86	16
Total	post	48.13	26.96	56
	pre	55.02	25.42	56
	Total	51.57	26.31	112

Tests of Between-Subjects Effects

Dependent Variable: PERCENT

Source	Type III Sum of Squares	df	Mean Square	F	Sig.
Corrected Model	9502.929[a]	13	730.995	1.064	.399
Intercept	297876.571	1	297876.571	433.639	.000
ENERGY	5881.929	6	980.321	1.427	.212
STRESS	1330.321	1	1330.321	1.937	.167
ENERGY * STRESS	2290.679	6	381.780	.556	.764
Error	67318.500	98	686.923		
Total	374698.000	112			
Corrected Total	76821.429	111			

a. R Squared = .124 (Adjusted R Squared = .007)

Post Hoc Tests

ENERGY

Multiple Comparisons

Dependent Variable: PERCENT
Tukey HSD

(I) ENERGY	(J) ENERGY	Mean Difference (I-J)	Std. Error	Sig.	95% Confidence Interval	
					Lower Bound	Upper Bound
12	24	22.88	9.27	.182	-5.02	50.77
	4	2.88	9.27	1.000	-25.02	30.77
	4w	4.56	9.27	.999	-23.33	32.46
	6	.94	9.27	1.000	-26.96	28.83
	8	5.19	9.27	.998	-22.71	33.08
	con	2.88	9.27	1.000	-25.02	30.77
24	12	-22.88	9.27	.182	-50.77	5.02
	4	-20.00	9.27	.328	-47.90	7.90
	4w	-18.31	9.27	.436	-46.21	9.58
	6	-21.94	9.27	.224	-49.83	5.96
	8	-17.69	9.27	.480	-45.58	10.21
	con	-20.00	9.27	.328	-47.90	7.90
4	12	-2.88	9.27	1.000	-30.77	25.02
	24	20.00	9.27	.328	-7.90	47.90
	4w	1.69	9.27	1.000	-26.21	29.58
	6	-1.94	9.27	1.000	-29.83	25.96
	8	2.31	9.27	1.000	-25.58	30.21
	con	.00	9.27	1.000	-27.90	27.90
4w	12	-4.56	9.27	.999	-32.46	23.33
	24	18.31	9.27	.436	-9.58	46.21
	4	-1.69	9.27	1.000	-29.58	26.21
	6	-3.63	9.27	1.000	-31.52	24.27
	8	.63	9.27	1.000	-27.27	28.52
	con	-1.69	9.27	1.000	-29.58	26.21
6	12	-.94	9.27	1.000	-28.83	26.96
	24	21.94	9.27	.224	-5.96	49.83
	4	1.94	9.27	1.000	-25.96	29.83
	4w	3.63	9.27	1.000	-24.27	31.52
	8	4.25	9.27	.999	-23.65	32.15
	con	1.94	9.27	1.000	-25.96	29.83
8	12	-5.19	9.27	.998	-33.08	22.71
	24	17.69	9.27	.480	-10.21	45.58
	4	-2.31	9.27	1.000	-30.21	25.58
	4w	-.63	9.27	1.000	-28.52	27.27
	6	-4.25	9.27	.999	-32.15	23.65
	con	-2.31	9.27	1.000	-30.21	25.58
con	12	-2.88	9.27	1.000	-30.77	25.02
	24	20.00	9.27	.328	-7.90	47.90
	4	.00	9.27	1.000	-27.90	27.90
	4w	1.69	9.27	1.000	-26.21	29.58
	6	-1.94	9.27	1.000	-29.83	25.96
	8	2.31	9.27	1.000	-25.58	30.21

Based on observed means.

Homogeneous Subsets

PERCENT

Tukey HSD[a,b]

ENERGY	N	Subset 1
24	16	34.31
8	16	52.00
4w	16	52.63
4	16	54.31
con	16	54.31
6	16	56.25
12	16	57.19
Sig.		.182

Means for groups in homogeneous subsets are displayed.
Based on Type III Sum of Squares
The error term is Mean Square(Error) = 686.923.

a. Uses Harmonic Mean Sample Size = 16.000.

b. Alpha = .05.

1-Way ANOVA Microleakage Pre and Post Stressing

Between-Subjects Factors

		N
ENERGY	12	8
	24	8
	4	8
	4w	8
	6	8
	8	8
	con	8

Descriptive Statistics

Dependent Variable: PERCENPR

ENERGY	Mean	Std. Deviation	N
12	58.50	18.19	8
24	38.38	14.13	8
4	53.00	30.91	8
4w	53.00	30.91	8
6	57.63	28.41	8
8	56.88	25.33	8
con	67.75	25.48	8
Total	55.02	25.42	56

Tests of Between-Subjects Effects

Dependent Variable: PERCENPR

Source	Type III Sum of Squares	df	Mean Square	F	Sig.
Corrected Model	3756.857[a]	6	626.143	.966	.458
Intercept	169510.018	1	169510.018	261.440	.000
ENERGY	3756.857	6	626.143	.966	.458
Error	31770.125	49	648.370		
Total	205037.000	56			
Corrected Total	35526.982	55			

a. R Squared = .106 (Adjusted R Squared = -.004)

Post Hoc Tests

ENERGY

Multiple Comparisons

Dependent Variable: PERCENPR
Tukey HSD

(I) ENERGY	(J) ENERGY	Mean Difference (I-J)	Std. Error	Sig.	95% Confidence Interval	
					Lower Bound	Upper Bound
12	24	20.13	12.73	.695	-19.01	59.26
	4	5.50	12.73	.999	-33.64	44.64
	4w	5.50	12.73	.999	-33.64	44.64
	6	.88	12.73	1.000	-38.26	40.01
	8	1.63	12.73	1.000	-37.51	40.76
	con	-9.25	12.73	.990	-48.39	29.89
24	12	-20.13	12.73	.695	-59.26	19.01
	4	-14.63	12.73	.909	-53.76	24.51
	4w	-14.63	12.73	.909	-53.76	24.51
	6	-19.25	12.73	.736	-58.39	19.89
	8	-18.50	12.73	.770	-57.64	20.64
	con	-29.38	12.73	.261	-68.51	9.76
4	12	-5.50	12.73	.999	-44.64	33.64
	24	14.63	12.73	.909	-24.51	53.76
	4w	.00	12.73	1.000	-39.14	39.14
	6	-4.62	12.73	1.000	-43.76	34.51
	8	-3.87	12.73	1.000	-43.01	35.26
	con	-14.75	12.73	.906	-53.89	24.39
4w	12	-5.50	12.73	.999	-44.64	33.64
	24	14.63	12.73	.909	-24.51	53.76
	4	.00	12.73	1.000	-39.14	39.14
	6	-4.62	12.73	1.000	-43.76	34.51
	8	-3.87	12.73	1.000	-43.01	35.26
	con	-14.75	12.73	.906	-53.89	24.39
6	12	-.88	12.73	1.000	-40.01	38.26
	24	19.25	12.73	.736	-19.89	58.39
	4	4.62	12.73	1.000	-34.51	43.76
	4w	4.62	12.73	1.000	-34.51	43.76
	8	.75	12.73	1.000	-38.39	39.89
	con	-10.13	12.73	.984	-49.26	29.01
8	12	-1.63	12.73	1.000	-40.76	37.51
	24	18.50	12.73	.770	-20.64	57.64
	4	3.87	12.73	1.000	-35.26	43.01
	4w	3.87	12.73	1.000	-35.26	43.01
	6	-.75	12.73	1.000	-39.89	38.39
	con	-10.88	12.73	.978	-50.01	28.26
con	12	9.25	12.73	.990	-29.89	48.39
	24	29.38	12.73	.261	-9.76	68.51
	4	14.75	12.73	.906	-24.39	53.89
	4w	14.75	12.73	.906	-24.39	53.89
	6	10.13	12.73	.984	-29.01	49.26
	8	10.88	12.73	.978	-28.26	50.01

Based on observed means.

Homogeneous Subsets

PERCENPR

Tukey HSD[a,b]

ENERGY	N	Subset 1
24	8	38.38
4	8	53.00
4w	8	53.00
8	8	56.88
6	8	57.63
12	8	58.50
con	8	67.75
Sig.		.261

Means for groups in homogeneous subsets are displayed.
Based on Type III Sum of Squares
The error term is Mean Square(Error) = 648.370.

a. Uses Harmonic Mean Sample Size = 8.000.

b. Alpha = .05.

Univariate Analysis of Variance

Between-Subjects Factors

		N
ENERGY	12	8
	24	8
	4	8
	4w	8
	6	8
	8	8
	con	8

Descriptive Statistics

Dependent Variable: PERCENPO

ENERGY	Mean	Std. Deviation	N
12	55.88	31.06	8
24	30.25	5.12	8
4	55.63	27.30	8
4w	52.25	21.50	8
6	54.88	30.27	8
8	47.13	23.85	8
con	40.88	37.34	8
Total	48.13	26.96	56

Tests of Between-Subjects Effects

Dependent Variable: PERCENPO

Source	Type III Sum of Squares	df	Mean Square	F	Sig.
Corrected Model	4415.750[a]	6	735.958	1.014	.427
Intercept	129696.875	1	129696.875	178.775	.000
ENERGY	4415.750	6	735.958	1.014	.427
Error	35548.375	49	725.477		
Total	169661.000	56			
Corrected Total	39964.125	55			

a. R Squared = .110 (Adjusted R Squared = .002)

Post Hoc Tests

ENERGY

Multiple Comparisons

Dependent Variable: PERCENPO
Tukey HSD

(I) ENERGY	(J) ENERGY	Mean Difference (I-J)	Std. Error	Sig.	95% Confidence Interval	
					Lower Bound	Upper Bound
12	24	25.63	13.47	.488	-15.77	67.02
	4	.25	13.47	1.000	-41.15	41.65
	4w	3.63	13.47	1.000	-37.77	45.02
	6	1.00	13.47	1.000	-40.40	42.40
	8	8.75	13.47	.995	-32.65	50.15
	con	15.00	13.47	.921	-26.40	56.40
24	12	-25.63	13.47	.488	-67.02	15.77
	4	-25.38	13.47	.500	-66.77	16.02
	4w	-22.00	13.47	.662	-63.40	19.40
	6	-24.63	13.47	.536	-66.02	16.77
	8	-16.88	13.47	.869	-58.27	24.52
	con	-10.63	13.47	.985	-52.02	30.77
4	12	-.25	13.47	1.000	-41.65	41.15
	24	25.38	13.47	.500	-16.02	66.77
	4w	3.38	13.47	1.000	-38.02	44.77
	6	.75	13.47	1.000	-40.65	42.15
	8	8.50	13.47	.995	-32.90	49.90
	con	14.75	13.47	.927	-26.65	56.15
4w	12	-3.63	13.47	1.000	-45.02	37.77
	24	22.00	13.47	.662	-19.40	63.40
	4	-3.38	13.47	1.000	-44.77	38.02
	6	-2.63	13.47	1.000	-44.02	38.77
	8	5.13	13.47	1.000	-36.27	46.52
	con	11.38	13.47	.979	-30.02	52.77
6	12	-1.00	13.47	1.000	-42.40	40.40
	24	24.63	13.47	.536	-16.77	66.02
	4	-.75	13.47	1.000	-42.15	40.65
	4w	2.63	13.47	1.000	-38.77	44.02
	8	7.75	13.47	.997	-33.65	49.15
	con	14.00	13.47	.942	-27.40	55.40
8	12	-8.75	13.47	.995	-50.15	32.65
	24	16.88	13.47	.869	-24.52	58.27
	4	-8.50	13.47	.995	-49.90	32.90
	4w	-5.13	13.47	1.000	-46.52	36.27
	6	-7.75	13.47	.997	-49.15	33.65
	con	6.25	13.47	.999	-35.15	47.65
con	12	-15.00	13.47	.921	-56.40	26.40
	24	10.63	13.47	.985	-30.77	52.02
	4	-14.75	13.47	.927	-56.15	26.65
	4w	-11.38	13.47	.979	-52.77	30.02
	6	-14.00	13.47	.942	-55.40	27.40
	8	-6.25	13.47	.999	-47.65	35.15

Based on observed means.

Homogeneous Subsets

PERCENPO

Tukey HSD[a,b]

ENERGY	N	Subset 1
24	8	30.25
con	8	40.88
8	8	47.13
4w	8	52.25
6	8	54.88
4	8	55.63
12	8	55.88
Sig.		.488

Means for groups in homogeneous subsets are displayed.
Based on Type III Sum of Squares
The error term is Mean Square(Error) = 725.477.

a. Uses Harmonic Mean Sample Size = 8.000.

b. Alpha = .05.

PART THREE

KHN **n = 3** **Flexure Bars**

	4 secs			avg	st dev		
surface	20.7	27.0	19.9	22.5	3.9	31.4	% of max
inside	16.6	14.8	16.0	15.8	0.9	22	% of max

	8 secs			avg	st dev		
surface	37.8	37.1	32.8	35.9	2.7	50	% of max
inside	39.5	33.4	36.4	36.4	3.1	50.7	% of max

	16 secs			avg	st dev		
surface	50.3	51.6	49.0	50.3	1.3	70.1	% of max
inside	50.7	51.0	47.2	49.6	2.1	69.1	% of max

	80 secs			avg	st dev		
surface	66.1	64.4	65.7	65.4	0.9	91.1	% of max
inside	62.4	71.8	62.3	65.5	5.5	91.2	% of max

Flexural Strength n = 5

	Force (lbs.)				Flexural Strength (MPa)			
	Control	16 sec	8 sec	4 sec	Control	16 sec	8 sec	4 sec
1	6.96	4.32	3.98	1.84	116.13	72.08	66.41	30.70
2	7.29	5.22	4.46	2.33	121.63	87.10	74.42	38.88
3	7.78	6.37	3.84	2.54	129.81	106.28	64.07	42.38
4	7.38	5.60	4.52	1.75	123.14	93.44	75.42	29.20
5	8.10	5.51	4.60	2.09	135.15	91.93	76.75	34.87
avg	7.50	5.40	4.28	2.11	125.17	90.17	71.41	35.21
st dev	0.44	0.74	0.34	0.33	7.41	12.35	5.76	5.51
				% of max	92.62	66.72	52.84	26.05

Flexural Modulus n = 5

	Force(lbs.)				Elastic Modulus (GPa)			
	Control	16 sec	8 sec	4 sec	Control	16 sec	8 sec	4sec
1	5.50	3.60	2.50	1.25	12.04	7.88	5.47	2.74
2	5.50	5.00	3.00	1.00	12.04	10.95	6.57	2.19
3	5.75	4.25	2.75	1.50	12.59	9.31	6.02	3.28
4	5.50	4.25	3.00	1.00	12.04	9.31	6.57	2.19
5	5.75	3.75	2.40	1.00	12.59	8.21	5.26	2.19
avg	5.60	4.17	2.73	1.15	12.26	9.13	5.98	2.52
st dev	0.14	0.55	0.28	0.22	0.30	1.20	0.61	0.49
				%max	97.4	72.5	47.5	20.0

Curing Light Transmission Study

Purpose: To determine what percentage of the power density delivered to the occlusal surface actually reaches the gingival margin.

Materials and Methods: Three 5 millimeter Z250 resin composite specimens were created in a flattened template (Figure 7). The composite was incrementally placed and represented the control group as described previously. All three specimens were mounted simultaneously in a square acrylic ring (Figure 8) with epoxy resin as before. The acrylic ring was encased in a black opaque cardboard wrap with a window cut out to allow light transmission only through the occlusal and gingival portion of a specimen. The encased acrylic ring was placed between the center of the tip of the standard VIP light guide and the center of the external orifice of the probe of the Power Max industrial radiometer. See figure above. The VIP curing light was calibrated to deliver 600 mW/cm^2. The specimen was exposed to the light and three readings were taken and an average calculated. The black cardboard wrap was moved to reveal the next resin composite specimen and three more readings were taken until all three specimens were tested. Next the acrylic ring with mounted specimens was replaced with only the outer sheet of the

Encased 5mm resin composite specimen between light guide and probe

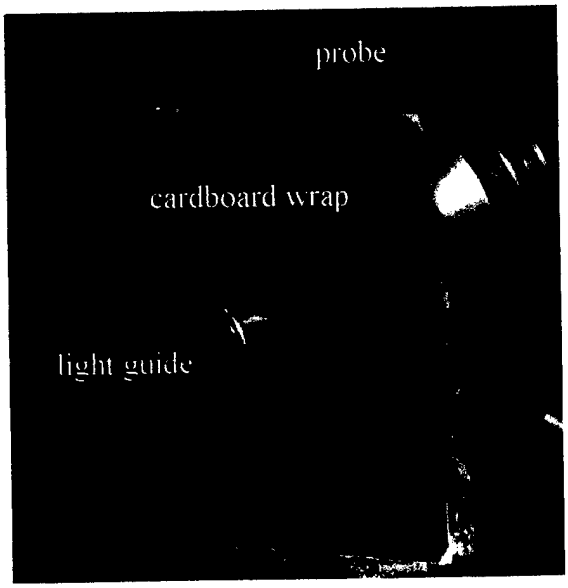

black cardboard wrap containing the entrance orifice to determine the total power exposure to the occlusal surface. Three power readings were recorded with the Power Max and an average calculated.

In order to create the most reproducible data using the Power Max the following technique was developed.

1) specimen in black wrap was placed between probe and light tip
2) Power Max was auto-zeroed
3) specimen was removed
4) VIP curing light was activated
5) specimen replaced
6) lowest, stabilized reading recorded

The same procedure was repeated with only the outer sheet of the black cardboard wrap containing the entrance orifice representing the occlusal surface.

The area of the occlusal and gingival surfaces of the black cardboard window was determined corresponding to the respective surfaces of the resin composite specimens.

Results:

Surface areas: occlusal surface of resin composite (entrance orifice): 0.0925 cm^2

gingival surface of resin composite (exit orifice): 0.064 cm^2

Power at gingival surface (n = 3)

Specimen	Power (mW)		
1	1.00	0.97	1.10
2	1.10	0.98	1.16
3	0.98	1.05	0.91

Average Power: 1.03 mW standard deviation: 0.08

Power density at gingival surface: 1.03 mW / 0.064 cm^2 = 16.1 mW/cm^2

Power at occlusal surface: (n = 1) Average: 92.4 mW

Power density at occlusal surface: 92.4 mW / 0.0925 cm^2 = 998.9 mW/cm^2

Percent change: 16.1 mW/cm^2 / 998.9 mW/cm^2 = 1.6%

Strain Gauge Study

Purpose: To determine the magnitude of strains developed at various levels in the resin composite restoration during cyclic loading and to estimate the resultant stresses.

Materials and Methods: Three single strain gauges (CEA-06-032UW-120, Measurements Group, Raleigh, NC) were bonded on the resin composite (Control Group) near the occlusal marginal ridge, at the gingival margin, and the dentinal gingival margin (Figure 24) using cyanoacrylate. The tooth was subjected to the same cyclic forces as before (18 to 85 Newtons at 1.25 Hertz). The generated strain was conditioned by a strain gauge conditioner (2100 System, Measurements Group, Raleigh, NC).

Results: Strain was recorded at 5 per second and the results are shown graphically over a 10 second span below.

Cyclic microstrain recorded over 10 seconds simultaneously at the dentinal gingival margin, composite gingival margin and near occlusal marginal ridge of 5 mm resin composite restoration of control group.

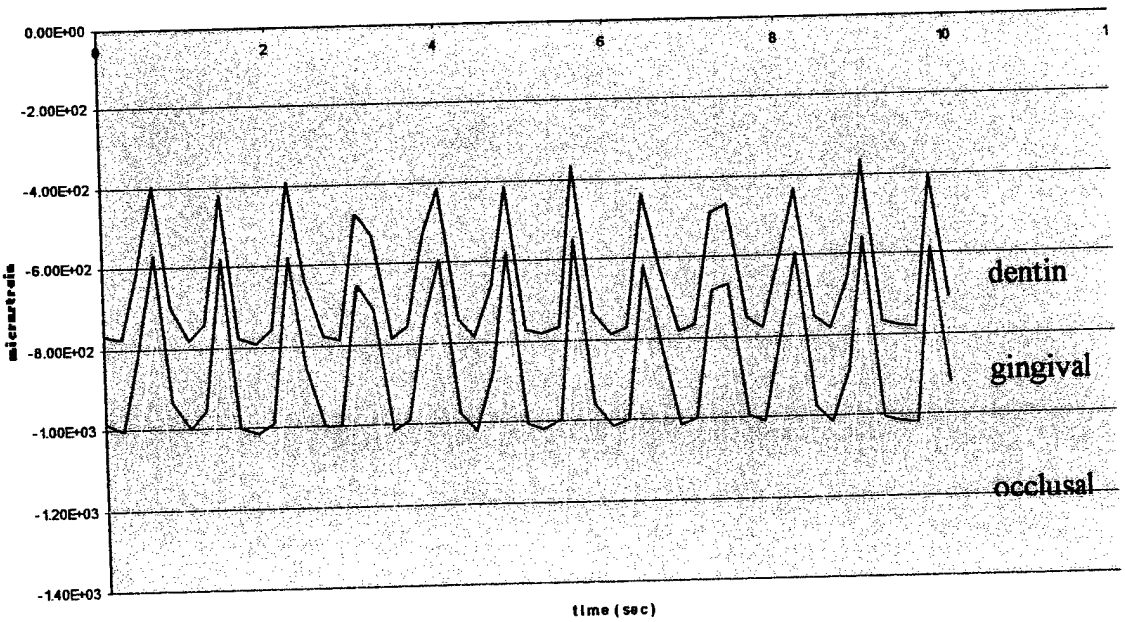

The average of 10 maximum and minimum microstrain values was determined from the graph and the results are shown below.

Maximum and minimum microstrain over 10 seconds

	occlusal		gingival		dentin	
	max	min	max	min	max	min
	1250	754	1000	570	778	397
	1260	753	1000	578	781	418
	1260	763	1010	579	790	392
	1260	830	1000	651	784	473
	1240	788	1020	596	786	415
	1270	753	1020	581	787	414
	1260	742	1020	551	784	369
	1270	799	1010	619	785	442
	1240	866	1010	667	783	470
	1250	776	1010	595	775	434
avg	1256	782	1010	599	783	422
Stress (MPa)	15.5	9.6	12.4	7.4	11.5	6.2

Assuming the control group was uniformly cured and using the flexural modulus of 12.3 GPa for Z250 as determined previously (Table 12) in Part 3, the resulting stress could be estimated by the product of the microstrain and the flexural modulus as shown above.

Oneway ANOVA Time vs flexural strength or modulus

Descriptives

FLEXURE

	N	Mean	Std. Deviation	Std. Error	95% Confidence Interval for Mean	
					Lower Bound	Upper Bound
4	5	35.220	5.520	2.468	28.366	42.074
8	5	71.420	5.754	2.573	64.275	78.565
16	5	90.160	12.345	5.521	74.832	105.488
80	5	125.140	7.405	3.312	115.946	134.334
Total	20	80.485	34.164	7.639	64.496	96.474

Descriptives

FLEXURE

	Minimum	Maximum
4	29.2	42.4
8	64.1	76.8
16	72.1	106.3
80	116.1	135.1
Total	29.2	135.1

ANOVA

FLEXURE

	Sum of Squares	df	Mean Square	F	Sig.
Between Groups	21093.846	3	7031.282	103.859	.000
Within Groups	1083.200	16	67.700		
Total	22177.046	19			

Post Hoc Tests

Multiple Comparisons

Dependent Variable: FLEXURE
Tukey HSD

(I) TIME2	(J) TIME2	Mean Difference (I-J)	Std. Error	Sig.	95% Confidence Interval	
					Lower Bound	Upper Bound
4	8	-36.200*	5.204	.000	-51.089	-21.311
	16	-54.940*	5.204	.000	-69.829	-40.051
	80	-89.920*	5.204	.000	-104.809	-75.031
8	4	36.200*	5.204	.000	21.311	51.089
	16	-18.740*	5.204	.012	-33.629	-3.851
	80	-53.720*	5.204	.000	-68.609	-38.831
16	4	54.940*	5.204	.000	40.051	69.829
	8	18.740*	5.204	.012	3.851	33.629
	80	-34.980*	5.204	.000	-49.869	-20.091
80	4	89.920*	5.204	.000	75.031	104.809
	8	53.720*	5.204	.000	38.831	68.609
	16	34.980*	5.204	.000	20.091	49.869

*. The mean difference is significant at the .05 level.

Homogeneous Subsets

FLEXURE

Tukey HSD[a]

TIME2	N	Subset for alpha = .05			
		1	2	3	4
4	5	35.220			
8	5		71.420		
16	5			90.160	
80	5				125.140
Sig.		1.000	1.000	1.000	1.000

Means for groups in homogeneous subsets are displayed.
a. Uses Harmonic Mean Sample Size = 5.000.

Oneway

Descriptives

ELASTIC

	N	Mean	Std. Deviation	Std. Error	95% Confidence Interval for Mean	
					Lower Bound	Upper Bound
4	5	2.520	.487	.218	1.916	3.124
8	5	6.000	.604	.270	5.250	6.750
16	5	9.120	1.180	.528	7.655	10.585
80	5	12.240	.329	.147	11.832	12.648
Total	20	7.470	3.763	.842	5.709	9.231

Descriptives

ELASTIC

	Minimum	Maximum
4	2.2	3.3
8	5.3	6.6
16	7.9	10.9
80	12.0	12.6
Total	2.2	12.6

ANOVA

ELASTIC

	Sum of Squares	df	Mean Square	F	Sig.
Between Groups	260.694	3	86.898	165.363	.000
Within Groups	8.408	16	.526		
Total	269.102	19			

Post Hoc Tests

Multiple Comparisons

Dependent Variable: ELASTIC
Tukey HSD

(I) TIME2	(J) TIME2	Mean Difference (I-J)	Std. Error	Sig.	95% Confidence Interval	
					Lower Bound	Upper Bound
4	8	-3.480*	.458	.000	-4.792	-2.168
	16	-6.600*	.458	.000	-7.912	-5.288
	80	-9.720*	.458	.000	-11.032	-8.408
8	4	3.480*	.458	.000	2.168	4.792
	16	-3.120*	.458	.000	-4.432	-1.808
	80	-6.240*	.458	.000	-7.552	-4.928
16	4	6.600*	.458	.000	5.288	7.912
	8	3.120*	.458	.000	1.808	4.432
	80	-3.120*	.458	.000	-4.432	-1.808
80	4	9.720*	.458	.000	8.408	11.032
	8	6.240*	.458	.000	4.928	7.552
	16	3.120*	.458	.000	1.808	4.432

*. The mean difference is significant at the .05 level.

Homogeneous Subsets

ELASTIC

Tukey HSD[a]

TIME2	N	Subset for alpha = .05			
		1	2	3	4
4	5	2.520			
8	5		6.000		
16	5			9.120	
80	5				12.240
Sig.		1.000	1.000	1.000	1.000

Means for groups in homogeneous subsets are displayed.

a. Uses Harmonic Mean Sample Size = 5.000.

Oneway ANOVA Time vs KHN surface or KHN center

Descriptives

KHNSURF

	N	Mean	Std. Deviation	Std. Error	95% Confidence Interval for Mean	
					Lower Bound	Upper Bound
4	3	22.533	3.889	2.245	12.873	32.194
8	3	35.900	2.707	1.563	29.174	42.626
16	3	50.300	1.300	.751	47.071	53.529
80	3	65.400	.889	.513	63.192	67.608
Total	12	43.533	16.840	4.861	32.834	54.233

Descriptives

KHNSURF

	Minimum	Maximum
4	19.9	27.0
8	32.8	37.8
16	49.0	51.6
80	64.4	66.1
Total	19.9	66.1

ANOVA

KHNSURF

	Sum of Squares	df	Mean Square	F	Sig.
Between Groups	3069.620	3	1023.207	164.151	.000
Within Groups	49.867	8	6.233		
Total	3119.487	11			

Post Hoc Tests

Multiple Comparisons

Dependent Variable: KHNSURF
Tukey HSD

(I) TIME	(J) TIME	Mean Difference (I-J)	Std. Error	Sig.	95% Confidence Interval	
					Lower Bound	Upper Bound
4	8	-13.367*	2.039	.001	-19.895	-6.839
	16	-27.767*	2.039	.000	-34.295	-21.239
	80	-42.867*	2.039	.000	-49.395	-36.339
8	4	13.367*	2.039	.001	6.839	19.895
	16	-14.400*	2.039	.000	-20.928	-7.872
	80	-29.500*	2.039	.000	-36.028	-22.972
16	4	27.767*	2.039	.000	21.239	34.295
	8	14.400*	2.039	.000	7.872	20.928
	80	-15.100*	2.039	.000	-21.628	-8.572
80	4	42.867*	2.039	.000	36.339	49.395
	8	29.500*	2.039	.000	22.972	36.028
	16	15.100*	2.039	.000	8.572	21.628

*. The mean difference is significant at the .05 level.

Homogeneous Subsets

KHNSURF

Tukey HSD[a]

TIME	N	Subset for alpha = .05			
		1	2	3	4
4	3	22.533			
8	3		35.900		
16	3			50.300	
80	3				65.400
Sig.		1.000	1.000	1.000	1.000

Means for groups in homogeneous subsets are displayed.
a. Uses Harmonic Mean Sample Size = 3.000.

Oneway

Descriptives

KHNCENT

	N	Mean	Std. Deviation	Std. Error	95% Confidence Interval for Mean	
					Lower Bound	Upper Bound
4	3	15.800	.917	.529	13.523	18.077
8	3	36.433	3.050	1.761	28.856	44.010
16	3	49.633	2.113	1.220	44.385	54.881
80	3	65.500	5.456	3.150	51.946	79.054
Total	12	41.842	19.241	5.554	29.617	54.067

Descriptives

KHNCENT

	Minimum	Maximum
4	14.8	16.6
8	33.4	39.5
16	47.2	51.0
80	62.3	71.8
Total	14.8	71.8

ANOVA

KHNCENT

	Sum of Squares	df	Mean Square	F	Sig.
Between Groups	3983.536	3	1327.845	119.689	.000
Within Groups	88.753	8	11.094		
Total	4072.289	11			

Post Hoc Tests

Multiple Comparisons

Dependent Variable: KHNCENT
Tukey HSD

(I) TIME	(J) TIME	Mean Difference (I-J)	Std. Error	Sig.	95% Confidence Interval	
					Lower Bound	Upper Bound
4	8	-20.633*	2.720	.000	-29.343	-11.924
	16	-33.833*	2.720	.000	-42.543	-25.124
	80	-49.700*	2.720	.000	-58.409	-40.991
8	4	20.633*	2.720	.000	11.924	29.343
	16	-13.200*	2.720	.006	-21.909	-4.491
	80	-29.067*	2.720	.000	-37.776	-20.357
16	4	33.833*	2.720	.000	25.124	42.543
	8	13.200*	2.720	.006	4.491	21.909
	80	-15.867*	2.720	.002	-24.576	-7.157
80	4	49.700*	2.720	.000	40.991	58.409
	8	29.067*	2.720	.000	20.357	37.776
	16	15.867*	2.720	.002	7.157	24.576

*. The mean difference is significant at the .05 level.

Homogeneous Subsets

KHNCENT

Tukey HSD[a]

TIME	N	Subset for alpha = .05			
		1	2	3	4
4	3	15.800			
8	3		36.433		
16	3			49.633	
80	3				65.500
Sig.		1.000	1.000	1.000	1.000

Means for groups in homogeneous subsets are displayed.

a. Uses Harmonic Mean Sample Size = 3.000.

EQUIPMENT

FOURIER TRANSFORM INFRARED SPECTROSCOPY (FTIR)

(DS20, Analect Instruments, Irvine, CA)

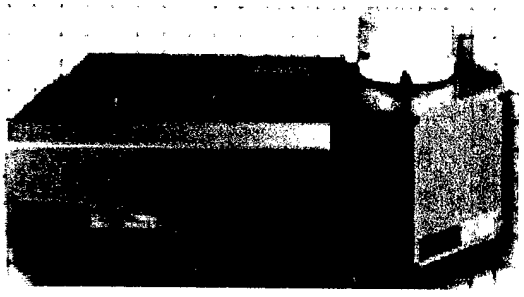

A Fourier transform is a complex mathematical computation that is performed by your computer. Infrared, an invisible part of the electromagnetic spectrum between visible light and radio waves refers to the radiation used by the spectrometer to perform its measurement. An FTIR spectrometer is an instrument that provides information about the molecules present in a given specimen of matter as well as the quantities.

An infrared source emits light that travels through the optical system of the spectrometer (the interferometer) to the resin composite specimen on the KCl crystal. The light excites the molecules in the specimen and the molecules in turn absorb some of the wavelengths of light while the remainder are transmitted to the detector. The detector then measures the amount of transmitted light. This measurement is then converted by the analog-to-digital converter (ADC) to a form that can be used by the computer software. The software performs the Fourier transform and some other operations. A display called a spectrum then appears on your computer screen. The spectrum is actually a graphic representation of your specimen in terms of the amount of light absorbed or transmitted by your sample at various frequencies along the spectrum.

The heart of the spectrometer is the interferometer, the instrument's optical system. The interferometer is a device that encodes the light from the infrared source.

After the specimen absorbs some of the light, the Fourier transform decodes the signal into the infrared spectrum. Infrared energy is transmitted from the source via mirrors to

Interferometer Diagram

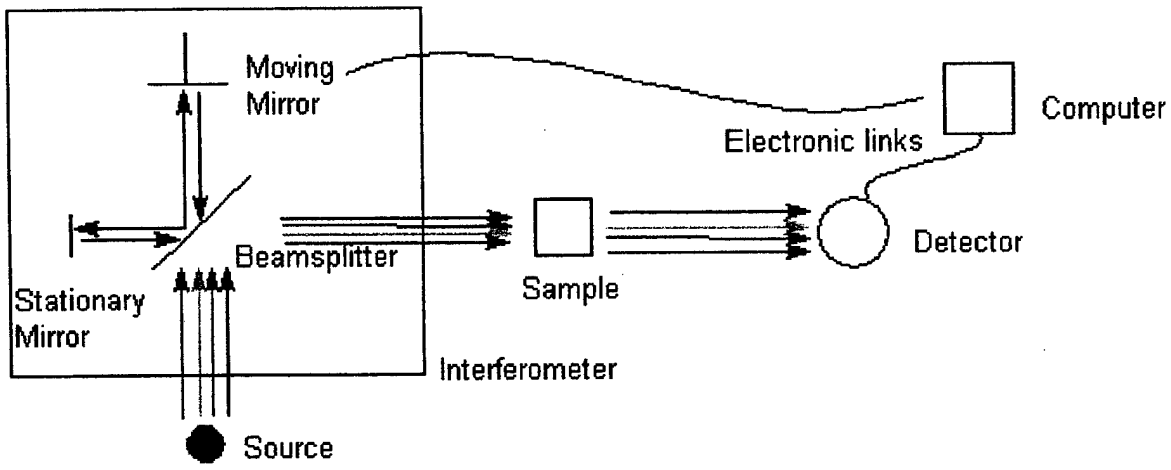

the beam-splitter where approximately half of the beam intensity is reflected toward the fixed-position mirror and the other half toward the moving mirror. The returning beam from each mirror travels back to the beam-splitter where the two beams are recombined, but the difference in path lengths creates constructive and destructive interference: an interferogram. The recombined beam passes through the sample. The sample absorbs all the different wavelengths characteristic of its spectrum, and then subtracts specific wavelengths from the interferogram. The detector now reports variation in energy versus time for all wavelengths simultaneously. A laser beam is superimposed to provide a reference for the instrument operation. A mathematical function called a Fourier tranform allows us to convert an intensity-vs-time spectrum into an intensity-vs-frequency spectrum.

The Fourier transform:

$$A(r)=\sum X(k)\exp(-2\pi\frac{irk}{N})$$

A(r) and X(k) are the frequency domain and time domain points, respectively, for a spectrum of N points.

The Fourier transform then converts the interferogram into a single-beam spectrum that is a representation of the same data in the frequency domain. That is, the single-beam spectrum shows the signal intensity for each frequency point in the range. After background data is taken (and then compensated for) this spectrum can be viewed in two modes: transmittance or absorbance.

In this project, tiny chips of resin composite, 10 to 30 microns thick, to be placed in the FTIR were removed from resin composite specimen using the tip of a scapel. The intensities of the double carbon bond (C=C) absorbance peak at 1637.3 cm^{-1} and the aromatic (C...C) reference peak at 1608.3 cm^{-1} were measured. The C...C peak originates from the aromatic rings in the Bis-GMA molecule and remains unchanged during the polymerization reaction. The ratio of the absorbance intensities of C=C/C...C were compared before and after polymerization using the following equation to determine the percent of reacted carbon double bonds or degree of conversion:

1 – [Abs (C=C) / Abs (C...C)] cured resin / [Abs (C=C) / Abs (C...C)] uncured resin X 100

Reference: Thermo Mattson Inc. "Chemist's Corner" website: www.mattsonir.com

KNOOP HARDNESS TESTER

(Kentron Microhardness, Torsion Balance Co., Clifton, NJ)

Hardness may be defined as the resistance to permanent surface indentation or penetration and is a force per unit area of indentation. The various hardness tests differ in the indenter material, geometry, and load. The indenter may be made of steel, tungsten carbide or diamond and be shaped as a sphere, cone or pyramid. The choice of hardness test depends on the material of interest, the expected hardness range and the desired degree of localization.[18]

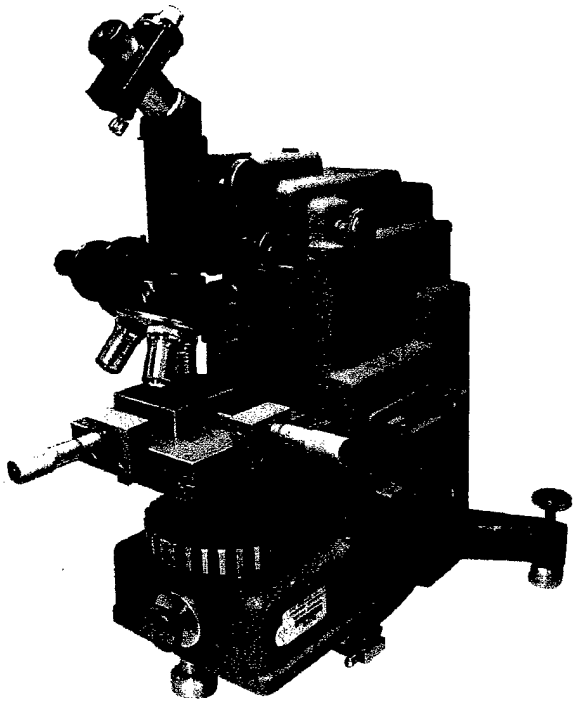

Photo by Patrick Pattamanuch

The Knoop indenter is cut in the shape of a diamond-based pyramid giving a diamond-shaped impression in which the long diagonal is very nearly 7 times the length of the short diagonal. Because of the difference in the lengths of the two diagonals, almost all of the elastic recovery of the indentations made with the Knoop indenter takes place in the transverse direction. Hence the measurement of the long diagonal together with the computed indenter constant gives a very close approximation of the un-recovered projected area of the indentation in square millimeters. The ratio of the applied load in kilograms to the approximate un-recovered projected area in square millimeters is called the Knoop Hardness Number for the specimen for that applied load.

The Knoop Hardness Number may be expressed by the formula:

$$KHN = L/Ap = L/l^2 \times C_p \text{ where}$$

KHN = Knoop Hardness Number

L = Load in kilograms applied to the indenter

Ap = Un-recovered projected area in square millimeters

l = Measured length of the long diagonal of the indentation in millimeters

C_p = Constant relating length (l) to the un-recovered projected area of the indentation. For this indenter, $C_p = 0.07028$

The Knoop indenter appears to be most useful in the investigation of the surface hardness of brittle materials such as glasses, hard carbides and oxides, thin layers of metals and small samples. The advantage of this method is that materials can be tested with a great range of hardness simply by varying the test load. The chief disadvantages are the need for a highly polished surface and a flat test sample.[18]

Reference: Kentron Micro Hardness Tester Operating Instructions

CUSTOM FATIGUE CYCLER

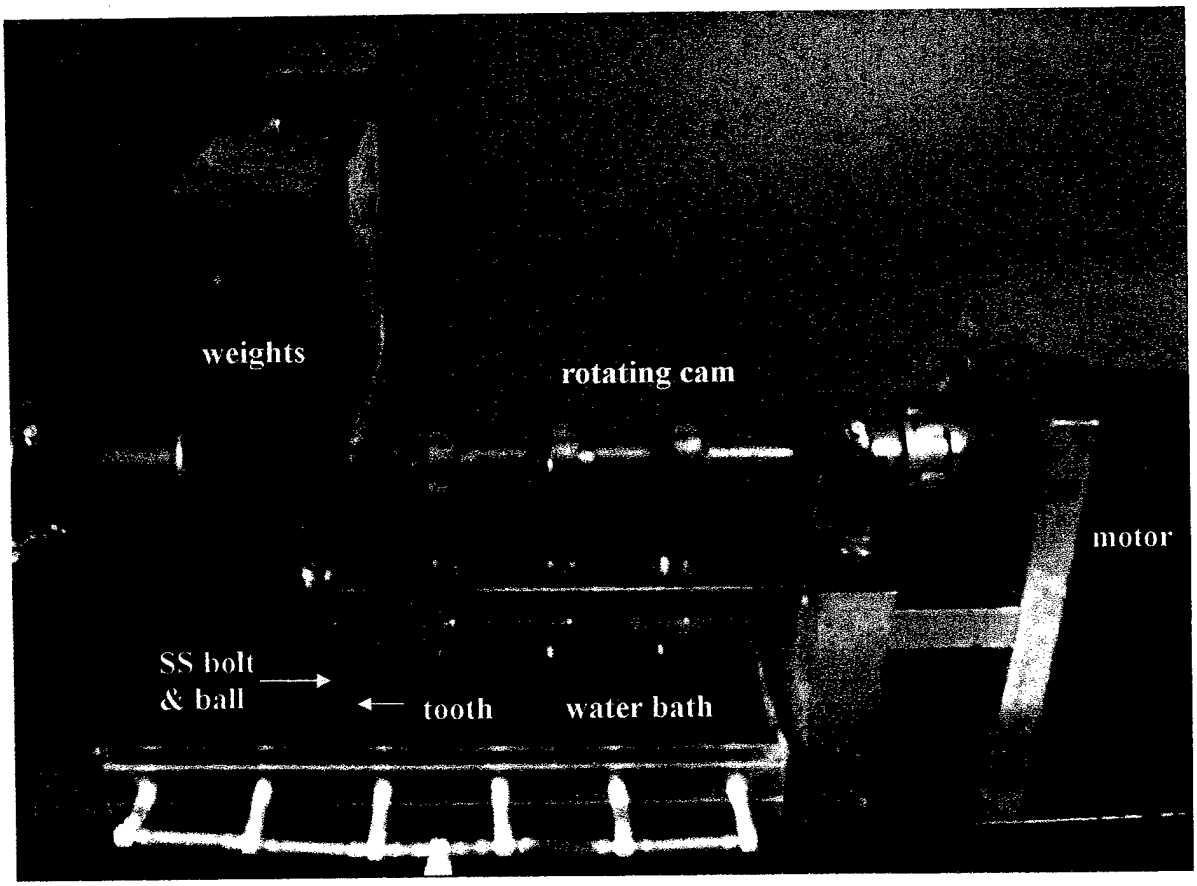

The OHSU custom-made fatigue cycler is capable of handling up to five specimens simultaneously. The number of dead weights and oscillations can be varied with a maximum of 85 Newtons and 1.25 Hertz. The unit operates with a DC motor rotating a cam system. The weights are supported by a spring assembly. The specimens may be bathed in re-circulating water at various temperatures with the use of a water bath. An electronic counter is available to terminate the oscillations at a preset number. The teeth were mounted in an acrylic ring. The ring and tooth assembly was locked into the cycler with adjustable plates. A 2 millimeter stainless steel sphere was cemented onto the occlusal surface of the resin composite restoration with chemically curing resin

cement. A stainless steel bolt, attached to the weight assembly system, was placed in contact with the surface of the steel sphere. The restorations were fatigued for up to 500,000 cycles from 18 to 85 Newtons at 1.25 Hertz while bathed in 37 degree centigrade water.

SCANNING ELECTRON MICROSCOPY

(JXA-6400, JEOL, Tokyo, Japan)

The Scanning Electron Microscope, or SEM, is an incredible tool for seeing the unseen worlds of micro-space. The SEM is capable of imaging samples of widely varying origin with a minimal preparation effort. A single SEM machine will allow magnifications from 10x up to 100,000x (the latter only under ideal conditions and with suitable samples). When an SEM is equipped with X-ray detectors, it becomes a micro-analysis device capable of measuring the elemental composition of a sample with high spatial resolution. The composition of the sample can be studied on a micrometer scale and can be visualized as an X-ray map. Conventional light microscopes use a series of glass lenses to bend light waves and create a magnified image. The Scanning Electron Microscope creates the magnified images by using electrons instead of light waves. Samples have to be prepared carefully to withstand the vacuum inside the microscope. Biological specimens are dried in a special way that prevents them from contracting. Because the SEM illuminates them with electrons, they also have to be made to conduct electricity. Our SEM samples are coated with a very thin layer of gold by a machine called a sputter coater. The sample is placed inside the microscope's vacuum column through an air-tight door. After the air is pumped out of the column, an electron gun [at the top] emits a beam of high-energy electrons. This beam travels downward through a series of magnetic lenses designed to focus the electrons to a very fine spot. Near the bottom, a set of scanning coils moves the focused beam back and forth across the specimen, row by row. As the electron beam hits each spot on the sample, secondary

electrons are knocked loose from its surface. A detector counts these electrons and sends the signals to an amplifier. The final image is built up from the number of electrons emitted from each spot on the sample.

Reference: Metalogic Products, Inc. www.metalogic.com